Electrospinning of Poly(acrylonitrile-*co*-glycidyl methacrylate) Nanofibrous Mats and their Applications

Dissertation

zur Erlangung des akademischen Grades
Doktor der Ingenieurwissenschaften
(Dr. -Ing.)
der Technischen Fakultät
der Christian-Albrechts-Universität zu Kiel

Tianhe Dai
Kiel
2011

1. Gutachter Prof. Dr. Volker Abetz

2. Gutachter Prof. Dr. Rainer Adelung

3. Gutachter Prof. Dr. Klaus Rätzke

Datum der mündlichen Prüfung: 19.12.2011

Table of Contents

List of Tables

List of Figures

Chapter 1. Introduction

Linear nanostructures such as: fibers, tubes, wires, rods, and belts have gained gradual attention in the past few years due to their unique properties and wide applications. A variety of advanced techniques including: electrochemical synthesis, solution-phase synthesis, vapor-liquid-solid growth, interfacial polymerization, electrophoresis, melt-blown technique, multicomponent processes, electrospinning, etc, have been innovated to prepare linear nanostructures with designed structure and composition.[1] Among these methods electrospinning probably is the simplest and most versatile one for fabricating linear nanostructures from kinds of polymers or composites.[1-6]

Conventional industrial spinning is restricted by the diameter of the nozzle and distance between the godet roll and winder, which results in the difficulty to produce fibers with the diameter below ten micrometers.[6] Electrospinning spins the spinning solution and reduces the diameter of viscoelastic jets and subsequent fibers via the electrostatic repulsions between surface charges, which is totally different from the conventional spinning process for fabricating macrofibers, therefore it avoids almost all the inborn weaknesses of the conventional spinning and accomplishes the elongation through a new manner.[1,5,6] Electrospinning provides much more possibilities for the fabrication of many materials into continuous long fibers with the diameter less than micrometer scale, even can reach several nanometers, which cannot be achieved by any other conventional fiber production techniques.[6-9]

The electrospun nanofibers and nanofibrous mats (ENMs) are notable for small diameters, large surface area to volume ratio, small pore size and extremely high

porosity. Due to these outstanding advantages electrospun nanofibers and ENMs already have had or will potentially have great applications as filtration membrane, catalysts/enzymes support, protective coating, drug delivery, scaffold for tissue engineering, wound healing, biosensor/chemosensor, fuel cell, micro/nano electronic device, and fiber reinforcement material. What is more, the most remarkable and inspiring thing is that electrospinning is not only employed in university laboratories, but also already has been widely applied in industries.[10-12]

Poly(acrylonitrile-co-glycidyl methacrylate) (PANGMA) is a new polymeric material developed by Helmholtz-Zentrum Geesthacht[13] which is a very good candidate for electrospinning novel nanofibers and nanofibrous mats. PANGMA is the copolymer of acrylonitrile (AN) and glycidyl methacrylate (GMA). It has not only the advantage of the chemical stability from the sturdy backbone of polyacrylonitrile but also the more critical functionality of further reacting ability from the free and active epoxy group on GMA. The epoxy group offers the opportunity in a variety of activation/coupling chemistries for crosslinking, surface modification, or covalent binding of capturers and ligands.

In this thesis, we describe the fabrication and three applications of a novel PANGMA electrospun nanofibrous mat (PANGMA-ENM). The PANGMA-ENM can be prepared by the electrospinning of PANGMA/DMF solution. The as-spun ENMs were modified via some subsequent physical or chemical treatments and then applied to the different areas. In numerous application directions of electrospun nanofibers, three of them were chosen: solvent-resistant nanomembranes, supports for the enzyme immobilization and affinity nanofilters for the protein filtration. The fabrication

process, fabrication parameters, properties of the nanofibers and nanomats, and the application results of the PANGMA-ENMs are described and discussed in detail in the following chapters of the thesis.

Why these three application directions (solvent-resistant nanomembranes, supports for the enzyme immobilization and affinity nanofilters for the protein filtration) were chosen to be our research contents? Firstly, these three applications of ENMs are very new and became hotspots in recent researches and they also do have very practical and wide prospects. They all tightly target most practical applications, which means they have the chance to be directly applied on a commercial level.[14,15] Secondly, they all highly involve in the epoxy group reaction, which can exactly take the advantage of PANGMA. These applications also have very close relationship with membrane engineering, especially with membranes for filtration, which is the research issue of our institute. Finally and the most importantly, the prior arts of ENMs applications in these areas all have lots of restrictions and disadvantages.[16,17] These disadvantages should be and could be made up or improved. For instance, ENMs can be used as the supports of the homogeneous catalysts in the catalysis field. Since most of the catalytic reactions are performed in organic solvents and at elevated temperatures, solvents and temperature resistant nanomembranes are urgently required. But the majority of available ENMs does not fulfill these requirements.[18,19] One possibility to overcome this drawback is to chemically crosslink the neat ENMs to make them become solvent and thermal resistable. Another example is about the application of ENMs in ultra- or nanofiltration. Normal ENMs have two universal and critical problems which limit their practical applications in those areas: relatively large pore size and weak mechanical properties.[20,21] A proper surface functional modification

can improve biological and mechanical stabilities of the ENMs and the binding of capturers on ENMs can greatly compensate their bad filtration ability due to their big pore sizes. From the two abovementioned examples it is clear that lots of worthwhile and meaningful work could be carried out. In this thesis, the methods and results of the improvements concerning the applications of ENMs in those areas will be described and discussed detailedly.

This doctoral thesis is organized as follows: Chapter 2 gives the theoretical background of this Ph.D work. In this chapter, the related theory and background knowledge used for the thesis, including the principle of electrospinning process, the principle of epoxy group reaction, crosslinking and surface modification, enzyme catalysts, the principle of enzyme immobilization, filtration and protein filtration, and affinity membrane are introduced and explained in more detail.

In chapter 3, characterization methods and devices used in this thesis are introduced and described. Measurement methods such as: Gel Permeation Chromatography (GPC), Attenuated Total Reflectance Fourier Transform Infrared Spectroscopy (ATR-FTIR), Ultraviolet-visible Spectroscopy (UV-vis), Scanning Electron Microscopy (SEM), Transmission Electron Microscopy (TEM), Bubble Point Test, Water Contact Angle Measurement, Tensile Strength Test, Differential Scanning Calorimetry (DSC), Thermogravimetric Analysis (TGA), Bradford Protein Assay, and other characterization methods are explained in detail.

The electrospinning process of PANGMA nanofibers and nanomats are particularly discussed in chapter 4. The detailed fabrication procedures are described and

explained. Factors and parameters which have influence on nanofiber diameter and morphology are discussed and compared.

Chapter 5 details the fabrication and application of solvent-resistant PANGMA-ENMs. As spun PANGMA-ENMs are crosslinked after electrospinning to gain the solvent-resistance. Different crosslinking routes and crosslinkers are compared and discussed. The effects of crosslinking temperature and crosslinking time on the crosslinking degree are studied and discussed. The solvents-resistance of crosslinked PANGMA-ENMs are tested via swelling test in different sorts of solvents and characterized by weight loss, swelling rate and SEM measurements after swelling test.

Chapter 6 introduces the application of PANGMA-ENMs as the support for the enzyme immobilization. The reaction routes and process of pre-functionalization of PANGMA-ENMs and the immobilization of enzyme are explained in detail. Different reaction routes and conditions are discussed and compared. The enzyme immobilized PANGMA-ENMs are applied as the catalyst for catalyzing the hydrolysis reaction of *p*-nitrophenol acetate. The catalytic activity, optimum pH and temperature, reusability, thermal ability and storage ability of the immobilized enzymes are investigated, discussed and compared with the pure enzyme particularly.

Chapter 7 narrates the application of this novel ENM in the filtration of proteins in water, which is done with the cooperation of Nanochemistry group of Kiel University. The fabrication and modification of PANGMA-ENMs into the affinity nanomembrane are presented in detail. This new fabrication method for the affinity ENMs is extremely simple and easy to operate compared with the previous reported

methods. The pore size and porosity, mechanical property, water wettability and permeability, filtration efficiency of the affinity PANGMA-ENMs are investigated, characterized and discussed. This novel affinity ENM is extremely suitable to be applied as the biofilter in the filtration of bioharzards in water or solutions.

Chapter 8 is the summary part. All the important conclusions obtained during the whole Ph.D work are repeated and summarized. Finally, a short acknowledgement to the persons who have given me kind and selfless helps for this Ph.D research is given in the end of the Ph.D thesis.

References:

[1] X. F. Lu, C. Wang, Y. Wei, Small, 2009, 5, 2349.

[2] M. A. Lim, Y. W. Lee, S. W. Han, I. Park, Nanotechnology, 2011, 22, http://dx.doi.org/10.1088/0957-4484/22/3/035601

[3] Y. Xia, P. Yang, Y. Sun, Y. Wu, B. Mayers, B. Gates, Y. Yin, F. Kim, H. Yan, Advanced Materials, 2003, 15, 353.

[4] S. Ramanathan, S. Patibandla, S. Bandyopadhyay, J. D. Edwards, J. Anderson, J. Mater. Sci.: Mater. Electron., 2006, 17, 651.

[5] J. Chen, B. Wiley, Y. Xia, Langmuir, 2007, 23, 4120.

[6] D. Li, Y. Xia, Advanced Materials, 2004, 16, 1151.

[7] J. Vonch, A. Yarin, C. M. Megaridis, J. Undergrad. Res., 2007, 1, 1.

[8] A. Frenot, I. S. Chronakis, Current Opinion in Colloid & Interface Science, 2003, 8, 64.

[9] S. Ramakrishna, K. Fujihara, W. E. Teo, T. Yong, Z. W. Ma, R. Ramaseshan, Materials Today, 2006, 9, 40.

[10] A. Greiner, J.H. Wendorff, Angewandte Chemie International Edition, 2007, 46, 5670.

[11] R. Dersch, M. Steinhart, U. Boudriot, A. Greiner, J. H. Wendorff, Polym. Adv. Technol., 2005, 16, 276.

[12] I. S. Chronakis, Journal of Materials Processing Technology, 2005, 167, 283.

[13] H.G. Hicke, I. Lehmann, Journal of Membrane Science, 2002, 198, 187.

[14] Z. M. Huang, Y. Z. Zhang, M. Kotaki, S. Ramakrishna, Comp. Sci. Technol., 2003, 63, 2223.

[15] K. Yoon, B. S. Hsiao, B. Chu, J. Mater. Chem., 2008, 18, 5326.

[16] P. Heikkila, A. Taipale, M. Lehtimaki, A. Harlin, Polym. Eng. Sci., 2008, 48, 1168.

[17] R. S. Barhate, C. K. Loon, S. Ramakrishna, J. Membr. Sci., 2006, 283, 209.

[18] C. Z. Chen, L. Wang, Y. Huang, Materials Letters, 2009, 63, 569.

[19] M. Stasiak, A. Studer, A. Greiner, J. H. Wendoff, Chem. Eur. J., 2007, 13, 6150.

[20] A. Srivastava, O. N. Srivastava, S. Talapatra, R. Vajtai, P. M. Ajayan, Nat. Mater., 2004, 3, 610.

[21] S. Kaur, R. Gopal, W. J. Ng, S. Ramakrishna, T. Matsuura, MRS Bull., 2008, 33, 21.

Chapter 2. Theoretical background

2.1 Electrospinning

2.1.1 General introduction

Electrospinning has drawn widespread attention in recent years due to its distinguished versatility and simplicity in fabricating nanofibrous materials. Currently, electrospinning is the only technique which can spin continuous long fibers with diameter below a few nanometers. Electrospinning can deal with nearly all kinds of raw materials from synthetic and natural polymers to polymers loaded with nanoparticles or carbon tubes, even can be expanded to metal and ceramic composites.[1] By the modification of the electrospinning setup, core–shell and hollow nanofibers can be produced and aligned nanofibrous structures also can be fabricated.[2-5] Electrospinning is not only used in university laboratories, but also has already applied in lots of fields of industry, such as catalysis, filtration, optoelectronics, sensor technology, pharmacy, food industry, biotechnology, etc.[1,6,7]

2.1.2 Historical background of electrospinning

The origin of electrospinning process can be traced down to 1930's. Formhals in 1934 patented a process for producing filaments using electric charge.[8,16] After that, he reported the spinning of cellulose acetate fibers from acetone by electrospinning.[9,10] In 1960's Taylor studied on the solution jet generated from droplet of polymer solution and found the conical shape of the droplet, which was later referred to as Taylor Cone.[11] Taylor determined that an angle of 49.3° is presented when the surface tension balances the applied electrical forces.[11,15] In subsequent years the structural morphology of electrospun fibers was of interest. Baumgarten[12] studied the

dependence of the fiber diameter to the viscosity of the spinning solution. Fibers obtained from the polymer melt were observed to be larger in diameter than those obtained from the polymer solution.[13,14,16] Hayati et al.[15] studied the influence of electric field and process parameters on the stability of the jet and found that semi conducting and insulating liquids can stabilize the spinning jets.[16]

Electrospinning obtained its new era of intensive academic attention in the 1990s.[17] Reneker and Doshi[17] initiated the research surge from studying the property and structure of polyethylene oxide (PEO) electrospun nanofibers by varying the solution concentration, applied voltage and working distance.[16] Deitzel et al.[18] revealed the electric field generated by the applied voltage could affect the bending of the jet, which determines the jet shape and finally the shape of the nanofibers, and also had influence on the formation of beads. Warner et al.[19] and Moses et al.[20] did very nice experimental characterization and evaluation on the aspect of fluid instabilities. Their results and conclusions are very key to the understanding of the electrospinning process.[21,16] Shin et al.[22] described the electrospinning process by experimental investigation and summarized the instabilities by systematically analyzing the relationship between electric field and flow rate. Spivak and Dzenis[23,24] reported that the nonlinear rheological constitutive equation used for polymer fluids (Ostwald de Waele power law) could be also applied for the stability analysis of polymer jets in the electrospinning process. Yarin et al.[25] calculated the bending electric force acting on an electrified polymer jet by a localized approximation, and then established an analogy between the bending instabilities driven electrical force and aerodynamical force. The results of the calculations were compared to the experimental data and the agreement of theory and experiment is discussed.

2.1.3 Details of electrospinning process

Generally, a common electrospinning setup consists of three major components (Figure 2.1): a high-voltage power supplier, a spinneret, and an electrically conductive collector. In most cases, an ordinary metallic needle acts as the spinneret and a piece of aluminum foil as the collector, respectively.[4] The spinning solution is loaded in a plastic or metal syringe, which is connected to the metallic needle. The syringe is placed at a particular distance away from the collector plate and connected to a syringe pump which can offer a constant and controllable feeding of the polymer solution. The needle of the syringe which loads the polymer solution is connected to the positive pole of the power supplier while the collector is grounded. For many experiments, especially for the electrospinning of ceramic nanofibers, the setup needs to be placed in a closed container in order to control the ambient conditions, such as humidity, temperature and solvent ventilation.[4] The collector can be constructed from different materials and in various shapes in order to fulfil the fabrication of all types of nanofibers.

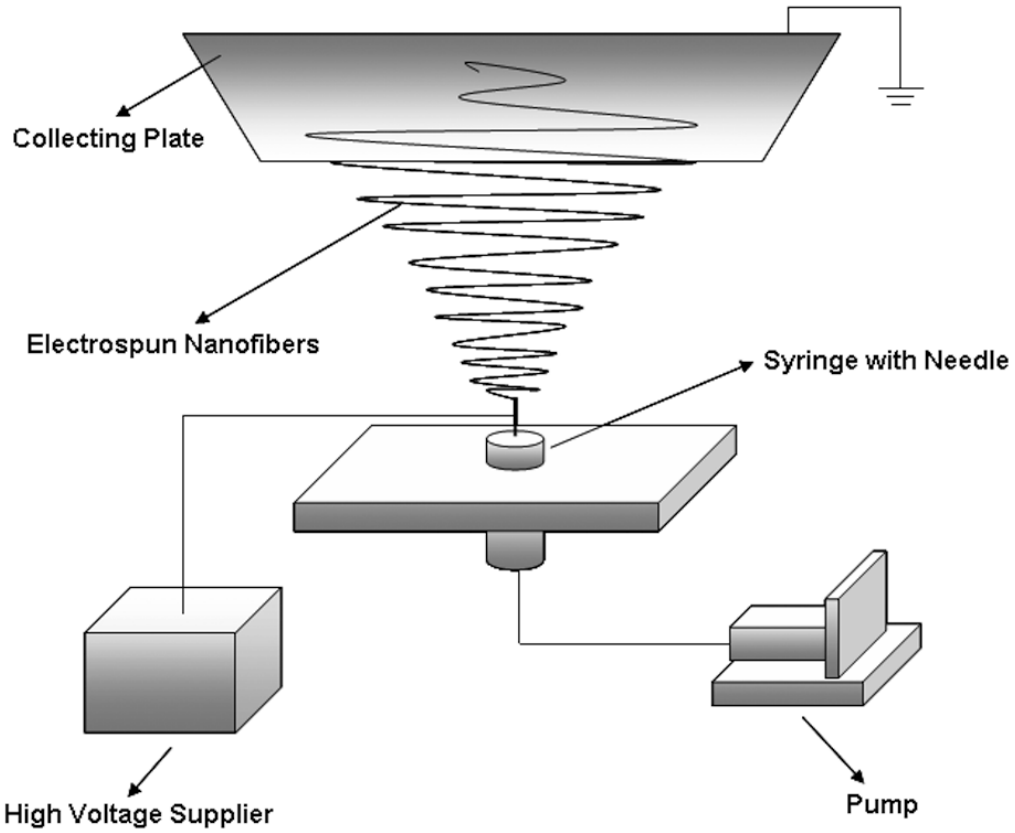

Figure 2.1 Schematic diagram of electrospinning setup and process

In a typical electrospinning process, a polymer solution, polymer melt or inorganic sol is ejected from a syringe with metal noodle under the strong electrostatic force from an electric field generated by the applied voltage. In conventional spinning techniques, the elongation of the fibers is completed by the tensile, gravitational, inertial, and rheological forces, while in electrospinning, the elongation is of the fibers is achieved by the the interaction of the applied electric field with the electrical charge carried by the jet.[26] When an electrical potential difference between the spinneret and the grounded collector is established, the surface of the polymer solution starts being charged by the electrical field, which results in the migration of ions through the solution. These migrated ions interact with the electrical field and form electrical

forces. With the potential difference increasing and finally above a threshold, the electrical forces overcomes the surface tension of the polymer solution and then a stable liquid jet emerges.[26,27] The jet is gradually stretched by the electrical force to form a continuous electrified jet, which first follows a straight path and then soon undergoes bending instability and finally is extremely elongated by its bending. During this process, the diameters of the jets decrease dramatically and the solvent evaporates rapidly. Finally the jets flight to the collector and dry out, leaving ultrathin fibers on the collector. Many of these ultrathin fibers eventually build up a non-woven mat which has huge surface area, high porosity and small pore sizes.[26,28,29]

2.1.4 Applications of electrospun nanofibers and nanomats

Electrospun nanofibers and nanomats nowadays have been attracting the attention of many research groups for advanced materials primarily due to their multi-functional properties required for application in specific areas like catalysis, filtration, tissue engineering, drug delivery systems, bio-sensors, protective textiles, nanocomposites and nanofiber reinforcement, storage cells for hydrogen fuel cells, etc (Figure 2.2).[30] A brief discussion on some of the applications of nanofibers and related nanomaterials is given in this section.

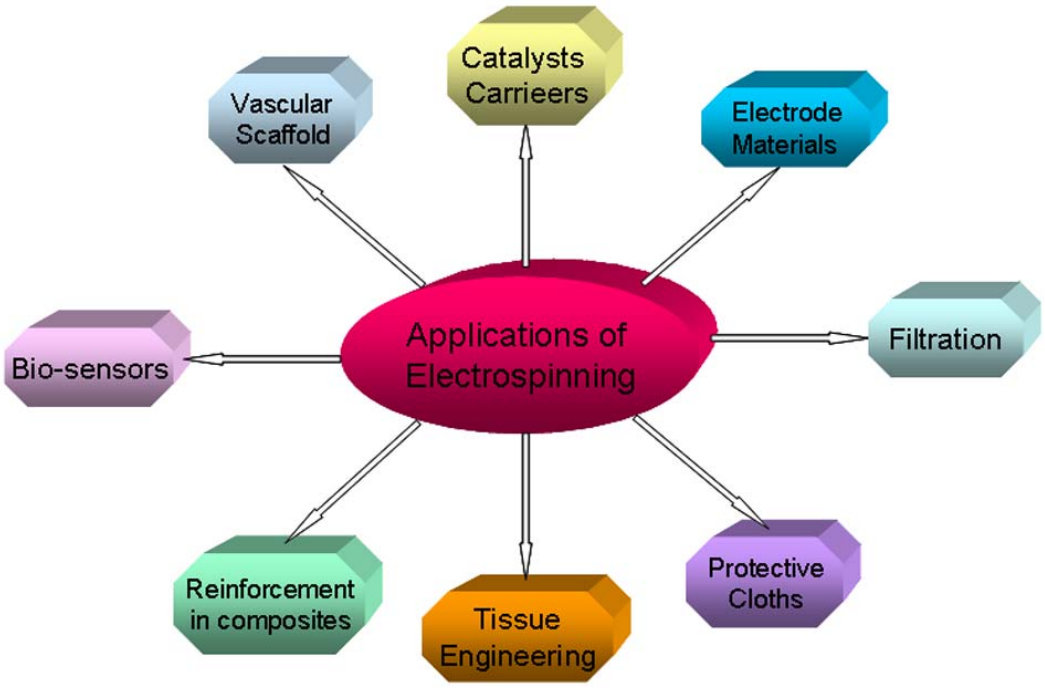

Figure 2.2 Applications of electrospinning and electrospun nanofibers

2.1.4.1 Catalysis applications

The main application of electrospun nanofibers and nanomats in catalysis field is that they can act as very good supports for the immobilization of homogeneous catalysts and enzymes.

The major disadvantage of homogeneous catalysts is the difficulty of separating the catalysts from the product. In homogeneous catalysis, reactants, products and catalysts are always in the same phase, this makes the separation become very difficult and complicated. It also causes a lot of trouble in recycling. Other disadvantages such like: weak thermal stability, toxicity, corrosion, the high cost and the creation of solid waste also hinder the further application of homogeneous catalysts in many applications.[31,32]

The immobilization of homogeneous catalysts in nanofibers presents an interesting solution to this problem.[1] After immobilization, the immobilized catalyst can almost keep the same structure and property as those in homogeneous catalysis, so it remains the advantages of the homogeneous catalyst, such as high activity and selectivity.[33] Meanwhile, because the catalyst has been fixed on the support, it also makes the immobilized catalyst become easier to separate and recover. In principle, the immobilization reaction of catalysts on nanofibers can be carried out in two ways. One way is that the reaction mixture can circulate around the catalyst fibers, and the other way is that nanofibers first are fixed on a carrier and then immersed repeatedly in the reaction vessel.[1]

Furthermore, electrospun nanofibers also can be used as carriers for enzymes. Enzymes can be chemically bound onto the electrospun fibers or directly dispersed in the nanofibers during the electrospinning process.[1,34,35] Enzymes applied as the catalysts are common and important in many chemical processes due to their high selectivity and mild reaction conditions.[36] Compared with pure enzymes, immobilized enzymes have some big advantages when such as easy separation, strong stability, and better availability for continuous operations. The efficiency and stability of these immobilized enzymes are mainly affected by the structure and property of the substrate material. Nanofibers and nanomats are recently very popular with acting as substrates for enzyme immobilization due to their large surface area per unit mass, organic origin closed to enzyme and the feasibility for high enzyme loading.[1,37] Their applications in enzyme immobilization will be detailed in §2.3.2, §2.3.3 and § 6.

2.1.4.2 Filtration applications

Polymer nanofibers are already used extensively as air filters for more than a decade. Conventional air filters are nomally made up of macrofibers with diameters in the micrometer range.[1,38] They trap particles which are floating in the air inside the filter, which means that all the layers in the filter are involved in the retention of the particle. As the trapped particles increase, the pressure drop across the filter also increases. When the pressure drop finally exceeds a certain limitation, the filter can be no longer used. The filter is usually partially cleaned by a pressure blast, whereby the particles are pushed out of the filter and collected. This cleaning mothed can not remove all the particles in filter, therefore the remaining pressure drop increases gradually after each cleaning, and eventually the filter must be replaced.[1,38] One concept for the modification of the filter is to cover the filter materials with a nanomat made of electrospun nanofibers.[39] The particles can be captured by this nanomat layer at the surface and will not contaminate the filter materials inside. By this way, the pressure drop remaining after each cleaning process is significantly reduced, and the filter lifetime can be prolonged ten times. This type of surface-modified filter has achieved great market success.[1,39]

Electrospun nanofibers also find inspiring applications in the filtration of water and solutions. These applications will be introduced and discussed in detail in §2.4 and § 7.

2.1.4.3 Protective textiles

Protective textiles must have properties like high moisture vapor transport, strong fabric breathability, and good toxicity resistance. Electrospun nanofibers and nanomats have been found to be good candidates for the application as protective

textiles. They are normally applied as the modifier for the enhancement of properties of the conventional textiles in combination with them.[40] Their functions are including: protecting against chemical or biological hazards, adjusting water-vapor permeability, optimizing thermal insulation, generating lotus effect, aerosol filtering, etc.[1] The nanoscaled size of nanofibers and nanomats dramatically benefits the transport processes of the material due to their relatively small pore dimensions and extremely large inner surface area.[41]

Gibson et al.[42] discussed the possibility of using nanofibrous mats over the conventional nonwoven elastomeric membrane for protective clothing. Nylon nanomats were applied over open cell polyurethane foams and carbon beads, which are used as a component in military chemical protective clothing systems. The air flow resistance and aerosol filtration properties of the nanomats coated foams were tested. Results indicate that these novel nanomats are extremely efficient at trapping airborne particles. And the high pressure drop is much reduced because the diameter of the nanofibers is comparable to the mean free path of air molecules. This novel nanomat also performs pretty well in the aspect of air flow resistance and aerosol filtration properties. Aerosol particle penetration is eliminated by minuscule levels of the nylon nanomats on the surface of the foam. This nanomat coated functional membrane for protective clothing applications exhibits high breathability, elasticity, and filtration efficiency. Ramaseshan et al.[43] used a functionalized nanofibrous membrane to degrade chemical warfare agents. This novel functionalized nanomembrance has strong ability of degradation and is very stable in these chemical agents. It is very suitable for combining with conventional textile media to form a protective garment. This type of protective wear would be much less heavy and allow

for moisture exchange. Such suits would offer the wearer both protection and comfort. Lee et al.[44] developed and researched nanofibers for different applications, especially for intermetallic-, metal-, and ceramic- matrix composites and high temperature coatings. They reported that nanofiber is a suitable candidate for these applications due to their wonderful properties, such as: strong scratch resistance, good compatibility, good interface stability, low flammability, low temperature ductility, and recyclability.

2.1.4.4 Tissue engineering

Nanostructured polymer materials, especially nanofibers and core-shell nanofibers, have already applied practically in medical and pharmaceutic field. A main reason for this wide applicability is that nanofibers are in the same size-scale with most of the biological molecules, for instance, proteins, viruses, and bacteria have dimensions all in nanoscaled. The following passages give some examples of the current progress of the applications of polymer nanofibers in tissue engineering, drug delivery and wound healing.[1,7,45]

Electrospun nanofibers due to their large surface area and high porosity have good applications as the candidates of tissue scaffolds. The extremely high surface to volume ratio of electrospun nanofibers offers much more space for the adherence of cells than the conventional fibers. The tissue scaffolding material must be selected carefully to meet the biocompatibility, which is very critical because the formation of the new tissue almost totally depends on the compatibility between the scaffolding material and body cells. The biocompatibility itself is based on the surface properties of the scaffolds materials.[46,47] Natural polymers of type I and type III collagen are the

main structural elements of the extracellular matrix (ECM) that supports tissue reconstruction, therefore electrospinning of collagen are mostly researched. For the synthetic polymers, firstly they should be biodegradable and secondly the size of these man-made nanofibrous scaffolds should be in the same scale with that of the natural ECM. Poly (D, l-lactide-co-glycolide) (PLGA) is the commonly used polymer for the electrospinning of nanoscaled fibrous scaffold in tissue engineering.[46-48] Mechanical properties like the Young's modulus and ultimate tensile strain are important for the application of electrospun nanofibers as tissue scaffolds.[46,49,50] Schields et al.[51] developed nanofibrous scaffolds of collagen type II by electrospinning and measured their mechanical properties. Tensile tests show that the Young's modulus and the ultimate tensile stress of the collagen II nanofibers scaffold can reach to about 170 MPa and 3.3 MPa, respectively. And these scaffolds also can produce a suitable environment for chondrocyte growth, indicating that electrospinning is a suitable technique for articular cartilage repair and replacement. Li et al.[52] fabricated a novel PLGA scafford with unique architecture by electrospinning process and measured its physical properties and also the cell attachment and proliferation. Results indicate that this novel PLGA nanofibrous scafford has nice mechanical property with a Young's modulus of 130 MPa, an ultimate tensile stress of 19 MPa, and an ultimate tensile strain of 20–120%. This nanofibrous scaffold also has good biocompatibility and good ability for the proliferation of cells. The architecture of this novel PLGA nanofiber scaffold is similar to that of natural extracellular matrix, indicating that the electrospun nanofibrous scaffold is suitable as a tissue substitute.

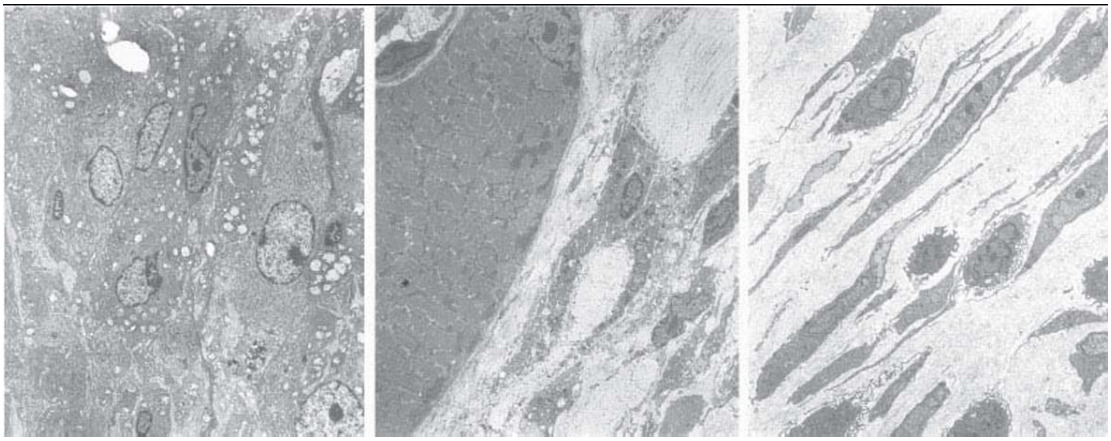

(a) **(b)** **(c)**

Figure 2.3 TEM micrographs of the PGA nanofiber scaffolds after one week of implantation: (a) 67 mg/mL PGA in HFP (no capsule seen), (b) 100 mg/mL PGA in HFP (smaller capsule at border with native muscle), (c) 143 mg/mL PGA in HFP (note large fibrotic capsule in white)[48]

2.1.4.5 Drug delivery

The nanostructured carriers for the delivery of drugs should meet some basic requirements, for instance, firstly they should be able to protect the drugs from decompositing in the blood circulation for enough time. Secondly they should be able to finish the release of the drug within the allotted time with a steady release rate. Moreover, they should also be able to have target-ability, which means they can guarantee the drug only to release in the targeted tissue but not in other tissues.[1,53] Nanofibrous mats due to their suitable pore size, large porosity and functionalized surface have been applied as the carrier for the drug delivery. Polymer nanofibers and nanomats perform well in the controlable delivery of drugs at a designed release rate in an assigned time period.[46,54] Kenawy et al.[55] developed novel carriers for drug delivery made up of electrospun nanomats from poly (ethylene-*co*-vinyl acetate) (PEVA) and poly lactic acid (PLA). They also tested the drug delivery performance of

these novel carriers with tetracycline hydrochloride as the model drug. Results show that the releases of tetracycline from all the electrospun nanomats are times drouble than those from the cast films. The electrospun nanomats also give a faster and smoother release of tetracycline. These positive results foretell a potential broad applicability of electrospun nanomats in the field of controlled drug delivery.

2.1.4.6 Wound healing

Electrospun nanofibers and nanomats also can be applied for the the treatment of large wounds such as brush burn and fire burn. Nanofibrous wound dressing has lots of advantages compared with conventional dressing. They give a quicker start of healing and higher healing efficiency than the conventional one due to their large surface area and porous structure, which can excrete the extracellular matrix components more rapidly to repair damaged tissue. The micrometer scaled pores of the nanomats are tiny enough to prevent the penetration of bacteria. Furthermore, the large surface area of the nanomat is very good for the adsorption of liquids, exudates, and bloods, which expands its application to hemostatic wound dressing.[1,56-59] The biggest advantage of electrospun nanofibrous wound dressings maybe is that they can greatly decrease the possibility of scarring after the wound cicatrisation because the nanofibrous structure of the nanomat can promote and control the healing of the wound in a homogeneous and controlled manner. And it is to be noted that the portable handheld electrospinning device has been developed, which makes the direct electrospinning of wound dress onto the skin for the first aid become possible in the future.[1,60,61]

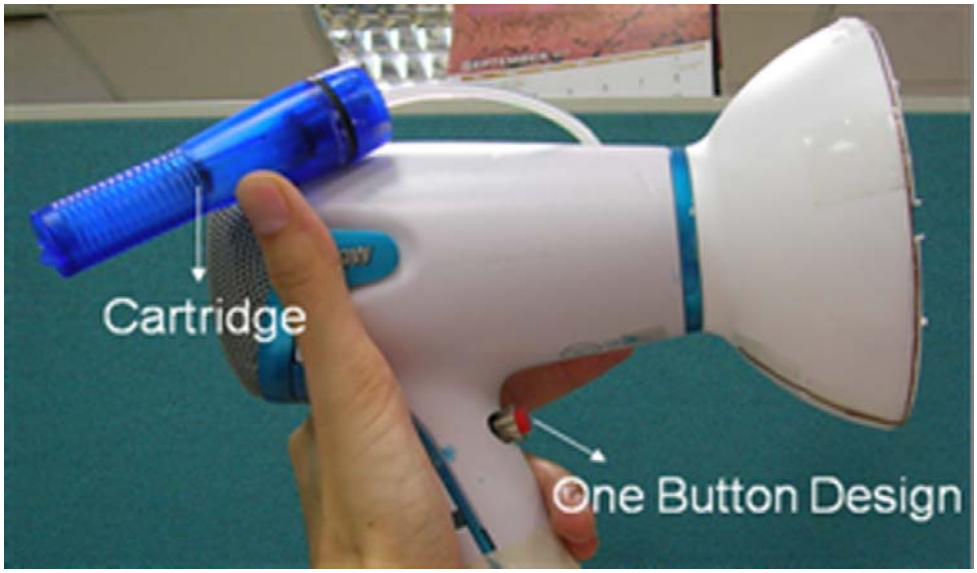

Figure 2.4 Handheld electrospinning device for the universal applications, also could be used for the preparing of wound dressings[60]

Khil et al.[62] electrospun polyurethane (PU) nanofibrous membranes and applied them as wound dressings. They also evaluated the performance of this nanofibrous wound dressing on pigs. The evaluation test shows that electrospun nanofibrous membrane has good and immediate adherence ability to the wet wound surface. It also shows controlled evaporative water loss, excellent oxygen permeability, and promoted fluid drainage ability. Histological examination confirms that epithelialization rate is increased and the exudate in the dermis is well controlled. Rujitanaroj et al.[63] fabricated gelatin nanofiberous mats with antibacterial activity against some common bacteria found on fire burn wounds and used them as antibacterial dressings. The antibacterial nanomats were prepared from gelatin solution containing 2.5 wt% $AgNO_3$ (first 12 hours aged to generate silver nanoparticles (nAg) for the antibacterium) by electrospinning. The release characteristic of Agt ions from either the nAg-containing gelatin nanomats was investigated by the total immersion method. The cumulative release of Agt ions from the nanomats is rather rapid during the first

60 min after submersion in the releasing medium, and increases gradually afterwards. The antibacterial activity of the novel nanofibrous dressing is very good against the common bacteria found on burn wounds, such as: P. aeroginosa, S. aureus, E. coli, and methicillin-resistant S. aureus. Rho et al.[64] fabricated type I collagen electrospun nanofibrous mats and investigated the wound-healing properties of these mats on wounds in mice. In the cell activity assessment, these electrospun collagen nanomats are found to promote cell adhesion and spreading of normal human keratinocytes. Additionally, these nanomats potentially provide a three-dimensional structure for cell attachment, growth, and migration. Therefore they conclude that these electrospun wound dressing has better healing effect of the wounds than those of the conventional dressings.

2.1.4.7 Nanofiber reinforcement

One of big and important application direction of nanofiber is fiber reinforcement nanocomposite material. Lots of nanostructures could be used as the reinforcement component including nanofibers, nanoyarns, nanoparticles, nanoclays and nanoplatelets. Among them, nanofibers seem to be the most easily-prepared and most wildly-used reinforcement material. The most important properties which decide the reinforcing performance of these nanofibers include mechanical strength, the compatibility to the matrix, and the ratio of the fiber length and diameter.[65-67]

Nanofibers as the reinforcement materials have many advantages compared with the conventional macroscopic reinforcement fibers. Reinforcement effect is mainly determined by the ratio of fiber length and diameter, so normally fibers with smaller diameters have better reinforcement effect. The average diameter of nanofibers can be

100–10000 times shorter than that of conventional fibers, therefore the reinforcement effect will be dramatically improved by using nanofibers. The large surface area of nanofibers also can improve the impact strength of the reinforced matrix.[1,68,69]

Nanofibers as the reinforcement materials without doubts have great prospect in many application area, but as well as the research on the nanofiber reinforcement is still in its starting period and lots of unknown are waited for the further discovery.

2.1.4.8 Applications of carbon and graphitic nanofibers

Carbon nanofibers (CNFs) have attracted gradually attention nowadays because their remarkable mechanical properties and other functions. These advantages make them be the ideal candidates for high-performance polymer composites. For instance, their strong mechanical properties enable them to be used as fillers in composites that find applications in synthetic and rubber industries. Those nanofillers provide the means to improve the properties of microstructured parts in which more conventional fillers physically cannot be accommodated.[46,70] Ma et al.[71] compounded polyethylene terphthalate (PET) resins with carbon nanofibers (CNF) with different methods. The morphology and mechanical properties of these composite materials have been studied. The results indicate that CNFs can be homogeneously dispersed into PET matrix. Compressive strength and torsional moduli of PET/CNF composite fiber increase obviously compared to the normal PET fiber.

2.1.4.9 Other applications

Nanofibers and nanomats also find different applications in other fields of industries. For example, Pawlowski et al.[72] electrospun piezoelectric polymers and developed

them for the application as a component on the lightweight wings for micro-air vehicles (MAV). The piezoelectric polyamide, (α-CN) APB-ODPA, was electrospun and the relationship between the morphologies and properties of it and the electrospinning conditions was studied. They conclude preliminary that this kind of piezoelectric polyamide can be electrospun into nanofiber and has optimistic prospect on the potencial applications. Wu et al.[73] reported the fabrication of high-performance transparent electrodes with copper nanofiber networks by electrospinning process. These nanofiber networks are excellent transparent electrode materials, with performances superior to the reported transparent electrodes so far in terms of transmittance and sheet resistance, e.g., high transmitance at low sheet resistance of 90% at 50 Ω/sq. The copper nanofiber networks also demonstrate great flexibility and stretchabilty. All of these advantages should continue to expand and open up new applications.

The above-mentioned brief introduction about the applications of nanofibers and nanomats show that their potencial applications in advanced functional materials are unlimited. The application of nanofibrous structures will definitely become wider, more diverse and more in-depth with the development of the nanotechnology and electrospinning technique itself. Researchers are making efforts to discover more unknown areas of nanofibrous structures, in the creating of fabrication techniques, in the studying of structure, properties, and performance, and in the searching of possible future applications.

2.2 Epoxide-amine reaction

2.2.1 Epoxide

An epoxide is a cyclic ether with a three-membered ring. This ring approximately defines an equilateral triangle with bond angles about 60°. The strain of the three-membered ring makes epoxides more reactive than other acyclic ethers.[75] Ethylene oxide is the most important epoxide and is made from oxidation of ethylene. Epoxides with more complex structures are synthesized by the epoxidation of alkenes.[74,75]

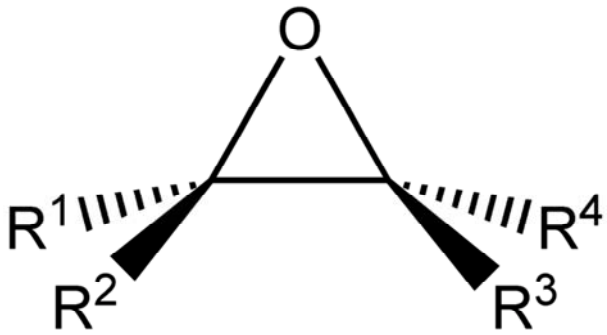

Figure 2.5 Schematic diagram of the molecular structure of epoxide[75]

A polymer containing unreacted epoxide units is called polyepoxide or epoxy.[75] Epoxy resins are a set of thermosetting polymers built up from monomers with epoxy groups. Epoxy resins can be cured with curing agents containing amines or anhydrides. After curing, a crosslinked network structure forms with good stablity, strong toughness, and resistance to corrosive chemicals. Epoxy resins are excellent adhesives, good structural materials, and useful surface coatings.[75,76]

2.2.2 Amine

Amines are organic compounds or functional groups that contain nitrogen atoms and they are basic. The general forms of amines are shown in Figure 2.6, R represents alkyl or aryl group. Amines are derivatives of ammonia in which one or more of the

hydrogens has been replaced by an alkyl or group.[77] In common nomenclature, the prefix "amino-" and the suffix "-amine" represent amine groups when they are in compound structure, and the prefix "N-" shows substitution on the nitrogen atom. Amines with multiple amino groups are called diamine, triamine, tetraamine and so forth. Important amines include amino acids, biogenic amines, amphetamine, barbituate, trimethylamine, and aniline.[77-80]

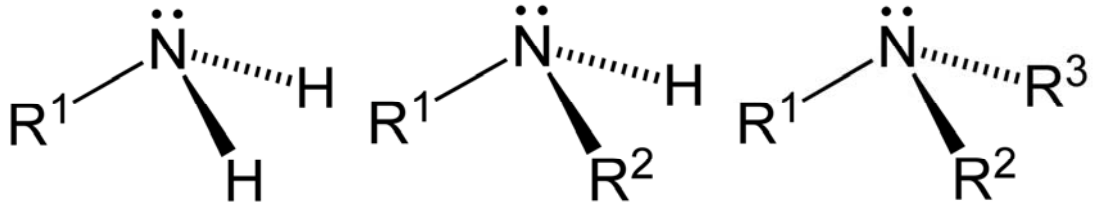

(a) **(b)** **(c)**

Figure 2.6 Schematic diagram of the amine groups: (a) primary amine, (b) secondary amine, (c) tertiary amine[77]

Amines are further devided into different classes according as how many of the hydrogen atoms are replaced. Primary, secondary, and tertiary amine represent one, two, and three hydrogen(s) have been substituted, respectively (Figure 2.6). Generally primary and secondary amines can react with electrophilic carbons to form C—N bonds. In strong contrast, tertiary amines tend to react as bases rather than nucleophiles. They are generally used as the accelerators for the reactions.[77,81,82]

2.2.3 Mechanisms of epoxide-amine reaction

The reaction mechanism involving cyclic compounds such as epoxides is identified as ring-opening polymerization.[83,84] This Ph.D dissertation only refers to the reaction mechanism of epoxide-amine systems, which was detailedly reported by Rozenberg in 1986.[83,85] In this reaction, epoxides can react either with primary or secondary

amines. Figure 2.7 (a) is the reaction mechanism for the conversion of a primary amine into a secondary amine by reacting with an epoxide. This generated secondary amine is able to react with another epoxide to generate a tertiary amine and thereafter forms a crosslinked network. As the reaction proceeds, the crosslinking degree increases and finally a three-dimensional network forms.

I. Primary amine – epoxy addition

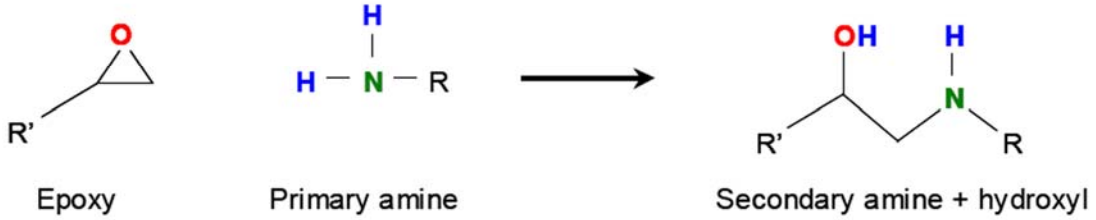

(a)

II. Secondary amine – epoxy addition

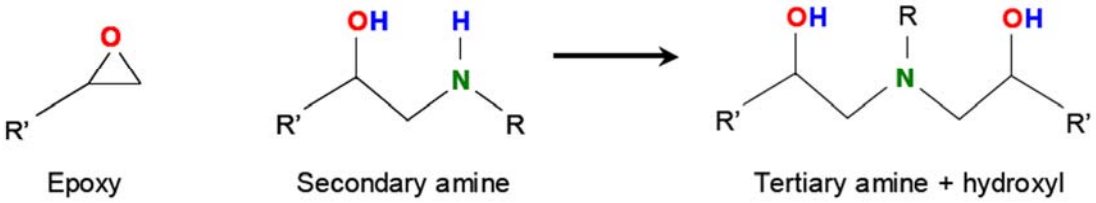

(b)

Figure 2.7 Schematic diagram of the epoxide-amine ring-opening reaction: (a) primary addition, (b) secondary addition[83]

Generally, the above reactions take place under two conditions: catalytic and autocatalytic.[83,86] In the early stage of the epoxide-amine reaction, absorbed moisture, residual hydroxyl groups in epoxy and solvents catalyze the reaction. Then, the hydroxyl groups generated by reactions also act as active catalysts. Rozenberg[85] explained the activation of carbon atoms in the epoxy ring by nucleophilic attack from those generated hydroxyl groups, which was identified as a "termolecular transition

state" (Figure 2.8). These secondary hydroxyl groups catalyze the reaction through the formation of a termolecular complex. Therefore the epoxide-amine reaction accelerates automatically, which is known as an autocatalytic reaction.[83-88]

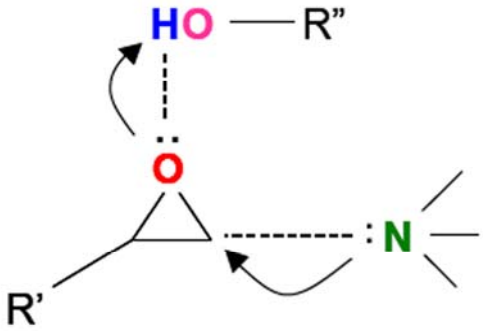

Figure 2.8 Termolecular transition state of the epoxide-amine addition in the presence of hydroxyl-containing groups[83,85]

2.2.4 PANGMA:

Poly(acrylonitrile-*co*-glycidyl methacrylate) (PANGMA) is a new polymer material developed by Helmholtz-Zentrum Geesthacht.[89] PANGMA is the copolymer of acrylonitrile (AN) and glycidyl methacrylate (GMA). It has not only the advantage of the chemical stability from the sturdy backbone of polyacrylonitrile but also the more critical functionality of further reacting ability from the free and active epoxy group on GMA. The epoxy group offers the opportunity in a variety of activation/coupling chemistries for the crosslinking by amines, grafting of catalysts ligands, and the covalent binding of enzymes and capturers. In these cases, the extremely simple and widespreadly used epoxide-amine reaction between PANGMA and the amines/ligands/enzymes/captures is performed.

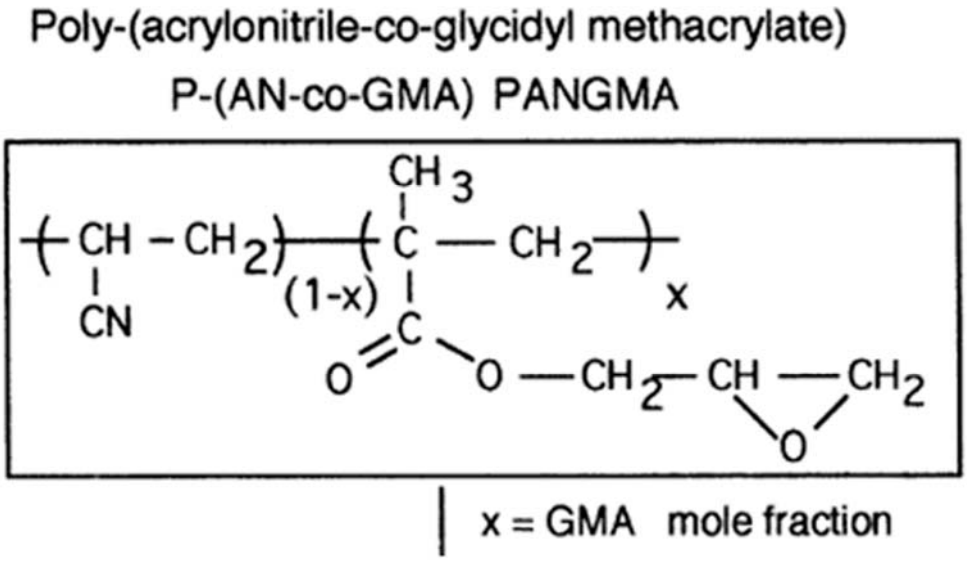

Figure 2.9 Schematic diagram of the molecular structure of PANGMA[89]

2.3 Catalysis and enzymes

2.3.1 Catalysis and catalysts

Catalysis plays a vital role in many industries, such as fuels industry, petrochemistry, fine chemistry, pharmacy, bio- and environmental engineering. For instance: nearly all the reactions in biological engineering require catalysts. Currently about 90% of chemical manufacturing processes involve catalytical steps.[90-92]

Catalysts are indispensable for catalysis. Catalysts can be classified into different types according to their chemical structure, physical state, or the reaction types which they catalyze. Most commonly, they are divided into three main large groups: heterogeneous catalysts, homogeneous catalysts and enzymes (Figure 2.12).[92,93]

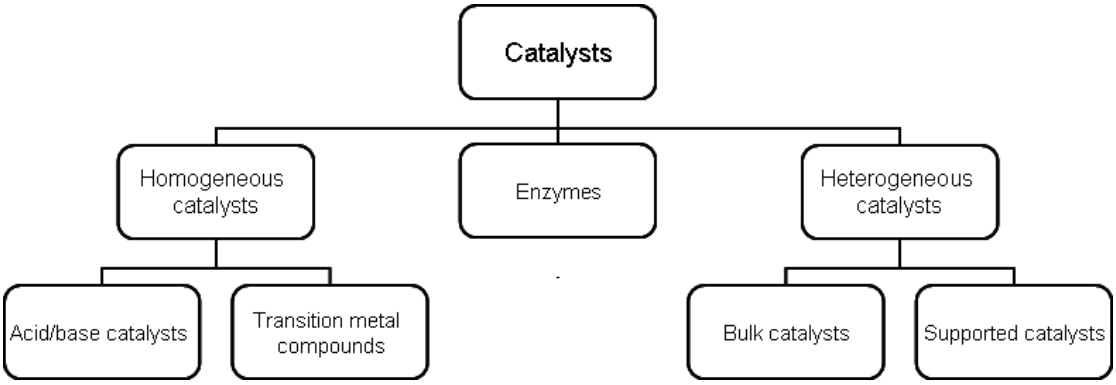

Figure 2.10 Classification of catalysts[92]

2.3.2 Enzymes

2.3.2.1 What is enzyme?

Enzymes are proteins which can catalyze many reactions of both living organisms and non-living things. Enzymes can rightly be called the catalytic machinery of living systems and have played a very important role in many aspects of life. Today nearly all the commercially prepared foods contain at least one ingredient which has relationship with enzymes.[95] Enzymes are also well applied in other industrial and daily life areas such like: laundry, dishwashing, paper manufacture, leather and textiles industries.[94-96]

2.3.2.2 Immobilization of enzyme

A popular strategy to apply enzymes in wider area is to immobilize them on a stable carrier. In general, immobilization will improve the catalytic activity and selectivity of enzymes as well as enhance the temperature and solvent stability, and the most important function is: immobilized enzymes can easily be recovered from the reaction medium and preferably be reused. This is particularly important because of the high enzyme costs.[97-99]

In general, there are three basic types of methods for enzyme immobilization:[100-102]

I. Carrier binding: binding enzymes onto solvent-stable carriers such as synthetic polymers, porous resin, inorganic/organic nanomaterials, etc.

II. Crosslinking: crosslinking of enzymes by using bifunctional or multifunctional crosslinkers such as glutaraldehyde, diamine, bisdiazobenzidine, hexamethylene diisocyanate, etc.

III. Encapsulating: incorporating (physically) enzymes into insoluble beads, microspheres or membranes, such as polysaccharides, polystyrenes, polyacrylates, polyamides, carbon, calcium alginate, etc.

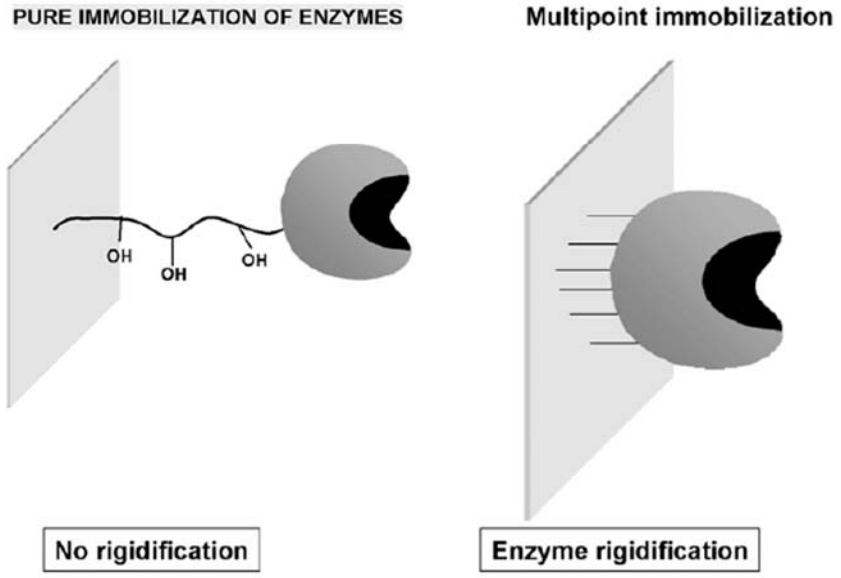

Figure 2.11 Different approaches of enzyme immobilization[101]

2.3.3 Electrospun nanofibers for the immobilization of enzymes

In recent years, there is a trend to use nanostructured materials as the support for the immobilization of enzymes since the large surface area of nanomaterials can effectively improve the unit enzyme loading. Nanoparticles, porous membranes and nonwoven nanomats are possible architectures. Compared with other architectures, electrospun nanofibers and nanomats have the following three big advantages, which

make them become excellent candidates for enzyme immobilization: firstly, electrospinning can deal with a variety of polymers, which can meet different requirements toward raw materials as the supports. Secondly, the high porosity and the interconnectivity of electrospun nanomats lower the mass transfer hindrance dramatically. Finally, nanofibers are very suitable for surface modification and surface functionalization to improve the enzyme loading and benefit the enzyme activity.[103-105]

Enzymes immobilized on electrospun nanomats have big advantages on the easy recovery and reuse, therefore they are very suitable for the application on continuous operations.[106,107] The immobilization of enzymes on both natural and synthetic polymeric electrospun nanomats has been widely reported.

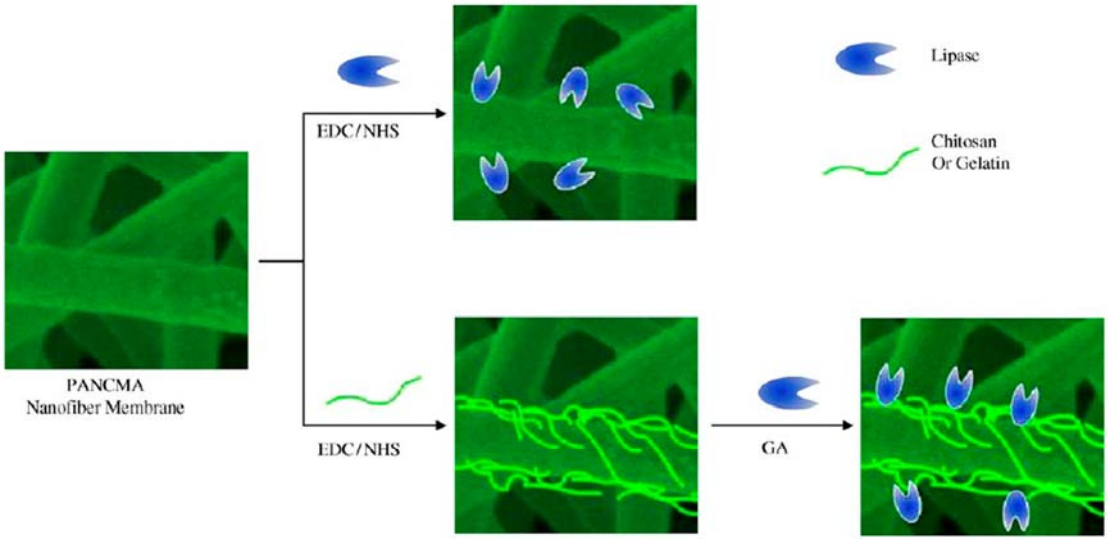

Figure 2.12 Schematic diagram of the immobilization of lipase on PANCMA nanofibers[103]

Jia et al.[108] electrospun functionalized polystyrene nanofibers which have reactive surfaces and covalently immobilized α-chymotrypsin onto these nanofibers. The

enzyme loading was up to 1.4 wt.% of the nanofibers and over 27.4% of the external nanofiber surface was covered with a monolayer of enzyme. The apparent hydrolytic activity of the immobilized α-chymotrypsin was found to be over 65% of that of the pure enzyme. The enzyme stability of this immobilized enzyme is also higher than other forms of immobilized enzymes. Ye et al.[103] electrospun nanofibers from poly(acrylonitrile-*co*-maleic acid) and used them for lipase immobilization. Two natural biomacromolecules, chitosan and gelatin, were tethered on the membrane surface as the surface modifiers. Results indicate that there is an increase of the activity retention of the immobilized lipase on the biomacromolecules modified nanomats compared to that on the neat one. Kim et al.[109] introduced enzyme aggregate coatings on the electrospun polymer nanofibers to improve the enzyme loading (Figure 2.13). Firstly, they covalently attached seed enzymes onto polystyrene/poly(styrene-co-maleic anhydride) blend nanofibers. Then they modified these enzyme immobilized nanofibers by a glutaraldehyde treatment to entrap and crosslink additional enzyme molecules and aggregates from the solution onto the surface of these enzyme immobilized nanofibers. The crosslinked enzyme aggregates greatly improve the activity and stability of these immobilized enzymes. The results show that the initial activity of aggregates-coated nanofibers is nine times higher than untreated nanofibres. This approach creates a useful biocatalytic immobilized enzyme system with potential applications in bioconversion, bioremediation, and biosensors. Kim and Park[110] electrospun biocompatible nanofibers from poly(ε-caprolactone) and poly(*d*,*l*-lactic-*co*-glycolic acid)-*b*-poly(ethylene glycol)-NH_2 (PLGA-*b*-PEG-NH_2) block copolymer and used them for the covalently immobilization of lysozyme. Results show that the nanomat is able to immobilize much greater amount of lysozyme compared to that of the solvent casting film, which demonstrates the this

novel nanomat has a promising prospect for immobilizing a wide range of bioactive molecules.

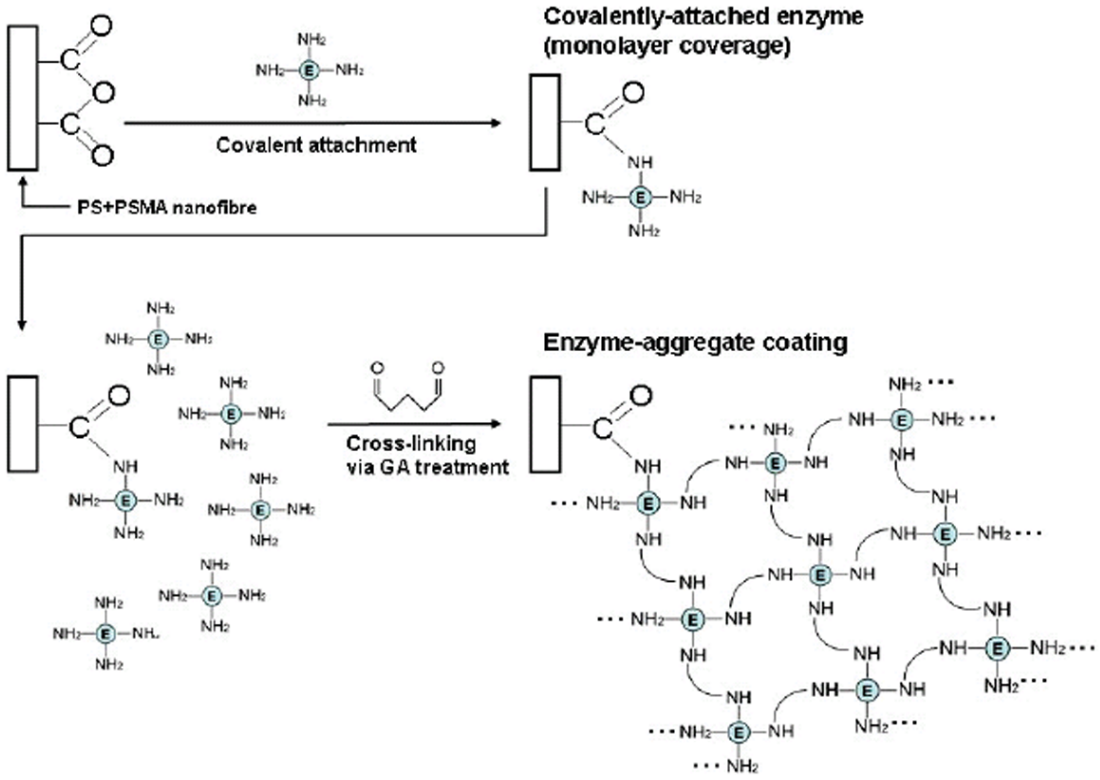

Figure 2.13 Schematic diagram for the preparation of covalently attached enzymes and enzyme-aggregate coatings on nanofibers[109]

2.4 Water filtration

2.4.1 Basic conceptions of filtration

Filtration is the mechanical or physical operation which is used for the separation of solids from fluids (liquids or gases) by passing the mixture through a permeable media which only allows fluids to pass.[111] In chemistry, filtration is a technique used either to remove impurities from an organic solution or to isolate an organic solid. These two commonly used filtration methods are called gravity filtration and vacuum filtration.[112] In biology, especially in water treatment and sewage treatment, filtration

refers to the removing of undesirable or deleterious components by adsorption into a biological film or biofilter.[111,113,114]

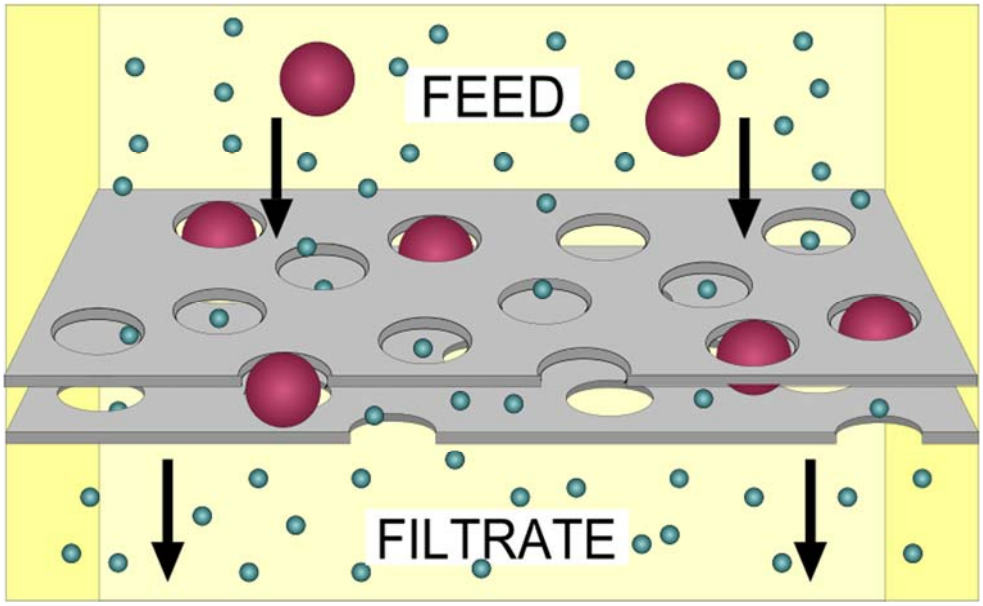

Figure 2.14 Schematic diagram of filtration[111]

There are some basic parameters for the characterization of the filtration, which should be introduced:[111,122]

I. Permeability: A measure of the ability of a filter to transmit fluids. Permeability is the grade of transmissibility of a filter, which means how much substance penetrates in a specific time, depending on the type of permeate, pressure, temperature, thickness of the filter and the area size. [111,115,116]

II. Feed: The substance feeding into a filtration process; that is, the mixture which must be divided into separated ingredients.[117]

III. Permeate: The substance permeating through the filter.[115]

IV. Flux: The rate of volume fluid flow through a unit area of filter. Water flux is often expressed as milliliter permeated water per minute per square centimeter of filter area (mL min^{-1} cm^{-2}).[118]

V. Pressure drop: A term used to describe the difference in fluid pressure from one point (upstream) to another point (downstream) in a pipe or tube. "Pressure drop" is usually caused by the frictional resistance against to the fluid flowing through pipe, conduit, filter media, or other flow-conducting system.[119,120]

VI. Filtration efficiency: The percentage of filtration objects which are removed from the feed by the filter. The filtration efficiency (FE) was determined using the formula below:

$$FE = (1 - C_{permeate}/C_{feed}) \times 100\% \quad (2\text{-}1)$$

where $C_{permeate}$ and C_{feed} are the concentration of the filtration object in permeate and in feed, respectively. The efficiency of a filter varies for different particles sizes and flux.[121]

2.4.2 Ultrafiltration and nanofiltration

Ultrafiltration (UF) is a membrane separation process driven by a pressure gradient for separating dissolved molecules in solution, in which hydrostatic pressure forces a liquid against a semipermeable membrane. Ultrafiltration is based on size, which means that molecules larger than the membrane pore size rating will be retained at the surface of the membrane while other components which are smaller than the membrane pore will pass through the pores with the water. This separation process is used in research for purifying and concentrating macromolecular (10^3 - 10^6 Da) solutions, especially protein solutions.[123] It is widely applied in a variety of industrial fields, including: food industry, pharmacy, biotechnology, power generation, and semiconductor manufacturing.[123-126]

Nanofiltration (NF) is a relatively recent membrane separation process which ranges somewhere between ultrafiltration (UF) and reverse osmosis (RO). The limitation of the size range of nanofiltration can reach up to a few nanometers. Nanofiltration membranes are usually characterized by the molecular weight cut-off (MWCO) and the MWCO of nanofiltration is typically less than 1000 Da.[127-129] Nanofiltration membranes also have selectivity for the charge of the dissolved components. Monovalent ions will pass the membrane and divalent and multivalent ions will be rejected.[128]

Typical applications of nanofiltration include water softening, desalination of dyestuffs, acid and caustic recovery, color removal, food and pharmaceutical application, etc.[130] Nanofiltration is mostly used in softening water such like surface water and fresh groundwater and removal of disinfection by-product precursors such as natural organic matter and synthetic organic matter. Recently, nanofiltration is gradually applied in food processing such as dairy, simultaneous concentration and partial demineralization.[127,131]

2.4.3 Electrospun nanofibers for the water filtration

Electrospun nanofibrous mats (ENMs) nowdays become very attractive in filtration technology due to their unique properties such as high porosity, micro- to nano-scaled pore sizes, interconnected open pore structure, high permeability for gases and a large surface area per unit volume. ENMs have achieved widely successfulness in the development of high-performance air filters.[132,133] The applications of ENMs in air filtration have been introduced in § 2.1.4.2.

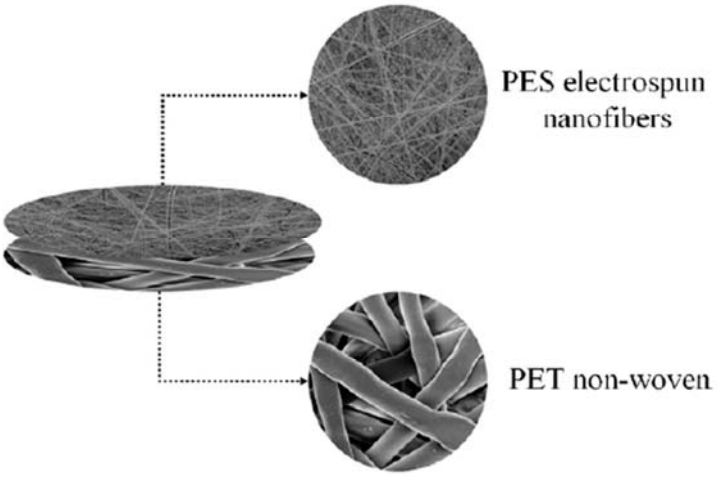

Figure 2.15 Nanofiber filter with sandwiched structure fabrication by HZG[137]

However, normal ENMs have two universal and critical problems which limit their practical applications in these areas: large pore size and weak mechanical property. Firstly, ENMs normally have a large pore size in the range of several micrometers resulting in the difficulty of filtrating submicro- and nanoparticles from water or organic solutions. However, many of the toxic metal particles, proteins and toxins in pollutants have sizes on the nanometer scale and therefore they are very difficult to be filtrated by normal ENMs. Secondly, the relatively wide distribution of both fiber size and pore size of ENMs will also reduce the filtration efficiency.[134-136] Finally, in some cases, the mechanical strength and fouling of ENMs should also be considered.[137-140]

Unfortunately, only few relevant publications and reports can be found in regard to solve the abovementioned problems, especially about the filtration of tiny particals or bioharzards in water or organic solutions.[141-144] People used several methods in the prior work to deal with these kinds of filtration but did not involve the details, furthermoer their methods and routes were really complex, normally involving plasma

treatments, chemical pre-functionalizations and a lot of complicated coupling reactions.[145-147] So how to solve those abovementioned problems? How to simplify the fabrication and modification process of the ENMs for the proteins filtration? The answers and solutions will be given in chapter 7.

2.5 References

[1] A. Greiner, J. H. Wendorff, Angewandte Chemie. Int. Ed., 2007, 46, 5670.

[2] Z. M. Huang, Y. Z. Zhan, M. Kotaki, S. Ramakrishna, Compos. Sci. Technol., 2003, 63, 2223.

[3] D. Li, Y. Xia, Adv. Mater., 2004, 16, 1151.

[4] D. Li, J. T. McCann, Y. Xia, M. Marquez, J. Am. Ceram. Soc., 2006, 89, 1861.

[5] D. H. Reneker, A. L. Yarin, E. Zussman, H. Xu, Adv. Appl. Mech., 2007, 41, 44.

[6] A. Frenot, I. S. Chronakis, Current Opinion in Colloid and Interface Science, 2003, 8, 64.

[7] S. Agarwal, J. H. Wendorff, A. Greiner, Polymer, 2008, 49, 5603.

[8] A.Formhals, US Patent 1975504, 1934.

[9] A.Formhals, US Patent 2160962, 1939.

[10] A.Formhals, US Patent 2187306, 1940.

[11] G. I. Taylor, Proc. Roy. Soc., 1969, 313, 453.

[12] P. K. Baumgarten, J. Colloid Interface Sci., 1971, 36, 71.

[13] B. Kalb, A. J. Pennings, Polymer, 1980, 21, 607.

[14] L. Larrondo, R. Mandley, J. Polym. Sci.: Polymer Physics Edn, 1981, 909.

[15] I. Hayati, A. I. Bailey, T. F. Tadros, J. Colloid Interface Sci., 1987, 117, 205.

[16] S. Bhargava, Dissertation, University of Akron, USA, 2007.

[17] J. Doshi, D. H. Reneker, J. Electrostatics. 1995, 35, 151.

[18] J. M. Deitzel, J. Kleinmeyer, J. K. Hirvonen, N. C. BeckTan, Polymer, 2001, 42, 8163.

[19] S. B. Warner, A. Buer, M. Grimler, S. C. Ugbolue, G. C. Rutledge, M. Y. Shin, National Textile Center Annual Report, 1998, 83.

[20] M. Moses, M. M. Hohman, Y. M. Shin, G. C. Rutledge, M. P. Brenner, Phys. Fluids, 2001, 13, 2201.

[21] A. Theron, E. Zussman, A. L. Yarin, Nanotechnology, 2001,12, 384.

[22] Y. M. Shin, M. M. Hohman, M. P. Brenner, G. C. Rutledge, Polymer, 2001, 42, 9955.

[23] A. F. Spivek, Y. A. Dzenis, Inst. Penn. Conf., 1999, 163, 175.

[24] A. F. Spivak, Y. A. Dzenis, Appl. Phys. Lett., 1998, 73, 3067.

[25] A. L.Yarin, S. Koombhongse, D.H. Reneker, J. Appl. Phys., 2001, 89, 5.

[26] D. H. Reneker, I. Chun, Nanotechnology, 1996, 7, 216.

[27] J. Watthanaaruna, V. Pavarajarna, P. Supaphol, Science and Technology of Advanced Materials, 2005, 6, 240.

[28] D.H. Reneker, A. L. Yarin, H. Fong, S. Koombhongse, J. of Appl. Phys., 2000, 87, 4531.

[29] S. Tan, X. Huang, B. Wu, Polymer International, 2007, 56, 1330.

[30] S. N. Patra, Ph.D dissertation, The University of Auckland, New Zealand, 2010.

[31] Franco Cozzi, Adv. Synth. Catal., 2006, 348, 1367.

[32] G. C. Bond, Homogeneous Catalysis – Principles and Applications, Clarendon Press, Oxford, 1987.

[33] G. Emig, E. Klemm, Technische Chemie. Einführung in die Chemische Reaktionstechnik, Springer, Berlin, 2005.

[34] S. H. Kim, S. Nair, B. C. Kim, M. B. Gu, J. Kim, Biomolecular Catalysis, ACS Symposium Series 86, American Chemical Society, 2008

[35] H. Jia, G. Zhu, B. Vugrinovich, W. Kataphinan, D. H. Reneker, P. Wang, Biotechnol Prog., 2002, 18, 1027.

[36] A. Zaks, M. Empie, A. Gross, Trends in Biotechnology, 1988, 6, 272.

[37] S. Viju, The Indian Textile Journal, Aug, 2008.

[38] Z. M. Huang, Y. Z. Zhang, M. Kotaki, S. Ramakrishna, Composites Science and Technology, 2003, 63, 2223.

[39] T. Matsuda, M. Ihara, H. Inoguchi, I. K. Kwon, K. Takamizawa, K. Keiichi, S. Kidoaki, J. Biomed. Mater. Res. Part A, 2005, 73, 125.

[40] Nano technology adds value to textile finishing, http://www.freewebs.com/textile-technology/nanotextile.htm

[41] H. L. Schreuder-Gibson, P. Gibson, P. Tsai, P. Gupta, G. Wilkes, Int. Nonwovens J., 2004, 13, 39.

[42] P. Gibson, H. Schreuder-Gibson, D. Rivin, Colloids Surf. A, 2001, 187, 469.

[43] R. Ramaseshan, S. Sundarrajan, Y. Liu, R. S. Barhate, N. L. Lala, S. Ramakrishna, Nanotechnology, 2006, 17, 2947.

[44] Y. Lee, G. Bhat, Processing and Fabrication of Advanced Materials for High Temperature Applications, Ed. T. S. Srivatsan, R. A. Varin, The Materials Society, Warrendale, PA, 2003.

[45] A. B. Balta, Master thesis, İzmir Institute of Technology, Turkey, 2010

[46] T. Subbiah, G. S. Bhat, R. W. Tock, S. Parameswaran, S. S. Ramkumar, J. Appl. Polym. Sci., 2005, 96, 557.

[47] J. L. Pariente, B. S. Kim, A. Atala, J. Biomed. Mater. Res., 2001, 55, 33.

[48] E. D. Boland, T. A. Telemeco, D. G. Simpson, G. E. Wnek, G. L. Bowlin, J. Biomed. Mater. Res. Part B, 2004, 71, 144.

[49] J. A. Matthews, G. E. Wnek, D. G. Simpson, G. L. Bowlin, Biomacromolecules, 2002, 3, 232.

[50] C. H. Lee, H. J. Shin, I. H. Cho, Y. M. Kang, I. A. Kim, K. D. Park, J. W. Shin, Biomaterials, 2005, 26, 1261.

[51] K. J. Shields, M. J. Beckman, G. L. Bowlin, J. S. Wayne, Tissue Eng., 2004, 10, 1510.

[52] W. J. Li, C. T. Laurencin, E. J. Caterson, R. S. Tuan, F. K. Ko, J. Biomed. Mater. Res., 2002, 60, 613.

[53] K. S. Soppimath, T. M. Aminabhavi, A. R. Kulkarni, W. E. Rudzinski, J. Controlled Release 2001, 70, 1.

[54] E. D. Boland, G. E. Wnek, D.G. Simpson, K. J. Pawlowski, G. L. Bowlin, J Macromol Sci: Pure Appl Chem., 2001, a38, 1231.

[55] E. R. Kenawy, G. L. Bowlin, K. Mansfield, J. Layman, D. G. Simpson, E. H. Sanders, G. E. Wnek, J of Controlled Release, 2002, 81, 57.

[56] B. S. Kim, D. J. Mooney, Trends Biotechnol., 1998, 16, 224.

[57] L. S. Nair, S. Bhattacharyya, C. T. Laurencin, Expert Opin. Biol. Ther., 2004, 4, 659.

[58] M.S. Khil, S. R. Bhattarai, H.Y. Kim, S.Z. Kim, K.H. Lee, J. Biomed. Mater. Res. Part B, 2004, 72, 117.

[59] A. G. Kanani, S. H. Bahrami, Trends Biomater. Artif. Organs, 2010, 24, 93.

[60] http://ilo.technologypublisher.com/technology/5095

[61] R. A. Coffee, PCT/GB97/01968, 1998.

[62] M.S. Khil, D.I. Cha, H.Y. Kim, I.S. Kim, N. Bhattarai, J. Biomed. Mater. Res. Part B, 2003, 67, 675.
[63] P. Rujitanaroj, N. Pimpha, P. Supaphol, Polymer, 2008, 49, 4723.
[64] K. S. Rho, L. Jeong, G. Lee, B. M. Seo, Y. J. Park, S. D. Hong, S. Roh, J. J. Cho, W. H. Park, B. M. Min, Biomaterials, 2006, 27, 1452.
[65] Fiber Reinforcements for Composite Materials (Ed.: A. R. Bunsell), Elsevier, Amsterdam, 1988.
[66] Structure and Properties of Composites: Material Science and Technology, 13 (Eds.: T.W. Chou, R.W. Cahn, P. Haasen, E. J. Kramer), VCH, Weinheim, 1993.
[67] L. R. Xu, L. Li, C. M. Lukehart, H. C. Kuai, Journal of Nanoscience and Nanotechnology, 2007, 7, 1.
[68] D. D. L. Chung, Carbon, 2001, 39, 1119.
[69] F. H. Hsieh, Master thesis, Ohio University, 2006.
[70] H. Ruckdäschel, J. K. W. Sandler, V. Altstädt, Tribology and Interface Engineering Series, Tribology of Polymeric Nanocomposites, 2008, 55, 2008, 149.
[71] H. Ma, J. Zeng, M. L. Realff, S. Kumar, D. A. Schiraldi, Composites Science and Technology, 2003, 63, 1617.
[72] K. J. Pawlowski, T. L. St.Clair, A. C. McReynolds, C. Park, Z. Ounaies, E. J. Siochi, J. S. Harrison, http://ntrs.nasa.gov/archive/nasa/casi.ntrs.nasa.gov/ 20040085790_2004090117.pdf
[73] H. Wu, L. B. Hu, M. W. Rowell, D. S. Kong, J. J. Cha, J. R. McDonough, J. Zhu, Y. Yang, M. D. McGehee,Y. Cui, Nano Lett., 2010, 10, 4242.
[74] L. G. Wade, http://www.britannica.com/EBchecked/topic/190485/epoxide
[75] http://en.wikipedia.org/wiki/Epoxide
[76] S. Rebsdat, D. Mayer, "Ethylene Oxide" in Ullmann's Encyclopedia of Industrial Chemistry, Wiley-VCH, Weinheim, 2005
[77] http://en.wikipedia.org/wiki/Amine
[78] J. E. McMurry, Organic Chemistry, 3rd Ed., Belmont: Wadsworth, 1992.
[79] http://hyperphysics.phy-astr.gsu.edu/hbase/organic/amine.html
[80] http://www2.chemistry.msu.edu/faculty/reusch/VirtTxtJml/amine1.htm
[81] P. L. Teh, M. Mariatti, A. N. R. Wagiman, K. S. Beh, Polym. Comp., 2008, DOI 10.1002/pc.20345.
[82] http://users.ox.ac.uk/~mwalter/web_05/year1/organonitrogen/amines.shtml
[83] R. S. Mahendran, Ph.D dissertation, The University of Birmingham, 2010.

[84] R. M. Luck, R. K. Sadhir, Eds. Expanding Monomers: Synthesis, Characterization and applications, Florida, CRC Press Inc., Florida, 1992.
[85] B. A. Rozenberg, Kinetics, Advances in Polymer Science, 1985, 75, 113.
[86] I. T. Smith, Polymer, 1961, 2, 95.
[87] J. D. R. Talbot, J. Polym. Sci. Part A, 2004, 42, 3579.
[88] E. Girard-Reydet, C. C. Richardi, H. Sautereau, J. P. Pascault, Macromolecules, 1995, 28, 7599.
[89] H.G. Hicke, I. Lehmann, Journal of Membrane Science, 2002, 198, 187.
[90] F. Cozzi. Adv.Synth.Catal., 2006, 348, 1367.
[91] E. Drioli, E. Fontananova, Membrane Reactors, Ullmann's Encyclopedia of Industrial Chemistry, Wiley-VCH Verlag GmbH, 2010.
[92] J. Hagen, Industrial Catalysis: A Practical Approach, Wiley-VCH Verlag GmbH, 1999.
[93] B.C. J. Gates, Catalytic Chemistry, Wiley, New York, 1992.
[94] J. Polaina, A. P. MacCabe (Ed), Industrial Enzymes: Structure, Function and Applications, Springer Verlag, 2007.
[95] Enzymes - a primer on use and benefits today and tomorrow, Enzyme Technical Association, Washington DC, 2001, http://www.enzymetechnicalassoc.org/ benefits_paper.pdf
[96] A. L. Smith (Ed), Oxford dictionary of biochemistry and molecular biology, Oxford University Press, Oxford, 1997.
[97] S. M. Silva, Ph.D dissertation, University of Minho, Guimarães, 2005.
[98] M. Leisola, J. Jokela, O. Pastinen, O. Turunen, H. Schoemaker, http://www.tkk.fi/Units/BioprocessEngineering/Kem-70.415/ INDUSTRIAL_USE_OF_ENZYMES.DOC
[99] T. H. Dai, N. Miletić, K. Loos, M. Elbahri, V. Abetz, Macromolecular Chemistry and Physics, 2011, 212, 319.
[100] T. Sato, T. Tosa, Enzymes, Immobilization Methods, Encyclopedia of Bioprocess Technology, John Wiley & Sons, Inc., 2003.
[101] C. Mateo, J. M. Palomo, G. Fernandez-Lorente, J. M. Guisan, R. Fernandez-Lafuente, Enzyme and Microbial Technology, 2007, 40, 1451.
[102] Y. Dror, J. Kuhn, R. Avrahami, E. Zussman, Macromolecules, 2008, 41, 4187.
[103] P. Ye, Z. K. Xu, J. W, C. Innocent, P. Seta, Biomaterials, 2006, 27, 4169.

[104] Z. G. Wang, L. S. Wan, Z. M. Liu, X. J. Huang, Z. K. Xu, Journal of Molecular Catalysis B: Enzymatic, 2009, 56, 189.
[105] K. Yoon, K. Kim, X. F. Wang, D. F. Fang, B. S. Hsiao, B. Chu, Polymer, 2006, 47, 2434.
[106] S. S. Ericksen, G. D. Szklarz, J. Biomol. Struct. Dyn., 2005, 23, 243.
[107] K. S. Ju, R. E. Parales, Appl. Environ. Microbiol., 2006, 72, 1817.
[108] H. F. Jia, G. Y. Zhu, B. Vugrinovich, W. Kataphinan, D. H. Reneker, P. Wang, Biotechnol. Prog., 2002, 18, 1027.
[109] B. C. Kim, S. Nair, J. Kim, J. H. Kwak, J. W. Grate, S. H. Kim, M. B. Gu, Nanotechnology, 2005, 16, 382.
[110] T. G. Kim, T. G. Park, Biotechnol. Prog., 2006, 22, 1108.
[111] http://en.wikipedia.org/wiki/Filtration
[112] Organic chemistry undergraduate courses, Chemistry and Biochemistry Department, University of Colorado, Boulder, http://orgchem.colorado.edu/hndbksupport/filt/filtration.html
[113]http://www.nesc.wvu.edu/pdf/dw/publications/ontap/2009_tb/filtration_DWFSOM51.pdf
[114] R. C. Brown, Air Filtration, Pergamon Press, Oxford, 1993.
[115] http://en.wikipedia.org/wiki/Permeation
[116] http://www.thefreedictionary.com/permeability
[117] http://www.thefreedictionary.com/feed
[118] http://en.wikipedia.org/wiki/Flux
[119] http://en.wikipedia.org/wiki/Pressure_drop
[120] http://www.answers.com/topic/pressure-drop-fluid-mechanics
[121] http://www.porex.com/by_function/by_function_filtration/filt_eff.cfm
[122] W. Liu, Ph.D Dissertation, University of Akron, Akron, OH, 2003.
[123] http://en.wikipedia.org/wiki/Ultrafiltration
[124] L. J. Zeman, A. L. Zydney, Microfiltration and Ultrafiltration: Principles and Applications, Marcel Dekker, Inc., New York, 1996.
[125] Membrane Processing, http://www.foodsci.uoguelph.ca/dairyedu/membrane.html
[126] http://www.pall.com/Aerospace_3185.asp
[127] http://en.wikipedia.org/wiki/Nanofiltration
[128] http://www.eurodia.com/html/nab.html

[129] K. Sutherland, What is nanofiltration?, Filtration + Separation, March 2009.
[130] Nanofiltration – Filtration overview, http://www.kochmembrane.com/sep_nf.html
[131] S. Srivastava, P. Goyal, Novel Biomaterials: Decontamination of Toxic Metals from Wastewater, Springer-Verlag, Berlin, Heidelberg, 2010.
[132] R.Gopal, S. Kaur, Z. Ma, C. Chan, S. Ramakrishna, T. Matsuura, Journal of Membrane Science, 2006, 281, 581.
[133] K. M. Yun, C. J. Hogan, Y. Matsubayashi, M. Kawabe, F. Iskandara, K. Okuyama, Chemical Engineering Science, 2007, 62, 4751.
[134] X. H. Qin, S. Y. Wang, Journal of Applied Polymer Science, 2006, 102, 1285.
[135] K.Yoon, B. S. Hsiao, B. Chu, Polymer, 2009, 50, 2893.
[136] A. Srivastava, O. N. Srivastava, S. Talapatra, R. Vajtai, P. M. Ajayan, Nat. Mater., 2004, 3, 610.
[137] S. S. Homaeigohar, K. Buhr, K. Ebert, J. Membr. Sci., 2010, 365, 68.
[138] D. Aussawasathien, C. Teerawattananon, A. Vongachariya, J. Membr. Sci., 2008, 315, 11.
[139] R. Gopal, S. Kaur, C.Y. Feng, C. Chan, S. Ramakrishna, S. Tabe, T. Matsuura, J. Membr. Sci., 2007, 289, 210.
[140] D. S. Wavhal, E. R. Fisher, J. Membr. Sci., 2002, 209, 255.
[141] X. Wang, X. Chen, K. Yoon, D. Fang, B. S. Hsiao, B. Chu, Environ. Sci. Technol., 2005, 39, 7684.
[142] P. Gibson, H. S. Gibson, D. Rivin, Colloids Surf. A: Physicochem. Eng. Aspects, 2001, 187, 469.
[143] C. H. Bamford, K. G. Al-Lamee, M. D. Purbrick, T. J. Wear, Journal of Chromatography, 1992, 606, 19.
[144] Z. W. Ma, M. Kotaki, S. Ramakrishna, Journal of Membrane Science, 2006, 272, 179.
[145] Z. W. Ma, K. Masaya, S. Ramakrishna, Journal of Membrane Science, 2006, 282, 237.
[146] Z. W. Ma, Z. W. Lan, T. Matsuura, S. Ramakrishna, Journal of Chromatography B, 2009, 877, 3686.
[147] Z. W. Ma, M. Kotaki, S. Ramakrishna, Journal of Membrane Science, 2005, 265, 115.

Chapter 3. General overview of characterization techniques and methods

3.1 Gel Permeation Chromatography (GPC)

Gel permeation chromatography (GPC) is a term used when the separation technique size exclusion chromatography (SEC) is particularly applied to polymers. As a technique, SEC was first developed in 1955 by Lathe and Ruthven.[1,3] The original of the term 'GPC' can be traced back to J. C. Moore of the Dow Chemical Company who investigated the technique in 1964.[2,3] It is often used to separate polymers, both for the molecular analysis and for the purification.[3]

When characterizing polymers, it is important to consider the polydispersity index (PDI) and the molecular weight (M_n, M_w, M_η and M_z). GPC allows for the determination of PDI as well as M_n and M_w.[3]

The experimental design of GPC is similar with other techniques of liquid chromatography. Firstly, samples are dissolved in an appropriate solvent (usually organic solvents). Then the sample solution is injected into a column after being filtrated for removing dust particles or microgels. A pump steadily pushes the fresh eluent to the column, in which carries on the separation of multi-component mixture. Usually multiple detectors are used to gain data as well as additional information about the polymer sample.[3-5]

GPC experiments in this thesis were performed on a chromatographic instrument with HPLC-pump 515 (Waters), autosampler 717 (Waters), and vertical heating furnace.

3.2 Attenuated Total Reflectance Fourier Transform Infrared Spectroscopy (ATR- FTIR)

Infrared spectroscopy (IR) is an absorption method used to obtain information of the molecular structure of most molecules in any physical state (solid, liquid, gas). This measurement technique is widely used in chemical, polymer, material research and industry.[6,7]

An infrared spectrum shows transmission or absorptions versus wavelength (cm^{-1}). If energy is absorbed by the molecules of the sample, the intensity of signals at particular frequencies will decrease, resulting in peaks on the spectrum. Samples for IR spectrum should not be thicker than 10 μm in order to get a good transmission and a clear spectrum. For thicker samples, a very popular technique called Attenuated Total Reflection (ATR) is used.[6]

Total internal reflection takes place when an electromagnetic radiation is incident on an IR transparent surface at an angle exceeds the critical angle. During this process part of the radiation also penetrates the sample and then returns in the crystal as if it is reflected within it. If an absorbing sample is placed on the surface of the crystal, the energy will be absorbed by the sample and spectral information of the sample will be read by the reflection beam. The depth of penetration is about several micrometers depending on the incidence angle of the beam and the wavelength of the light. More detailed information can be found in literature.[6,8,9]

In this doctoral thesis, ATR-FTIR is used to monitor the chemical changes taking place during the reactions on nanofibers. All the FTIR measurements were performed

on an FTIR spectrophotometer (Bruker Equinox 55, Bruker Optics) in the mid-infrared range from 4000 to 500 cm^{-1}.

3.3 Ultraviolet-visible Spectroscopy (UV-vis)

Ultraviolet-visible spectroscopy is an absorption technique mainly used for the identification and the quantitative determination of some functional groups in molecules.[10]

The extent of the absorption of molecules can be correlated with their concentration by the Beer-Lambert law:[11]

$$\log_{10} I_0 / I = \varepsilon \, l \, c \qquad (3\text{-}1)$$

where: I_0 = intensity of the incident radiation, I = intensity of the transmitted radiation, ε = molar absorption coefficient, l = path length of the absorbing solution (cm), c = molar concentration of the absorbing species. Therefore the ε can be calculated by knowing concentration of the absorbing species and the maximum wavelength. On the other hand, assaying of the absorbing species can be made if the above parameters are obtained. More information about UV-vis spectroscopy can be found in literature.[12]

A UV-vis spectrophotometry (HITACHI U-3000, HITACHI) was applied for all the UV-vis measurements in this thesis.

3.4 Scanning Electron Microscopy (SEM)

Scanning electron microscope (SEM) is a very important and widely used tool which is capable of producing high resolution images of samples' surface. SEM uses a focused beam of high-energy electrons to generate a variety of signals at the surface

of solid specimens.[14] The signals derived from electron-sample interactions demonstrate information about the sample including surface morphology, chemical composition, and crystalline structure. In most applications, some areas of the surface of the sample are selected as the representative for collecting information and data of the sample. A 2-dimensional image is generated to display these informations. SEM is also capable of making analyses of selected locations on the sample.[13,14]

SEM could be divided into two major types based on the different type of electron gun: conventional SEM (using thermionical electron gun) and Field Emission Scanning Electron Microscope (FE-SEM). FE-SEM works with electrons instead of light. In a typical FE-SEM, electrons are liberated from a field emission source and accelerated by a high electrical field. Firstly, primary electrons are focused and deflected by electronic lenses in the high vacuum column and then a narrow beam is produced and this beam bombards the object. Consequently, secondary electrons are emitted from each spot on the object and then catched by a detector. Finally, an electronic signal is produced by the detector and then amplified and transformed to a digital image file which is visable and processable further.[15,16]

Field Emission scanning electron microscope (LEO Gemini 1550 VP, Zeiss) was used in this work. The SEM images in this thesis were taken using an accelerating voltage at 10 kV after sputter-coating with Au/Pd. The average diameters of the nanofibers were calculated from 10 different randomly chosen single values. Details about the construction and working principle of the SEM are available elsewhere.[17]

3.5 Transmission Electron Microscopy (TEM)

In transmission electron microscope (TEM), a highly energetic beam of electrons is generated and then penetrates through the specimen for the detecting of the sample's inner structure. These electrons are scattered with different angles by the sample depending on the density of atoms encountered with the beam.[18] The transmitted electron signal is amplified by a series of electromagnetic lenses and forms a image, which is finally focused and captured by a CCD camera. These obtained electron diffraction patterns are used to determine the microstructures of the sample, e.g. the grain size, lattice, the crystalline structure, etc.[19,20]

A 200 keV TEM (Tecnai G2 F20, Fei) was used in this work to evaluate the dimensions of the electrospun fibers. Other details about TEM can be found elsewhere.[21]

3.6 Bubble Point Test

In this thesis, the inter-fiber pore size of the nanomats was determined with the liquid-gas displacement method, which measures the requisite pressure for blowing gas through a liquid-filled pore in a membrane. The relationship between the pore size and the corresponding pressure is given by the Young-Laplace equation:

$$R = 2 \gamma \cos \theta / \Delta P \qquad (3\text{-}2)$$

where R is the radius of the pore (m), ΔP is the differential gas pressure, γ is the surface tension of wetting liquid (J/m), and θ is the contact angle.[22]

The measurements were performed with a Porometer 4.900 from Porous Materials Inc. (PMI). The PANGMA-ENM stamps with a diameter of 3 cm were immersed in the

wetting fluid Porewick® from PMI (surface tension = 16×10^{-7} J/m= 16 dyn/cm) for more than 15 min and then placed into the test cell. By an automated procedure a successively increasing pressure was applied across the membrane sample using nitrogen as pressurizing gas. At a certain pressure the surface tension of the pore filling liquid in the largest pores is exceeded. The liquid is displaced and the gas flow through the open pore is monitored. By further pressure increase the liquid in the smaller pores is displaced until all pores are open. Based on the flux data through the membrane the pore size distribution is calculated by the internal PMI software.[23,24]

3.7 Water Contact Angle Measurement

The commonest and simplest method for measuring water contact angle is the sessile drop method. Sessile drop method is measured with a contact angle goniometer by capturing the profile of liquids on a solid substrate. Current systems capture and analyze the contact angle by using high resolution cameras and software.[25,26] The droplet of liquid is deposited by a syringe which is perpendicular to the surface of the sample. Meanwhile, a high resolution camera is in charge of capturing the image. The image is displayed on the monitor and analyzed by image analysis software.[26,27]

The water wettability of the nanofibers and ENMs was measured by a contact angle meter (Krüss DSA100E) with the image processing system from Data Physics Instruments. The liquid used for the measurement was H_2O (HPLC grade) and the measurement was performed at room temperature. Ten measurements were carried out for each sample for the calculation of final average values.

3.8 Tensile Strength Test

The commonest testing machine used in tensile strength test is the universal testing machine. This type of machine has two crossheads: one is adjustable for the fixing of different shape of specimen and the other is movable to apply and control the tension added on the test specimen. There are two types: hydraulic powered and electromagnetically powered machines.[28,29]

In this thesis, the tensile strength tests were performed on a Zwick-Roell universal testing machine with a 0.02 N load cell. The tensile strength, stiffness and elongation of the samples were recorded automatically by the machine and the average data of them were calculated from at least ten independent specimens.

3.9 Differential Scanning Calorimetry (DSC)

Differential scanning calorimetry is a technique used to study the thermal transitions of a polymer. Most DSC machines have two pans and a platform connected to a heating source. One pan holds the sample to be measured while the other pan is left empty as a reference. A computer controls the heating source to heat the two pans at a totally equal rate. In most experiments, 10 ℃ per minute is used as the most general heating rate. The computer precisely controls that the heating rate remains exactly the same for the whole duration of the experiment and also ensures that the sample pan and the reference pan are heated with the exactly same heating rate. Since one of the pans has samples in it, it needs more heat to keep the temperature of the pan increasing at the same rate as the reference pan. The difference of the heat consuming is measured and recorded by the form of electric currents. These currents are

calibrated against materials with known phase transition enthalpies like indium or chloroform.[30,31]

The resultant curves on DSC graph can offer lots of very important information such as T_g, T_m, and T_c. The T_g of a sample can be observed if there is a change in slope in the endothermic direction. This shows that heat is being absorbed by the sample. The T_m of a non amorphous sample can be observed by a peak in the endothermic direction. The T_c of a sample can be seen with a sharp peak in the exothermic direction. This peak is useful because it reflects the capability of a polymer to form crystals, while an amorphous sample cannot have a crystallization peak. This information is very useful and important for indicating structural and phase changes of samples. In addition, the enthalpy of melting can be obtained by calculating the area under the melting curve on the DSC graph.[32,33]

DSC was performed with Netzsch DSC 204 Phoenix® using indium standards. The glass transition temperature (T_g) was determined by means of a dynamic scan at 10 ℃/min from 20 to 300 ℃.

3.10 Thermogravimetric Analysis (TGA)

Thermogravimetric analysis (TGA) is one of important technique in many thermal analysis techniques. TGA measurements provide important information for selecting materials for certain end-use applications, for predicting product performance and for improving product quality.[34] TGA also provides complimentary and supplementary heat information of materials for DSC. It can be specially applied in the study of

polymeric materials, including thermoplastics and thermosets, elastomers, polymer membranes, synthestic fibers, coatings, polymer composites, etc.[34-36]

TGA measurements in this thesis were performed on a thermogravimetric analyzer of Netzsch 209 TG with a heating rate of 10 ℃/min and a temperature range of 20 to 700 ℃ in argon atmosphere.

3.11 Bradford Protein Assay

The Bradford protein assay is a spectroscopic analytical method used to measure the concentration of protein in a solution. It is based on an absorbance shift of the dye Coomassie Brilliant Blue G-250 from 465 nm to 595 nm caused by its binding to protein.[37] Coomassie Brilliant Blue G-250 exists in two different color forms, red (under acidic conditions) and blue. The red form is converted to the blue form once the dye binds with the protein and subsequently forms a protein-dye complex which will stabilize the blue form of the Coomassie dye. The amount of the protein-dye complex in solution is in proportion to the protein concentration and therefore can be a measure for the calculation of the protein amount. This protein-dye complex has a high extinction coefficient thus can be measured by UV-vis spectrum. The bound form of the dye has a maximum absorption at 595 nm on spectrum.[37,38]

The increase of absorbance at 595 nm is proportional to the amount of bound dye, and of course also proportional to the amount of protein in the sample.[37] The protein amount can be calculated by reading the absorbance at 595 nm on the UV-vis spectrum. The protein assay is a very rapid process and is very convenient to process large numbers of samples.[37-39]

In this thesis, the amount of residual protein was determined by Bradford's method. Bovine serum albumin (BSA) was used as the standard to construct the calibration curve. Each reported value was the average of at least three experimental values.

3.12 References

[1] G. H. Lathe, C. R. J. Ruthven, Biochem J., 1956, 62, 665.

[2] J. C. Moore, J. Polym. Sci., 1964, 2, 835.

[3] http://en.wikipedia.org/wiki/Gel_permeation_chromatography

[4] D. Helmut, Gel Chromatography, Gel Filtration, Gel Permeation, Molecular Sieves: A Laboratory Handbook, Springer Verlag, 1969.

[5] B. Trathnigg, Prog. Polym. Sci., 1995, 20, 615.

[6] http://www.research.philips.com/technologies/matanalysis/downloads/16-ir-tn.pdf

[7] N. J. Harrick (ed.), Internal Reflection Spectroscopy, New York: John Wiley & Sons, Inc., 1967.

[8] L.M. Harwood, C. J. Moody, Experimental organic chemistry: Principles and Practice (Illustrated ed.), Wiley-Blackwell, 1989.

[9] W.S. Lau, Infrared characterization for microelectronics, World Scientific, 1999

[10] UV-vis spectroscopy – theoretical principles, http://teaching.shu.ac.uk/hwb/chemistry/tutorials/molspec/uvvisab1.htm

[11] http://en.wikipedia.org/wiki/Beer%E2%80%93Lambert_law

[12] M. Prabhakar, M. A. Dubinskii, In Ultraviolet Spectroscopy and UV Lasers, Marcel Dekker, 2002.

[13] http://en.wikipedia.org/wiki/Scanning_electron_microscope

[14] S. Swapp, http://serc.carleton.edu/research_education/geochemsheets/techniques/SEM.html

[15] http://www.vcbio.science.ru.nl/public/pdf/fesem_info_eng.pdf

[16] S. L. Flegler, K. L. Klomparens, J. W. Heckman, Scanning and Transmission Electron Microscopy, Oxford University Press, UK, 1993.

[17] J. I. Goldstein, D. E. N. bury, P. Echlin, D. C. Joy, C. Fiori, E. Lifshin, Scanning Electron Microscopy and X-ray Microanalysis, Plenum Press, New York, 1981.

[18] http://www.sv.vt.edu/classes/MSE2094_NoteBook/96ClassProj/experimental/electron.html
[19] http://en.wikipedia.org/wiki/Transmission_electron_microscopy
[20] A. Khan, Vol. Ph. D, Ohio University, Athens OH, 2006,135.
[21] D. B. Williams, C. B. Carter, Transmission Electron Microscopy, Plenum Press, New York, 1996.
[22] A. Hernfindez, J. I. Calvo, P. Prfidanos, F. Tejerina, Journal of Membrane Science, 1996, 112, 1.
[23] K. Ebert, D. Fritsch, J. Koll, C. Tjahjawiguna, J. Mem. Sci., 2004, 233, 71.
[24] D. P. Li, M. W. Frey, Y. L. Joo, Journal of Membrane Science, 2006, 286, 104.
[25] http://en.wikipedia.org/wiki/Contact_angle
[26] http://en.wikipedia.org/wiki/Sessile_drop_technique
[27] http://membranes.edu.au/wiki/index.php/Goniometer_Method
[28] http://en.wikipedia.org/wiki/Tensile_testing#cite_ref-davis2_3-3
[29] C. Horst, Springer Handbook of Materials Measurement Methods, Berlin: Springer, 2006.
[30] R. Damnjanovic, Master thesis, Universtity of South Florida, 2005
[31] B. Wunderlich, Thermal Analysis, New York: Academic Press, 1990.
[32] J. A. Dean, The Analytical Chemistry Handbook, New York: McGraw Hill, 1995.
[33] D. A. Skoog, F. J. Holler, T. Nieman, Principles of Instrumental Analysis, 5th ed., New York, 1998.
[34] W. J. Sichina, http://depts.washington.edu/mseuser/Equipment/RefNotes/TGA_Notes.pdf
[35] H. Qin, Q. S. Su, S. M. Zhang, B. Zhao, M. S.Yang, Polymer, 2003, 44, 7533.
[36] E. Mansfield, A. Kar, T. P. Quinn, S. A. Hooker, Analytical Chemistry, 2010. doi:10.1021/ac102030z
[37] http://en.wikipedia.org/wiki/Bradford_protein_assay
[38] M. M. Bradford, Anal. Biochem., 1976, 72, 248.
[39] T. Zor, Z. Selinger, Anal. Biochem., 1996, 236, 302.

Chapter 4. Electrospinning of poly(acrylonitrile-*co*-glycidyl methacrylate) (PANGMA) nanofibers

4.1 Brief introduction

Electrospinning is the most convenient and versatile method for generating nanoscaled fibrous materials among a number of fabricating method.[2] Electrospinning has been investigated for preparing long nanofibers for many kinds of polymers, ceramics and metal oxides. Enormous efforts have been made to improve the methods and devices of electrospinning, so this fabrication technique has gradually become mature and sophisticated. Electrospinning also broadens its applications into more and more different areas.[1-6]

This chapter focuses on the electrospinning process. First, the basic properties of PANGMA - the raw polymer for the electrospun nanofibers were introduced and characterized. Then the fabricating procedures of PANGMA nanofibers and electrospun nanofibrous mats (ENMs) will be particularly depicted. The effect of electrospinning conditions on the parameters of the PANGMA nanofibers and ENMs will be investigated and studied in detail. The discussion is divided into four parts concerning on four important parameters of nanofibers and ENMs: fiber diameter, fiber morphology, thickness of ENM and pore size of ENM. For each parameter, the influence of the spinning conditions, including: solution concentration, solution viscosity, applied voltage, spinning distance and feed rate on the parameter will be particularly studied and discussed. The influence of additives, such as citric acid and triethylbenzylammonium chloride (TEBAC) on the diameter of the PANGMA nanofibers is also investigated. Optimal electrospinning conditions are summarized,

and by controlling them we can obtain the ideal morphology and structure of the PANGMA nanofibers and ENMs.

4.2 Experimental

4.2.1 Materials

PANGMA was synthesized at Helmholtz-Zentrum Geesthacht with a molecular weight (M_n) of ca.100,000 g/mol and GMA content of 10 mol %.[7] Citric acid and triethylbenzylammonium chloride (TEBAC) were purchased from Sigma-Aldrich & Co. N'N-dimethylformamide (DMF) was purchased from Merck KGaA. All the chemicals were directly used without further purification.

4.2.2 Electrospinning

PANGMA was dissolved in DMF with moderately stirring for 48 h to obtain a homogeneous and transparent PANGMA/DMF solution. The solution concentration was in the range from 16 wt% to 24 wt%. The solution was then transferred into a 5 mL glass syringe with steel needle which had an inner diameter of 0.8 mm. 15 to 30 kV high positive voltages were applied to the solution via the needle. A rectangular counter electrode covered with the aluminum foil was used as the collector. Feed rate of the range from 0.5 to 2.5 mL/h was given by a syringe pump (HARVARD PHD 4400, Harvard Apparatus.Co) and a spinning distance (the distance between the tip of needle and aluminum foil) was varied from 15 to 25 cm. The electrospinning time was usually from 2 h to 8 h to obtain sufficient thickness of the ENM. Different additives, including citric acid and triethylbenzylammonium chloride (TEBAC) were added to the spinning solution in order to study their influence on the diameter of the nanofiber.

After electrospinning, the ENM was detached and then dried under vacuum at 30 ℃ for 24 h to remove all the liquids.[5,6]

4.2.3 Measurements and characterizations

The molecular weight of the synthesized PANGMA was determined by gel permeation chromatography (GPC) on a HPLC-pump 515 (Waters), autosampler 717 (Waters) plus a vertical heating furnace with DMF as the solvent.

The structure of the PANGMA was detected by Attenuated Total Reflection Fourier transform infrared spectroscopy (ATR-FTIR) with a FTIR spectrophotometer (Bruker Equinox 55, Bruker Optics) in the mid-infrared range from 4000 to 500 cm^{-1}.

The viscosity of PANGMA/DMF solution was measured by a rheometer (Brookfield R/S Plus, Brookfield Viscometers).

The conductivity of PANGMA/DMF solution was measured by a HZG conductivity cell connected to commercial conductivity meter (WTW, LF 530).

The morphology of PANGMA electrospun nanofibers and ENMs was observed with a scanning electron microscope (LEO Gemini 1550 VP, Zeiss) at 10 kV accelerating voltage after sputter-coating with gold/palladium. The average diameters of the nanofibers were calculated from 10 different single values randomly by the internal software of the SEM.

The inter-fiber pore size of the PANGMA-ENM was determined with the bubble point method which was performed with a Porometer 4.900 from Porous Materials Inc. (PMI). The PANGMA-ENM stamps with a diameter of 3 cm were immersed in the wetting fluid Porewick® from PMI (surface tension = 16×10^{-7} J/m= 16 dyn/cm) for more than 15 min and then placed in the test cell. Based on the flux data through the membrane the pore size distribution is calculated by the internal PMI software.[8]

4.3 Results and discussion

4.3.1 Molecular weight and chemical structure of PANGMA

GPC and ATR-FTIR were used to characterize the basic properties such as molecular weight and chemical structure of PANGMA nanofibers. Figure 4.1 shows the GPC trace of the PANGMA sample. The detected number average molecular weight (M_n) of PANGMA is 98,053 g/mol and the GPC curve also indicates a bimodal distribution of molecular weight.

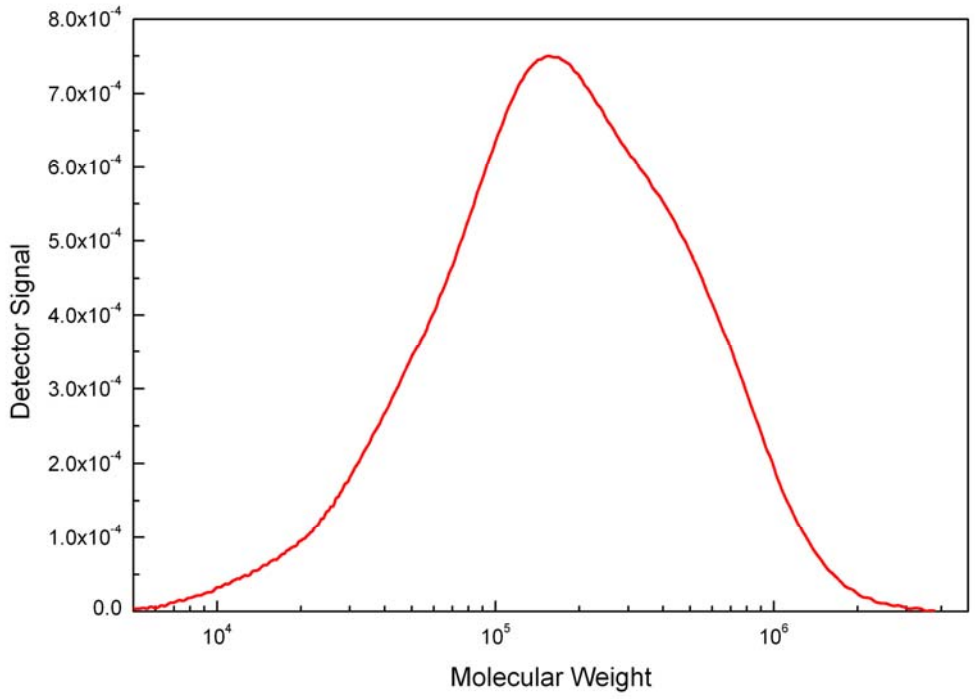

Figure 4.1 Molecular weight distribution of PANGMA

ATR-FTIR measurement was performed to investigate the chemical structure of neat PANGMA nanofibers. Figure 4.2 shows the FTIR spectrum of the copolymer which is built from acrylonitrile (AN) and glycidyl methacrylate (GMA). The peak at 2240 cm^{-1} of nitrile group, at 1453 cm^{-1} corresponding to CH bending and at 2930 cm^{-1} representing the $-CH_3$ symmetric stretching all reveal the existing of acrylonitrile backbone in PANGMA molecules.[9-11] Meanwhile, a strong peak at 1729 cm^{-1} is the ester vibration of carbonyl groups in the GMA part. The oscillations of the C-O bond in GMA structure are observed at the wavenumbers bands at 1210, 840 and 890 cm^{-1}. Particularly, an obvious peak near 908 cm^{-1} demonstrates the existence of the epoxide group in PANGMA nanofibers.[12-14]

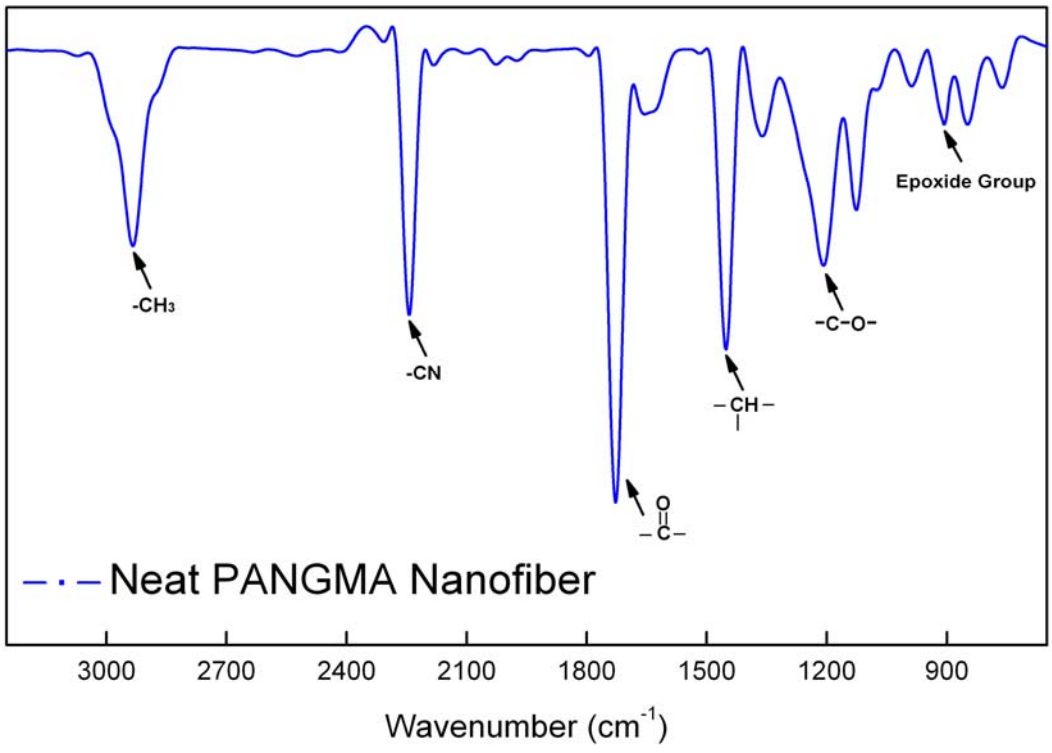

Figure 4.2 FTIR spectrum of neat PANGMA nanofibers

4.3.2 Diameter of PANGMA nanofiber

It has been observed and confirmed by lots of previous research work that the diameter of the electrospun nanofibers can be affected by several electrospinning

variables such as solution concentration, solution viscosity, solution conductivity, applied voltage, feed rate and spinning distance.[15-19] Therefore these spinning parameters were studied and discussed in order to verify that the existing theories also work in PANGMA/DMF system, and also discover some new and unique phenomenons and rules in the new system. Best spinning conditions for fabricating PANGMA nanofibers with optimum diameters were also disclosed in the end.

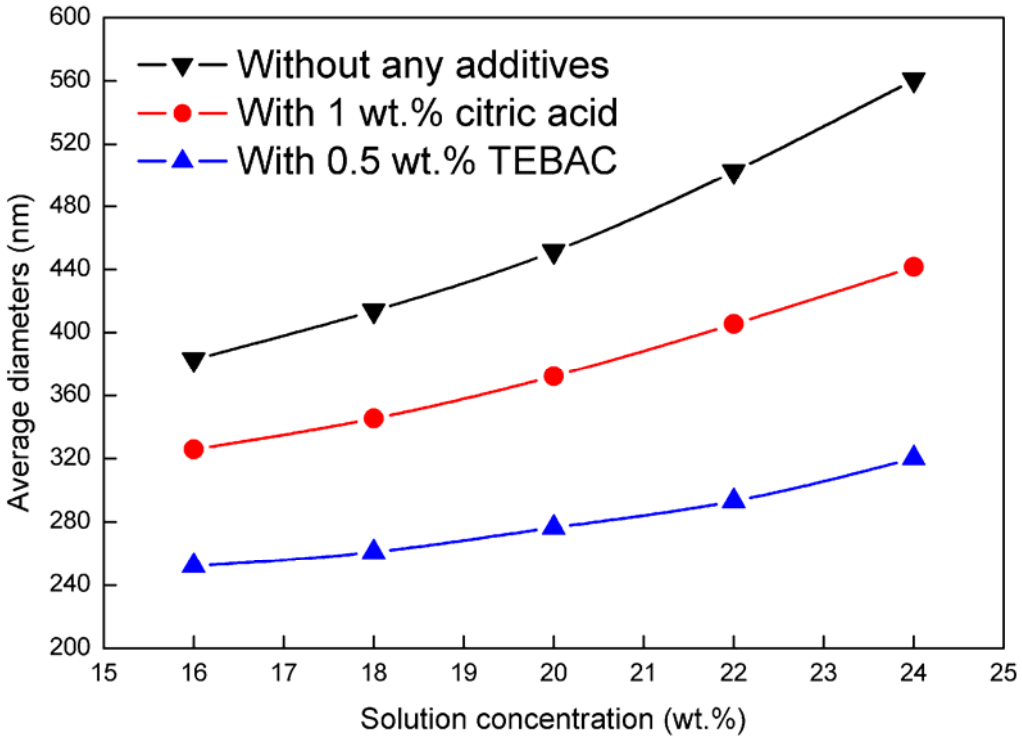

Figure 4.3 Average diameter of PANGMA nanofibers prepared with different solution concentration and additives

At first the effect of solution concentration on the diameter of PANGMA nanofibers was investigated and studied. Five series of polymer solutions with different concentration (16, 18, 20, 22 and 24 wt%) of PANGMA dissolved in DMF were prepared for electrospinning. Electrospinning results (Fig. 4.3 and Fig. 4.4) show that the diameter of the electrospun fibers increases with the increase of polymer

concentration in solution. Apparently, the average fiber diameter was found to increase monotonically from ca. 380 nm at 16 wt% to ca. 560 nm at 24 wt%. (Fig. 4.3) A minimum polymer concentration to electrospin a uniform fibers was found to be 16 wt% and beaded fibers were formed if the solution concentration was below this value (Fig. 4.4(a)). Despite some non-uniformity of fiber size and roughness of fiber surface morphology were observed, ultrafine PANGMA fibers were successfully fabricated by electrospinning.

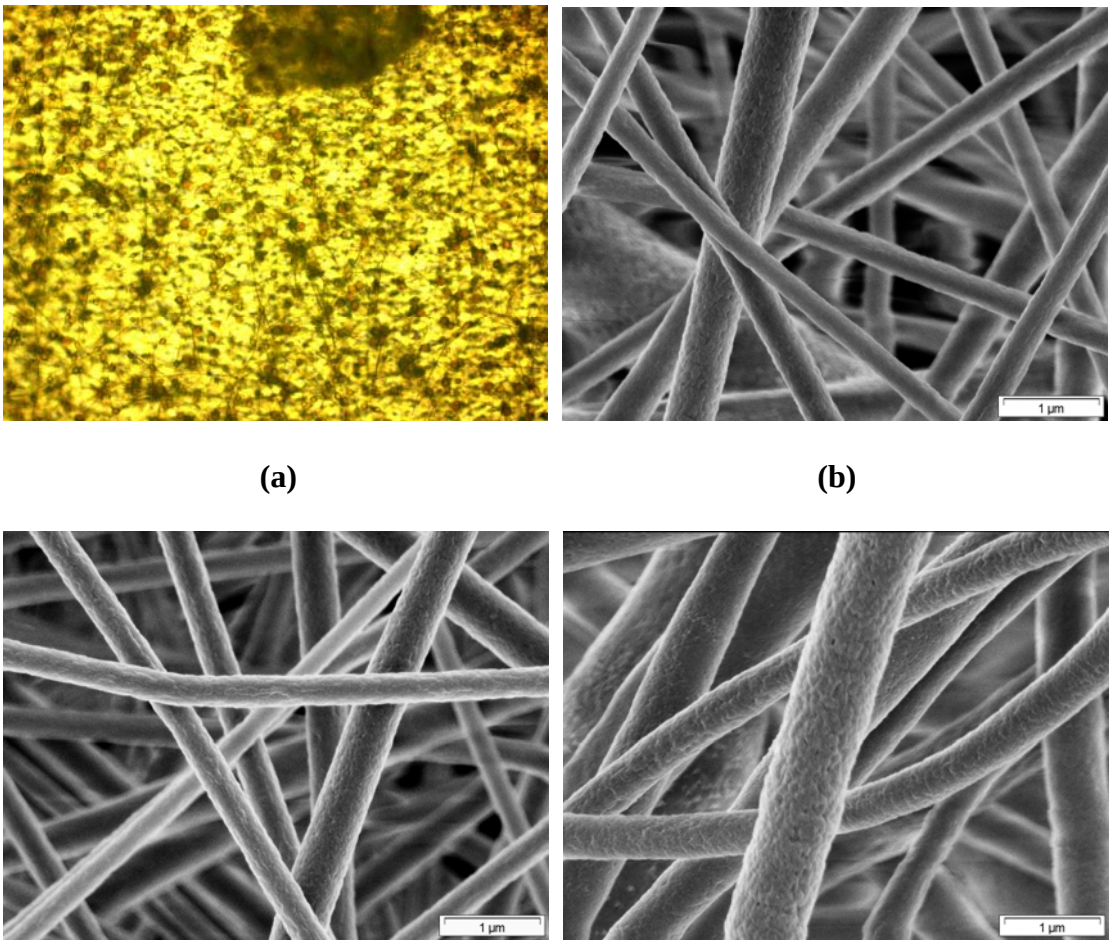

(a) **(b)**

(c) **(d)**

Figure 4.4 Optical micrograph and SEM micrographs of PANGMA nanofibers electrospun from spinning solution with different concentration: (a) 14%, (b) 16%, (c) 20%, and (d) 24%

Mit-uppatham et al.[21] gave the explanations of the influence of solution concentration on the electrospun fiber diameter: first, the increased concentration makes the jet stand against the strong stretching force which is from the Coulomb repulsion, resulting in the consequential larger diameter of the jet and the electrospun fibers. In addition, the larger diameter will hamper the extent of the bending instability which is crucial to the total moving distance of the jet segment flying to the collector, leading to the hindrance of the thinning of the jet segment.[20,21]

Besides solution concentration, solution viscosity is also one of the most important parameters to determine the diameter and morphology of electrospun nanofibers.[19] In binary systems which consist of only the polymer and the solvent, viscosity is mainly related to concentration. But sometime the assortment of the solvent may also affect the viscosity because intermolecular interactions in solution also have influence on it. Thin fibers with beads are formed at low viscosities and thicker fibers are generated gradually with the increasing viscosity, while beads decrease because they merge into the thickening fibers, which together lead to thick fibers with smooth morphologies finally.[21-26] Figure 4.5 shows the relationship between the average diameter of PANGMA nanofibers and the solution viscosity. The plotted curve shows a crescent dependency between the fiber diameter and the solution viscosity, which is similar to the exponential curve. This result is totally consistent with most reported results and conclusions.[27,28] An increased viscosity of electrospinning solution will stabilize the jet since the movement of the polymer chains will be restricted by it. Thus a higher viscosity can limit the ability of the jet of stretching and results in the form of thicker fibers.[22,28]

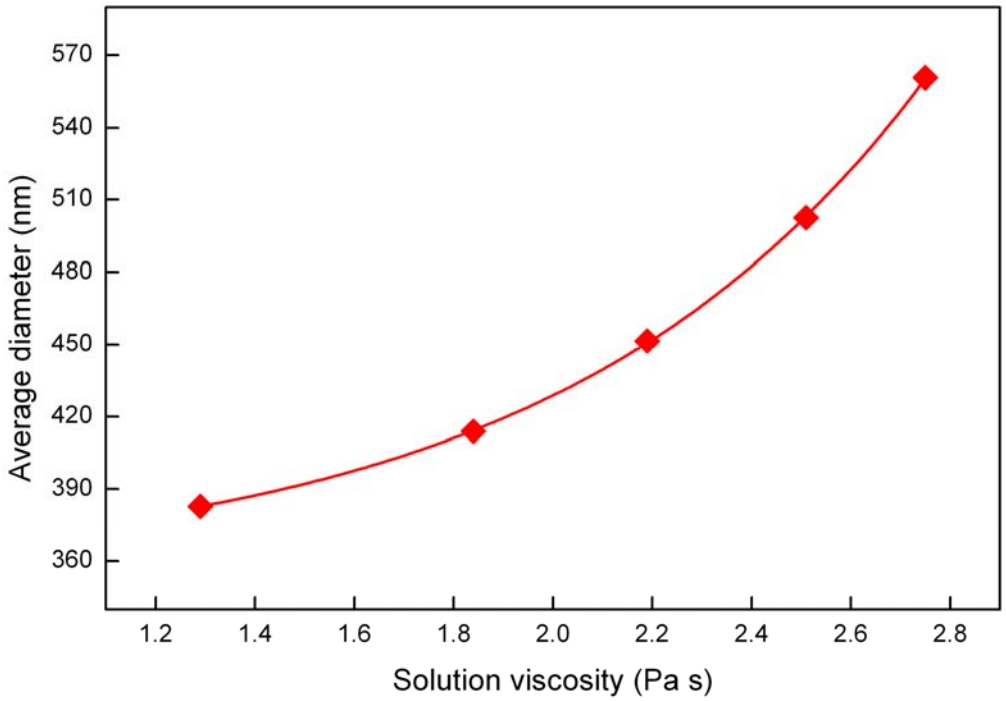

Figure 4.5 Relation between solution viscosity on average diameter of PANGMA nanofibers

It was already reported that the diameter of electrospun fibers can be affected by the applied voltage, but not significantly.[29-31] In this doctoral work, in order to confirm the past researches, four different levels of applied voltage from 15 to 30 kV were applied to study their influence on the diameter of the resulted electrospun fibers. It was observed that the diameter of the electrospun fibers was not dramatically changed with varied applied voltage. The average diameter only has a slight decrease with the increase of applied voltage (Figure 4.6). According to the reported conclusions, higher voltage results in smaller diameter.[32-34] Applied voltage can affect some factors such as elongation level and morphology of the jet.[32] A higher applied voltage introduces a stronger electrical force, which leads to a larger elongation and a stronger bending instability of the spinning jet. These factors all result in thinner eventual fibers. Our results on PANGMA electrospun nanofibers have verified these reported conclusions.

Although some tendencies of decreased diameter of PANGMA nanofibers are shown when higher voltages are applied, the voltage does not play a significant role in controlling the fiber diameters.

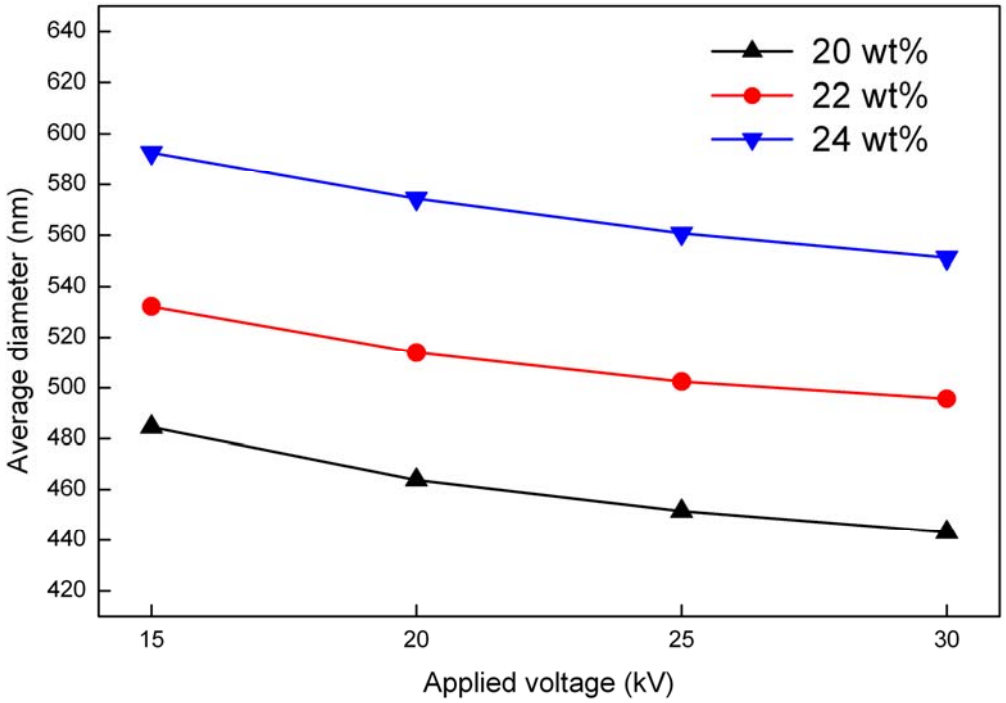

Figure 4.6 Influence of the applied voltage on the average diameter of PANGMA electrospun nanofibers

By adding small amount of organic acid (citric acid) or organic salt (triethylbenzylammonium chloride (TEBAC)) into the spinning solution, the diameters could be further reduced. Figure 4.3 shows the variation of the average diameter of PANGMA nanofibers with and without adding additives in spinning solution. It is clear that the average fiber diameter decreases dramatically from ~500 to ~280 nm after additives are added.

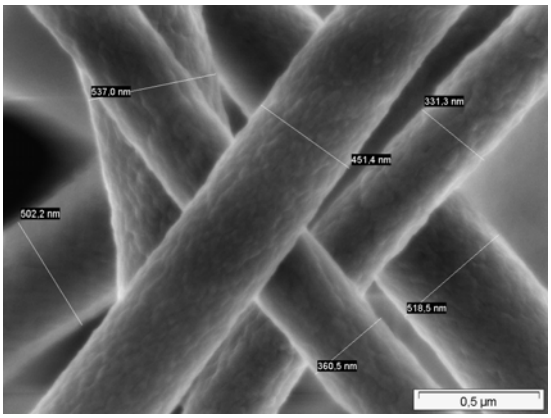

(a)

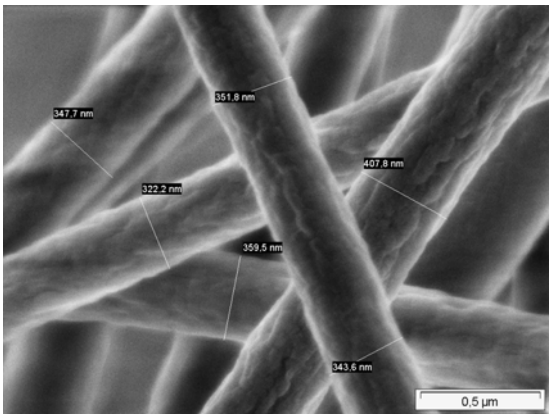

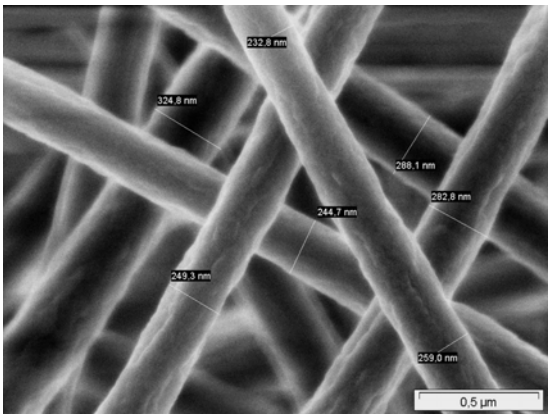

(b) **(c)**

Figure 4.7 SEM micrographs of PANGMA nanofibers electrospun from different solution: (a) without any additives, (b) with 1 wt.% citric acid, (c) with 0.5 wt.% TEBAC, the concentration of spinning solution is 22 wt.%

The SEM photos of the nanofibers electrospun from solution with 1 wt.% citric acid, with 0.5 wt.% TEBAC and without any additives also illustrate the decreasing tendency of the fiber diameter. It is obvious that the fibers electrospun from solutions show thinner diameters (Figure 4.7(b), addition of citric acid, and Figure 4.7(c), addition of TEBAC compared to neat PANGMA fibres (Figure 4.7(a)). Some literatures have reported that additives can have influence on the diameters of nanofibers through the way of altering the conductivity of the spinning solution.[35,36]

Generally, the electrical conductivity of the spinning solution reflects the charge density on a jet. The charge density can determine the elongation level of the jet via influencing the electrical force.[32] Therefore, under the same spinning conditions, a solution with higher electrical conductivity will lead higher elongation of jet, resulting in the reduction of the diameter of the generated electrospun fibers. Experiments were performed to study the relationship between fiber diameters and the conductivity of spinning solution, also to verify the existing theories.

The solution conductivity was measured with a HZG conductivity cell connected to a commercial conductivity meter (WTW, LF 530). The data were summarized in Figure 4.8. The average diameters of the nanofibers were calculated from 10 different single values randomly and listed also in Figure 4.3. It could be seen clearly that the solution conductivity increases dramatically when the additives are added. These results well confirm that higher solution conductivity can result in producing nanofibers with thinner diameter. A small amount of additives can change the solution conductivity strongly and thus reduce the diameter of the nanofibers.

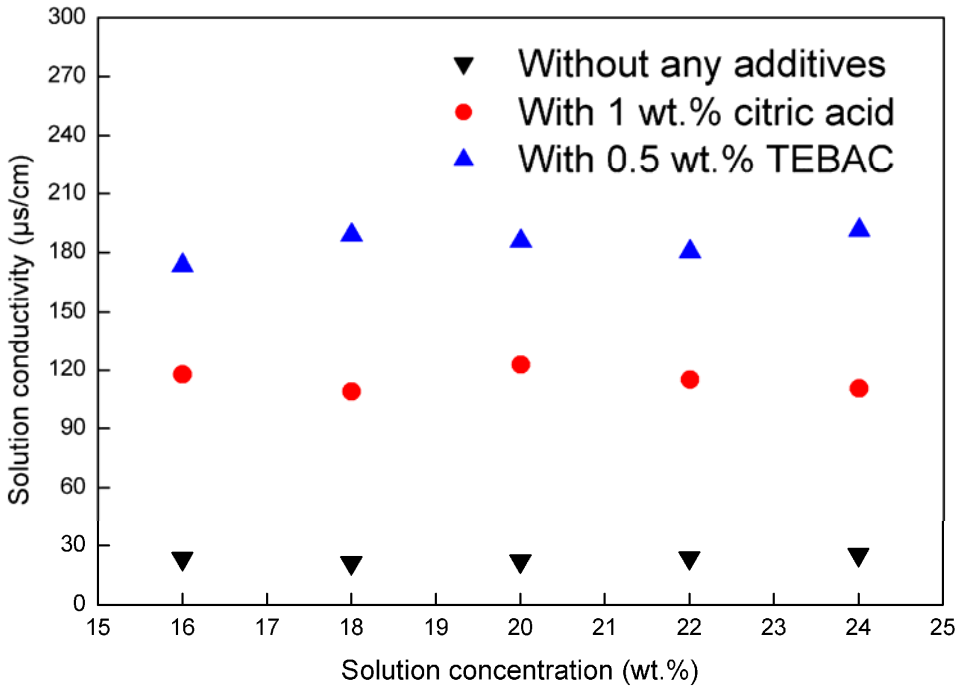

Figure 4.8 Solution conductivity of PANGMA/DMF solution with and without adding additives

The rest of the electrospinning conditions such as: feed rate of the spinning solution, spinning distance, air humidity, ambient temperature…only have very limited influence on the diameter of PANGMA electrospun nanofibers. For instance, it is reported and verified by our experiments that feed rate has almost no influence on the diameter of the produced nanofiber.

4.3.3 Morphology of PANGMA nanofiber

A variety of morphologies and structures of the PANGMA nanofibers and ENMs are shown in Figure 4.9. The nanofibers have uniform and beadless morphology only with slightly rough surface (Figure 4.9(c)). It is unexpected that the inside structure of these nanofibers seem to be nodular, instead of compact. A possible reason of forming this structure is the phase inversion during the drying process of nanofibers after

electrospinning. DMF is a high boiling point solvent with low volatility in room temperature (Vapor pressure: 490 Pa at 25 ℃). It does not evaporate completely during the electrospinning process and the residual DMF will spontaneously form some solvent rich regions inside the nanofibers. After this remaining DMF diffuses out, the former solvent rich regions transform into small pores and then such nodular structure forms.

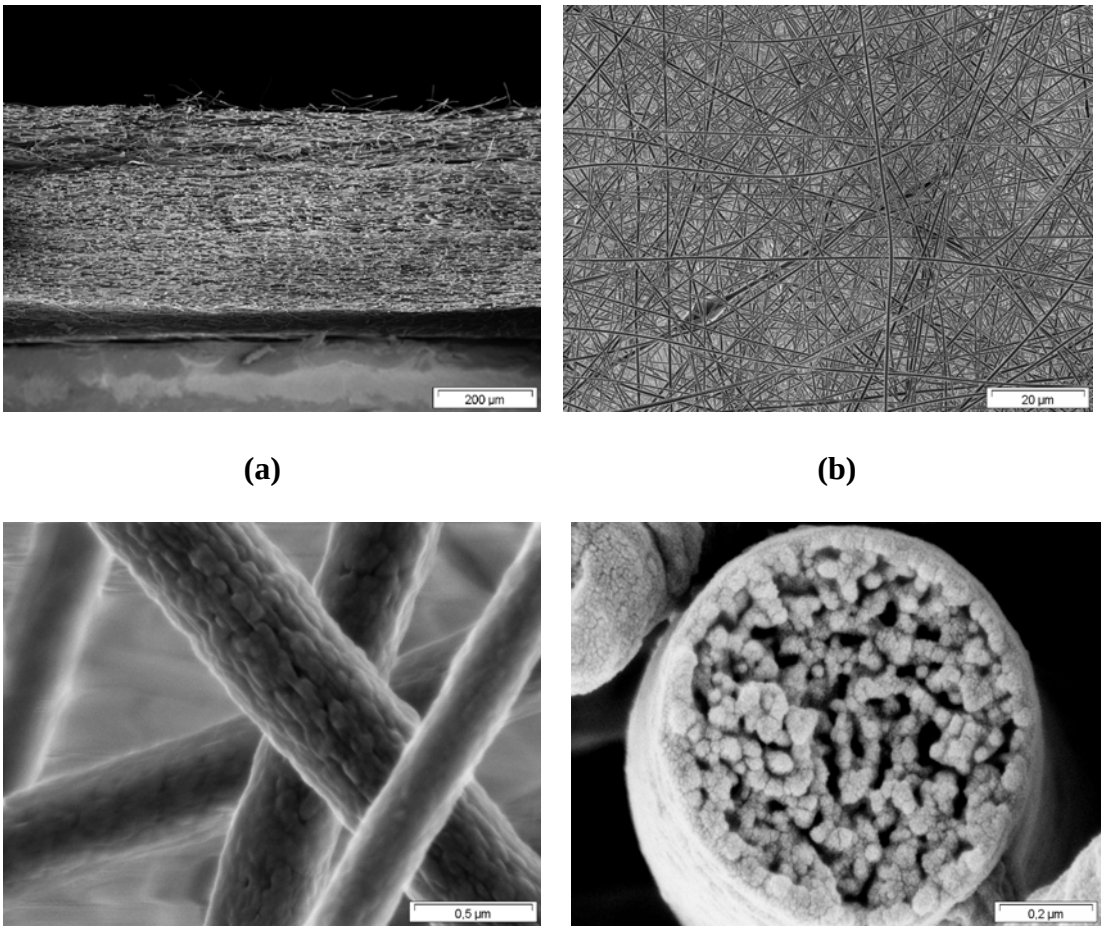

(a) **(b)**

(c) **(d)**

Figure 4.9 SEM micrographs of PANGMA nanofibers with different morphologies: (a) cross-section of ENMs, (b) x 1000, (c) x 50000, (d) cross-section of single nanofiber

As mentioned before, nanofibers electrospun from solutions with lower concentrations have beaded structures and even break when the solution concentration is very low (Figure 4.4(a)). Meanwhile, nanofibers electrospun from concentrated solutions have no beads but rougher surface. A explanation for such phenomenon is raised by Heikkiliä et al.[22]: low concentrations result in low viscosities. Low viscosities give low degree of the entanglements of polymer chain, therefore the viscoelastic force in a given jet segment is not large enough to counter the higher Coulomb force, which leads to the nonuniformity of the spinning jet and even causes the break-up of the jet into small pieces. Under the influence of surface tension, finally these small jet pieces finally round up to form small droplets and turn to beads after drying up. This phenomenon has been familiarized in industry as the electrospraying process and has been widely used in many applications such as paint spraying, ink-jet printing and powder coating.[21] At higher concentrations and of course higher viscosities, the charged jet does not break up into small droplets due to the increased chain entanglements.[33] These chain entanglements are enough to prevent the break-up of the jet and meanwhile to allow the Coulomb stress further elongate the jet during its flight to the target. However, if the concentration is not high enough but also not too low, a combination of smooth fibers and droplets could be obtained, therefore finally beaded fibers are obtained on the target.[37]

Another possible reason is that at lower concentrations electrospun nanofibers are harder to dry up before they reach the collector. Since the wet fibers will not be strained by the electric force when they are laid on the target, a solidification process will happen, which is driven by the surface tension and the relaxation process due to the viscoelastic property of the wet fibers. This process would result in the beaded

morphology. In contrast, at higher concentrations the electrospun nanofibers are mostly dried before they reach the target and therefore avoid the relaxation process.[16]

Applied voltage also can affect the morphology of PANGMA nanofiber.[38-40] The nanofibers produced under the normal range of the applied voltage (15-30 kV) have a cylindrical morphology with few beads. When the applied voltage is further increased above 30 kV, the electrospun fibers still can maintain a cylindrical morphology, but with an increase of the number of beads in the ENM.[40] This indicates that above a critical voltage there are some changes in the shape of the electrospun nanofibers. A broader distribution of fiber diameters was also observed at a higher applied voltage. Increasing the applied voltage will increase the electrostatic repulsive force on the jet, which will keep against the formation of more stable, smooth and uniform nanofibers.

The spinning distance (distance between the needle tip and collector) had no significant effect on the morphology of PANGMA electrospun nanofibers. The nanofiber morphology can be slightly changed by changing the feed rate of solution, a few of big beads were observed on the PANGMA nanofibers electrospun with higher feed rate. J. M. Deitzel et al.[40] gave their explanations: the change in the shape of the nanofiber reflects a change in the mass balance that occurs at the end of the capillary tip. Increasing the feed rate causes the increase of the delivery rate of solution to the tip. When the flow rate exceeds a critical value, the delivery rate of the solution jet to the capillary tip will exceed the maximal loading for the removing of the solution by the electric forces. This shift in the mass balance results in a sustained but increasingly less stable jet, and the maintenance of a conical shape of the nanofiber becomes harder and harder.[39] The density of beads increases with the increase of the

jet instability at the tip of the spinning jet and finally nanofibers with big beads are formed.

From the preceding discussion, it is seen that such spinning parameters as applied voltage, spinning distance and feed rate do not exhibit a strong influence on the morphology of PANGMA nanofibers compared with that of solution concentration. PANGMA nanofibers electrospun with the spinning conditions of 22 wt% solution concentration, 25 kV applied voltage, 25 cm spinning distance and 1.2 mL/h feed rate have best fiber morphology on the whole.

4.3.4 Thickness of the PANGMA-ENM

The thickness of the electrospun nanofibrous mats (ENMs) is a very important parameter, especially in their application on water filtration and enzyme immobilization field. ENM thickness can directly affect the filtration efficiency of the ENM. A thicker ENM theoretically has larger capacity of filtrating particles and contaminations, but it will also result in the decrease of water permeability. According to Darcy's law,[41-43] the water flux through a filtration membrane can be expressed by the following equation:

$$J = (\varepsilon r^2 \Delta P) / (8\mu\tau\Delta x) \qquad (4\text{-}1)$$

where J is the water flux ($m^3\ m^{-2}\ s^{-1}$), ε is the porosity (–), r is the pore radius (m), ΔP is the pressure difference across the membrane (Pa), μ is the dynamic viscosity (Pa s), τ is the tortuosity (–), and Δx is the membrane thickness (m). From this law it is clear that the water permeability is inversely proportional to the thickness of ENM, therefore the water permeability decreases with the increase of ENM thickness. On the other hand, increasing ENM thickness will increase the effective filtration area

and pores of the ENM, which is of benefit to the filtration efficiency of the ENM. Therefore the thickness of the ENM should be well controlled in a suitable range according to its applications.

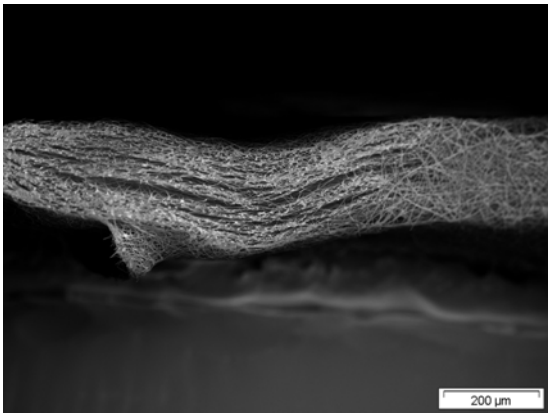

(a)

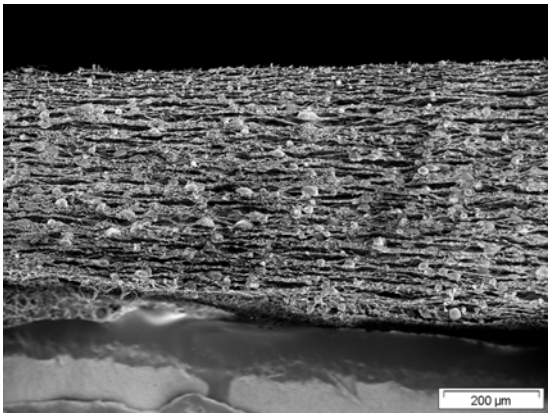

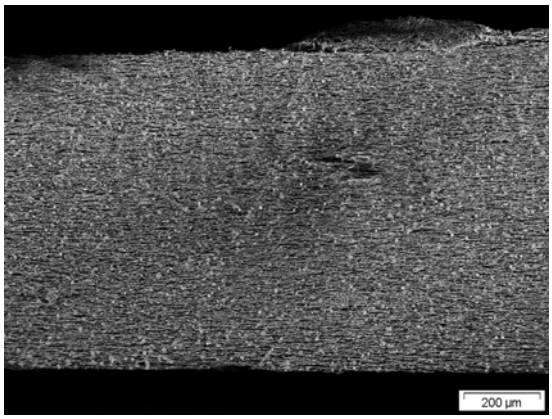

(b) **(c)**

Figure 4.10 SEM micrographs for the cross-sections of PANGMA-ENMs prepared with different feed rate and electrospinning time:
(a) feed rate of 1.0 mL/h for 2 h; (b) 1.2 mL/h for 3 h; and (c) 1.5 mL/h for 4 h

It is well-known that feed rate and electrospinning time have the most direct influence on the thickness of the nanomats among these electrospinning conditions.[44,45] Figure 4.10 shows the cross-section morphologies of PANGMA-ENMs fabricated at different feed rates and electrospinning times. It is obvious that the thickness increases

with the increase of feed rate and electrospinning time. A higher feed rate offers more polymers in unit time, resulting in producing larger amount of electrospun nanofibers per unit time per unit area, which finally will increase the thickness of the unit ENM in that unit area. Electrospinning time affects the average pore size by increasing the layer of nanofibers. PANGMA-ENMs with any required thickness can be fabricated by controlling the feed rate and electrospinning time (Figure 4.11).

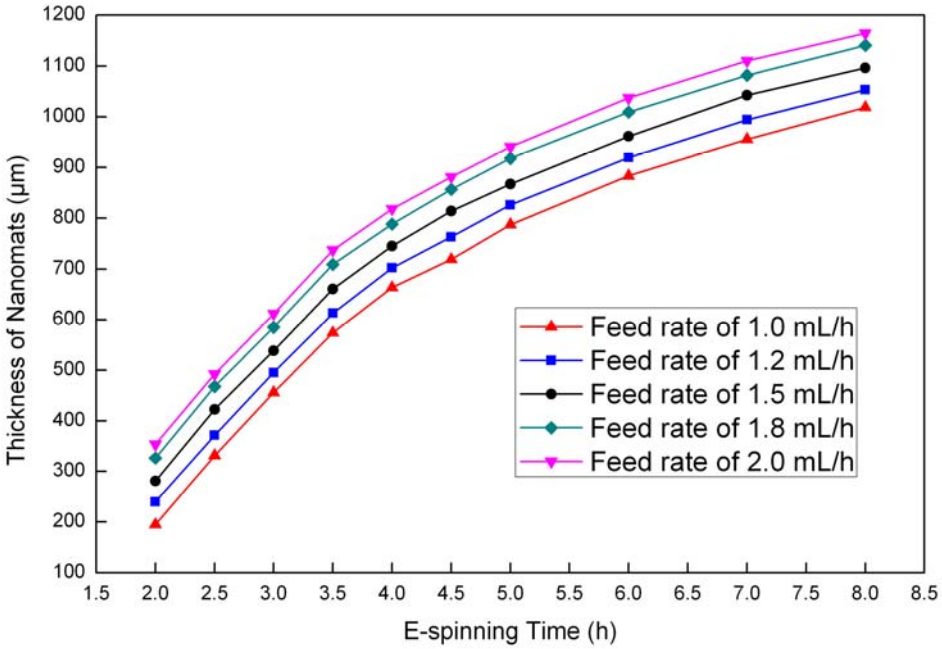

Figure 4.11 Relationship between the thickness of PANGMA-ENMs and feed rate and electrospinning time

4.3.5 Pore size of the PANGMA-ENM

Pore size is another important parameter which can affect the performance of ENMs in filtration and catalysis field. According to eq. 4.1, permeability is proportional to the pore size square. Therefore pore size has greater influence on the water permeability than the thickness. On the other hand, the pore size of the ENM could not be too large because in that case the tiny particles and contaminations in water or solution could pass through it more easily. It is very detrimental for the filtration and

separation. So it is pretty important and crucial to control the pore size of the ENM in a certain range for the application.[46,47]

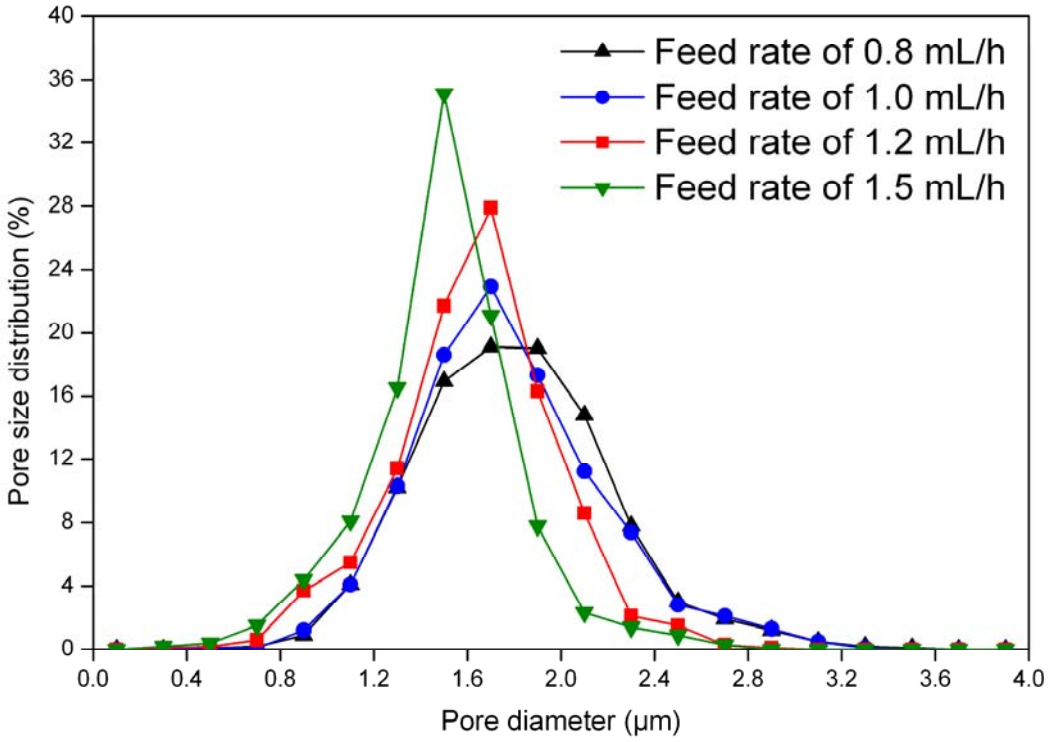

Figure 4.12 Pore size distribution of different PANGMA-ENMs fabricated with different feed rates

Figure 4.12 shows the pore size distribution of PANGMA-ENMs prepared with different feed rates of PANGMA/DMF solution. Samples electrospun with higher feed rate of solution have smaller average pore size than those electrospun with lower feed rate. The average pore size of samples shifts from about 1.8 μm to about 1.4 μm when the feed rate increases from 0.8 mL/h to 1.5 mL/h. Samples electrospun at higher feed rate also have narrower pore size distribution. The explanation for this phenomenon is that a higher feed rate increases the number of nanofibers in unit area of ENMs. As a result, the average pore size decreases due to the increase of nanofiber density. In addition, it is mentioned in the foregoing paragraphs that feed rate have no obvious influence on the diameter of the nanofiber. A higher feed rate will not cause

thicker fibers, which will result in a significant difference in the spacing between the nanofibers in ENM. Eichhorn and Sampson[48] found that at a given mass the larger pore sizes are expected for those samples which have bigger fiber diameter since less number of fibers with larger diameter will be generated per unit area than those with smaller diameter. A higher feed rate does not affect the fiber diameter, therefore there is no offset from fiber diameter on the pore size of PANGMA-ENMs. Finally smaller pore sizes are observed on the ENMs electrospun with higher feed rates.

4.4 Conclusions

PANGMA nanofibers and ENMs were successfully fabricated by electrospinning PANGMA/DMF solution. The fabricating procedures and the effect of spinning conditions on the properties of nanofibers and ENMs were detailed and studied. The solution concentration has largest influence in these spinning conditions on the diameter of PANGMA nanofibers. Increasing solution concentration will increase the average diameter and unify the fiber morphology. Solution viscosity also has influence on nanofiber diameter. The average diameter of PANGMA nanofibers increases with the increase of solution viscosity and the tendency fits to an exponential relationship. Applied voltage also affects the average diameter of PANGMA nanofibers. Diameter decreases slightly with the increase of the applied voltage. On the other hand, the feed rate and spinning distance have no obvious influence on the nanofiber diameter. Adding additives, such as citric acid and triethylbenzylammonium chloride (TEBAC) can further decrease the average diameter of the PANGMA nanofibers. After the additives were added into the spinning solution, the conductivity of the solution increased dramatically and then resulted in thinner fibers.

The morphology of the PANGMA nanofibers also could be controlled by adjusting the spinning conditions properly. Solution concentration can change the morphology of PANGMA nanofibers. Nanofibers with a lot of beads were observed when the solution concentration was below 16 wt% while beads-free nanofibers were obtained when the concentration was above 20 wt%. Applied voltage and feed rate also could limitedly affect the nanofiber morphology. Big beads could arise and further increase when the applied voltage or the feed rate exceeds a certain range. Spinning distance has almost no effects on the morphology of PANGMA nanofibers.

The parameters of the PANGMA-ENM, such as thickness and pore size of the ENM also could be controlled and optimized by adjustment of the relevant spinning conditions. Higher feed rate and longer electrospinning time could increase the thickness of the ENMs. Higher feed rate also could decrease the average pore diameter and narrow the pore size distribution of PANGMA-ENMs.

4.5 References:

[1] A. Greiner, J. H. Wendorff, Angew. Chem. Int. Ed., 2007, 46, 5670.
[2] D. Li, Y. N. Xia, Adv. Mat., 2004, 16, 1151.
[3] I. S. Chronakis, J. Mater. Process. Technol., 2005, 167, 283.
[4] Z. M. Huang, Y. Z. Zhang, M. Kotaki, S. Ramakrishna, Compos. Sci. Technol., 2003, 63, 2223.
[5] T. H. Dai, H. Yu, K, Zhang, M. F. Zhu, Y. M. Chen, H. J. Adler, J. Appl. Polym. Sci., 2008, 107, 2142.
[6] T. H. Dai, N. Miletić, K. Loos, M. Elbahri, V. Abetz, Macromolecular Chemistry and Physics, 2011, 212, 319.
[7] H. G. Hicke, I. Lehmann, Journal of Membrane Science, 2002, 198, 187.
[8] K. Ebert, D. Fritsch, J. Koll, C. Tjahjawiguna, J. Mem. Sci., 2004, 233, 71.

[9] S. Cetiner, H. Karakas, R. Ciobanu, M. Olariu, N. U. Kaya, C. Unsal, F. Kalaoglu, A. S. Sarac, Synthetic Metals, 2010, 160, 1189.
[10] R. E. Farsani, S. Raissi, A. Shokuhfar, A. Sedghi, World Academy of Science, Engineering and Technology, 2009, 50, 430.
[11] S. B. Deng, R. B. Bai, J. P. Chen, Journal of Colloid and Interface Science, 2003, 260, 265.
[12] T. Godjevargova, V. Konsulov, A. Dimov, Journal of Membrane Science, 1999, 152, 235.
[13] L. B. Canto, L. A. Pessan, Polymer Testing, 2002, 21, 35.
[14] O. H. Lin, R. N. Kumar, H. D. Rozman, M. A. M. Noor, Carbohydrate Polymers, 2005, 59, 57.
[15] W. G. Cui, X. H. Li, S. B. Zhou, J. Wenig, Journal of Applied Polymer Science, 2007, 103, 3105.
[16] X. H. Zong, K. Kim, D. F. Fang, S. F. Ran, B. S. Hsiao, B. Chu, Polymer, 2002, 43, 4403.
[17] V. Beachley, X. J. Wen, Materials Science and Engineering C, 2009, 29, 663.
[18] L. S. Lee, K. H. Choi, H. D. Ghim, S. S. Kim, D. H. Chun, H. Y. Kim, J. Appl. Polym. Sci., 2004, 93, 1638.
[19] L. Li, Y. Jia, Z. R.Yang, Mater. Lett., 2008, 62, 511.
[20] L. Dong, J. Huang, Y. Zheng, Mater. Lett., 2007, 61, 2556.
[21] C. Mit-uppatham, M. Nithitanakul, P. Supaphol, Macromol. Chem. Phys., 2004, 205, 2327.
[22] P. Heikkiliä, A. Harlin, European Polymer Journal, 2008, 44, 3067.
[23] A. Koski, K. Yim, S. Shivkumar, Mater. Lett., 2004, 58, 493.
[24] K. H. Lee, H. Y. Kim, H. J. Bang, Y. H. Jung, S. G. Lee, Polymer, 2003, 44, 4029.
[25] L. Li, Y. L. Hsieh, Polymer, 2005, 46, 5133.
[26] V. Pornsopone, P. Supaphol, R. Rangkupan, S. Tantayanon, Polym. Eng. Sci., 2005, 45, 1073.
[27] S. Tang, Y. C. Zeng, X. H. Wang, Polym. Eng. Sci., 2010, 50, 2252.
[28] B. Ding, H. Y. Kim, S. C. Lee, D. R. Lee, K. J. Choi, Fibr. Polym., 2002, 3, 73.
[29] X. M. Mo, C. Y. Xu, M. Kotaki, S. Ramakrishna, Biomaterials, 2004, 25, 1883.
[30] M. M. Demir, I. Yilgor, E. Yilgor, B. Erman, Polymer, 2002, 43, 3303.
[31] C. J. Buchko, L. C. Chen, Y. Shen, D. C. Martin, Polymer, 1999, 40, 7397.

[32] S. H. Tan, R. Inai, M. Kotaki, S. Ramakrishna, Polymer, 2005, 46, 6128.

[33] M. G. McKee, G. L. Wilkes, R. H. Colby, T. E. Long, Macromolecules, 2004, 37, 1760.

[34] S. F. Fennessey, R. J. Farris, Polymer, 2004, 45, 4217.

[35] X. H. Qin, E. L.Yang, N. Li, S. Y. Wang, Journal of Applied Polymer Science, 2007, 103, 3865.

[36] S. J. Kim, C. K. Lee, S. I. Kim, Journal of Applied Polymer Science, 2005, 96, 1388.

[37] J. Sutasinpromprae, S. Jitjaicham, M. Nithitanakul, C. Meechaisue, P. Supaphol, Polym. Int., 2006, 55, 825.

[38] V. Jacobs, R. D. Anandjiwala, M. Maaza, Journal of Applied Polymer Science, 2010, 115, 3130.

[39] C. X. Zhang, X. Y. Yuan, L. L. Wu, Y. Han, J. Sheng, European Polymer Journal, 2005, 41, 423.

[40] J. M. Deitzel, J. Kleinmeyer, D. Harris, N. C. B. Tan, Polymer, 2001, 42, 261.

[41] Z. Wang, D. Z. Liu, W. J. Wu, M. Liu, Desalination, 2006, 201, 175.

[42] P. Gibson, H. S. Gibson, D. Rivin, Colloids Surf. A: Physicochem. Eng. Aspects, 2001, 187, 469.

[43] I. H. Huisman, B. Dutrê, K. M. Persson, G. Trägårdh, Desalination, 1997, 113, 95.

[44] M. Gandhi, H. J. Yang, L. Shor, F. Ko, Polymer, 2009, 50, 1918.

[45] X. F. Wang, K. Zhang, Y. Yang, L. L. Wang, Z. Zhou, M. F. Zhu, B. S. Hsiao, B. Chu, Journal of Membrane Science, 2010, 356, 110-116.

[46] A. A. Tseng, A. Notargiacomo, T. P. Chen, J. Vac. Sci. Technol. B, 2005, 23, 877.

[47] J. C. Huie, Smart Mater. Struct., 2003, 12, 264.

[48] S. J. Eichhorn, W. W. Sampson, J. Roy. Soc. Interf., 2005, 2, 309.

Chapter 5. Crosslinked PANGMA electrospun nanofibrous mat applied as a solvent resistant membrane

5.1 Brief Introduction

Solvent resistant membrane is a very strong and practical separation or protection membrane with high potential in many branches of industry, ranging from petrochemistry to pharmaceuticals.[1–3] These membranes are robust enough to resist the erosion from the common used solvents, meanwhile selectively allow the filtration objects pass through.[4,5] Whu et al.[6] modelled a semi-batch reactor process using a solvent resistant membrane as the separation media. They succeeded to separate the catalyst by the solvent resistant membrane from those strong solvents which can easily dissolve normal membranes. Their study academically demonstrated the potential application of solvent resistant membranes in the field of catalyst recycling.

Electrospun nanofibrous mats (ENMs) are very promising as candidates for the solvent resistant membrane because of their huge surface area, relatively small pore size and highly porous structure. Since lots of the chemical and catalytical reactions are performed in aprotic solvents such as dimethylformamide (DMF), N-methylpyrrolidinone (NMP), dimethylacetamide (DMAc) and dimethylsulfoxide (DMSO) and also sometimes at elevated temperatures, an ideal solvent resistant membrane should combine chemical, mechanical and thermal stability with excellent rejections and high permeabilities.[7-9]

However, unfortunately majority of the existing electrospun nanofibers or ENMs do not fulfill these requirements due to their common deficiencies such as poor thermal

stability, bad solvent stability, and low mechanical strength.[10–12] For instance, electrospun poly(vinyl alcohol) (PVA) fibers can dissolve in water easily.[13,14] These disadvantages severely restrict their applications in these aprotic solvents such as DMF, NMP, DMAc and DMSO. In most current industries, solute recovery and solvent purification generally still rely on conventional separation techniques such as energy consuming distillations or waste generating extractions.[15-17]

Lots of methods including surface modification,[18] heat treatment,[10,11,19] and chemical crosslinking[12,14,20–25] have been brought forward to solve these problems and made improvements. Among them, the chemical crosslinking is an effective one, which can endue the electrospun nanofibers with the ability of solvent and temperature resistance. Crosslinking generally promotes resistance to chemical attack and reduces the mobility of the polymer chains.[24,26-29] Several papers have reported on generating chemically crosslinked ultrafine fibers by electrospinning. Yi et al.[21] reported that crosslinked eggshell membrane protein ultrafine fiber could be fabricated by dipping it in DCC (a catalyst) after electrospinning. Zeng et al.[22] prepared photocurable PVA derivative electrospun fiber and found that the fibers proved to be water stable after UV irradiation for more than 3 min. Li and Hsieh[23] reported that poly(acrylic acid) (PAA) electrospun fibers could be rendered insoluble in water by crosslinking with the addition of ß-cyclodextrin and heating at 140 ℃ for 20 min.[31]

In this chapter we describe the newest results for a novel solvent resistant electrospun nanofibrous mat (ENM), which can be obtained from PANGMA in two steps: 1) electrospinning PANGMA/DMF solution and 2) chemically crosslinking via

ammonolysis. The novel ENM can be considered promising for potential applications as solvent and thermal resistant membrane for the solvent resistant filtration or the catalytical applications.

5.2 Experimental

5.2.1 Materials

PANGMA was synthesized at Helmholtz-Zentrum Geesthacht with a molecular weight (M_n) of ca. 100,000 and GMA content of 10 mol%.[30] Ammonium hydroxide solution (27 wt%) was purchased from Fluka & Co. Ethylenediamine (EDA), butylenediamine (BDA), hexamethylenediamine (HMDA) and *p*-xylylenediamine (*p*-XDA) were purchased from Sigma-Aldrich & Co. N,N-dimethylformamide (DMF), N,N-dimethylacetamide (DMAc), dimethyl sulfoxide (DMSO), tetrahydrofuran (THF) and toluene were purchased from Merck KGaA. All chemicals were directly used without further purification.

5.2.2 Preparation of PANGMA-ENMs via electrospinning

PANGMA was dissolved in DMF at room temperature with moderate stirring for 48 h to form a homogeneous solution. The polymer concentration was fixed at 22 wt%. The solution was placed in a 5 mL glass syringe with a metal needle with the inner diameter of 0.8 mm. A high voltage generator was connected to the middle of the needle. A rectangular counter electrode covered with the aluminium foil was used as the collector. Electrospinning was performed at a voltage of 25 kV and a spinning distance of 25 cm. The feed rate of the solution was controlled by a syringe pump (HARVARD PHD 4400, Harvard Apparatus.Co) to be maintained at 1.5 mL/h and the electrospinning time was 4 h to obtain ENM of sufficient thickness. After

electrospinning the ENMs were detached and washed with methanol and deionized water to remove the DMF and impurities. Subsequently, the ENMs were dried under vacuum at 50 ℃ for 24 h to remove residual liquids.[31,32]

5.2.3 Crosslinking of the as-spun PANGMA-ENMs with different crosslinkers

The as-spun PANGMA-ENMs were crosslinked with different crosslinkers to gain the solvent and thermal resistance. The crosslinkers include different kinds of diamines and 27 wt% ammonium hydroxide solution. The reaction was performed at 50 ℃ for different time intervals. Finally, the nanomats were carefully washed with deionized water and dried under vacuum at 50 ℃ for 24 h.

5.2.4 Measurements and characterizations

The solvent-resistance of crosslinked PANGMA-ENMs was tested by immersing them in different solvents (toluene, THF, DMF, DMAc and DMSO). For the swelling experiments the ENMs were cut into pieces of 4 cm x 4 cm. Then the initial weight of the ENMs was taken (W_0). The samples were then immersed for 72 h in the respective solvent at room temperature and finally the weight of the thus treated sample was determined (W_1). Subsequently, the samples were washed with methanol and deionized water and then dried as described before. The weight of the dried samples is referred to as W_2. The swelling ratio (S) and the weight loss (WL) were calculated by the following equations:

$$S = W_1 / W_2 \quad (5\text{-}1)$$

$$WL = (W_0 - W_2) / W_0 \times 100\% \quad (5\text{-}2)$$

The experiments were performed with 5 pieces of the respective samples. The data given in the paper are the average values of these 5 experiments.

The structures of both neat and crosslinked PANGMA-ENMs were characterized by Attenuated Total Reflection Fourier transform infrared spectroscopy (ATR-FTIR) with an FTIR spectrophotometer (Bruker Equinox 55, Bruker Optics) in the mid-infrared range from 4000 to 500 cm^{-1}.

The morphology of neat and crosslinked PANGMA-ENMs were observed with a scanning electron microscope (LEO Gemini 1550 VP, Zeiss) at 10 kV accelerating voltage after sputter-coating with gold. The average diameters of the nanofibers were calculated from 10 different single values randomly by the internal software of the SEM.

The thermal properties of neat and crosslinked PANGMA-ENMs were studied by differential scanning calorimetry (DSC) and thermogravimetric analysis (TGA). DSC measurements were carried on with a Netzsch DSC 204 Phoenix® using indium standards. The glass transition temperature (T_g) was determined by means of a dynamic scan at 10 ℃/min from 20 to 200 ℃. TGA measurements were performed on a thermogravimetric analyzer of Netzsch 209 TG with a heating rate of 10 ℃/min and a temperature range of 20 to 700 ℃ in argon atmosphere.

The inter-fiber pore size of the PANGMA-ENMs was determined with the bubble point method which was performed with a Porometer 4.900 from Porous Materials Inc. (PMI). The PANGMA-ENM stamps with a diameter of 3 cm were immersed in the wetting fluid Porewick® from PMI (surface tension = 16×10^{-7} J/m= 16 dyn/cm) for more than 15 min and then placed in the test cell. Based on the flux data through the membrane the pore size distribution is calculated by the internal PMI software.[33]

5.3 Results and discussions

5.3.1 Electrospinning of PANGMA nanofibers

PANGMA nanofibers were obtained by electrospinning PANGMA/DMF solution with the following spinning conditions: solution concentration of 22 wt%, applied voltage of 25 kV, feed rate of 1.5 mL/h, spinning distance of 25 cm and spinning time of 4 h. Their morphologies are shown in Figure 5.1. These spinning conditions were chosen for further experiments because with them PANGMA nanofibers with best uniformity of both diameter and morphology could be electrospun. The fabricated ENMs have a uniform distribution of fiber size and are practically free of beads (Figure 1(a)).

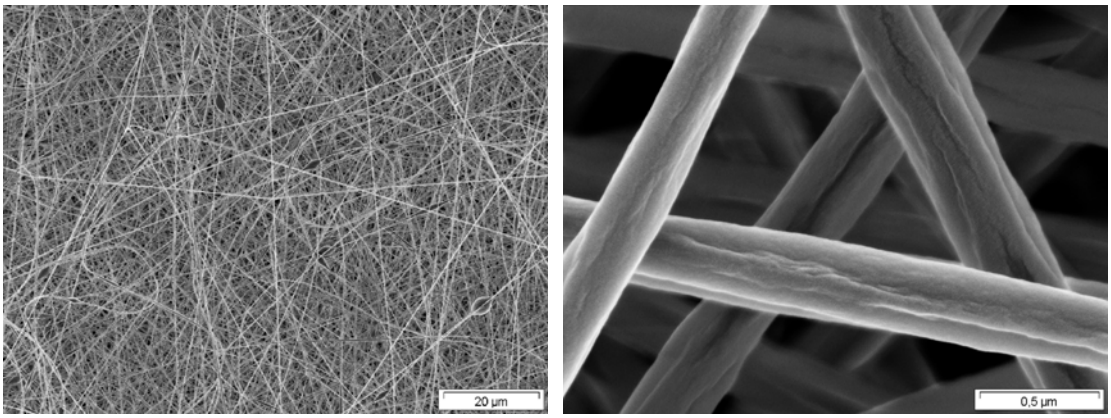

(a) **(b)**

Figure 5.1 SEM micrographs of PANGMA nanofibers and ENMs: (a) structure of the ENM, (b) surface morphology of the nanofiber

5.3.2 Crosslinking and solvent resistance measurement of PANGMA-ENMs

PANGMA-ENM contains epoxy groups which are very suitable for the crosslinking with many compounds which contain active hydrogen, such as amines, carboxylic acids, phenols and alcohols. But as mentioned in §2.2.3, amines show the best reactivity among these crosslinkers. Aliphatic primary amine could directly react with

epoxy group at room temperature dispensing with any accelerants, while other crosslinkers like carboxylic acids and alcohols could only react if the reaction temperature is above 200 ℃ or when the accelerants are introduced.[34-36]

Two different kinds of crosslinkers, diamines with different chain lengths and ammonia hydroxide solution were used for the crosslinking of PANGMA-ENMs, and their crosslinking ability and effect were investigated and compared. The mechanisms of crosslinking with diamines and with ammonia are slightly different with each other and detailed as follows: During the crosslinking with diamines, firstly the epoxy groups on the PANGMA nanofibers are attacked by the primary amine groups which are at the terminal of the diamine chain, and then secondary amine groups and hydroxyl groups are formed as a result of the ring-opening reaction of epoxide (Figure 5.2(a)). One diamine molecule contains two primary amine groups and these two amine groups tend to react with epoxy groups on different PANGMA nanofibers due to the nearer distance and lower steric hindrance of two epoxy groups on two different nanofibers, leading to the formation of the crosslinked structure. Small amount of inner-crosslinking also happens between the epoxy groups on the same PANGMA polymer chain.[37,38] For the crosslinking with ammonia, the process of the crosslinking reaction is a little bit different from that with diamine. Firstly, primary amine groups are formed by the conversion of epoxy groups by ammonia. As the reaction proceeds further, epoxy groups may react with the already formed primary amine groups and further form secondary amine groups and these formed secondary amines may possibly further react and form tertiary amine. This mechanism makes the epoxy-ammonia reaction tend to result in a 3-dimensional network of the crosslinked

PANGMA molecules. These tertiary amines are the nodal points of this polymer network (Figure 5.2(b)).[39,40]

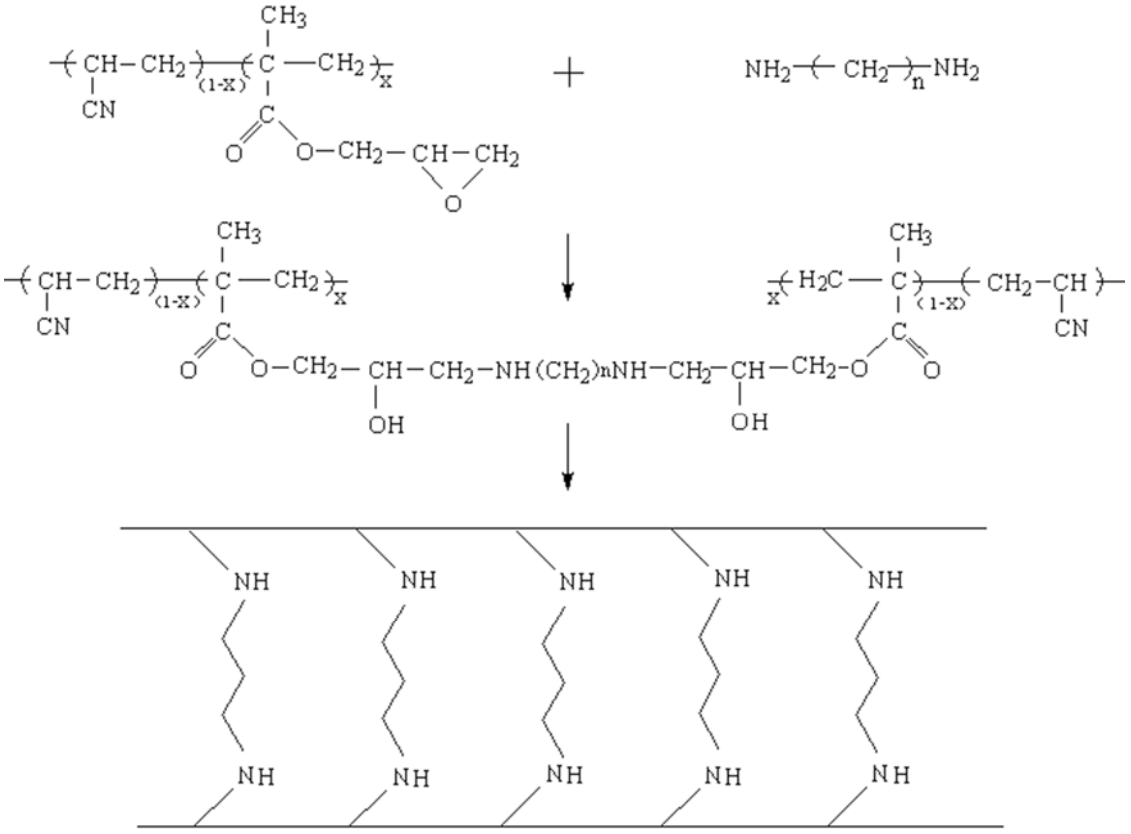

(a)

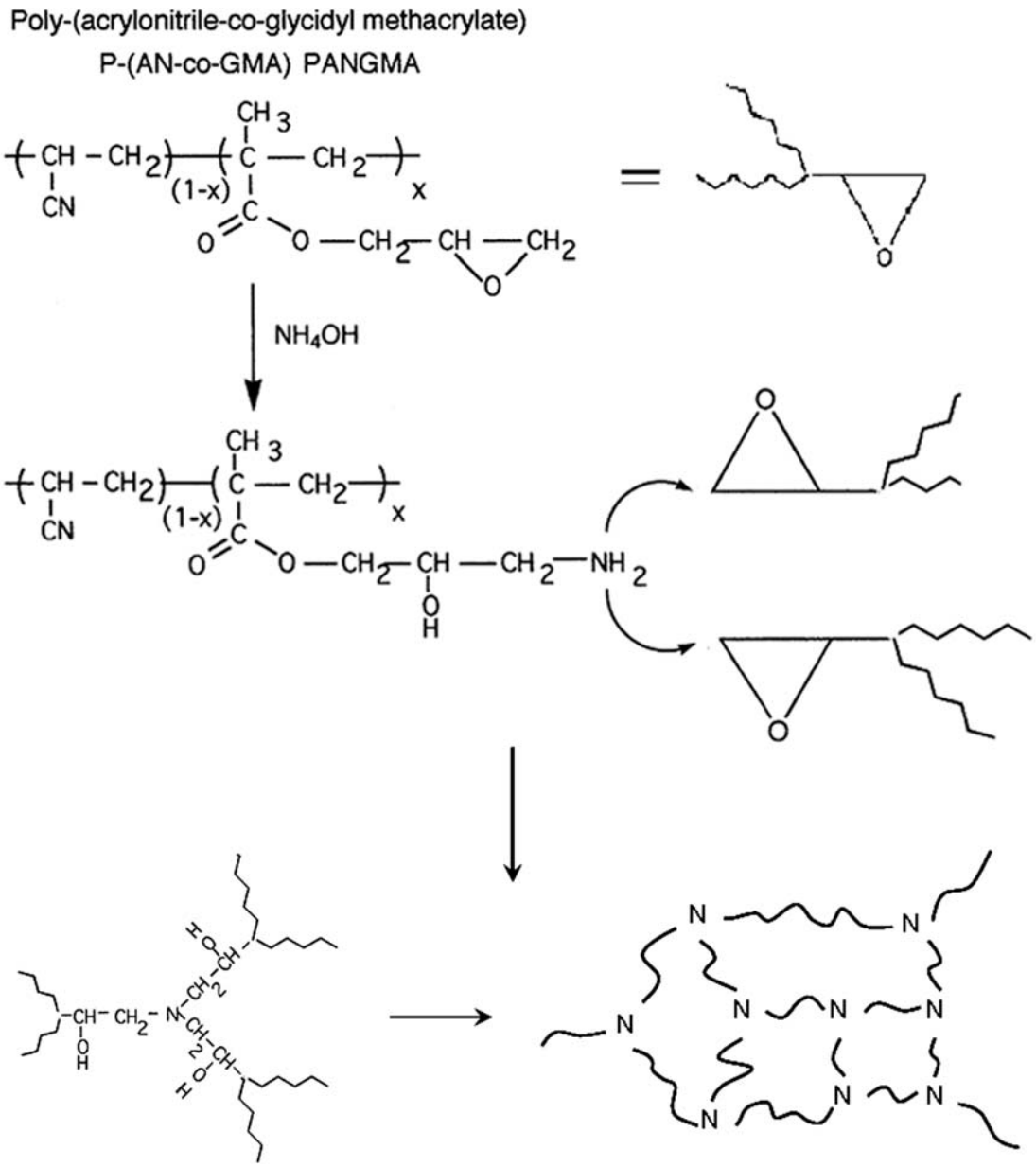

(b)

Figure 5.2 Crosslinking reaction route of the as-spun PANGMA nanofibers: (a) crosslinking with diamine, (b) crosslinking with ammonia[30]

The crosslinking reaction was performed at 50 ℃ with different crosslinkers for different crosslinking time to obtain the best crosslinking conditions. The solvent resistance of the crosslinked PANGMA-ENM was characterized by determining the

weight loss and the swelling rate of the ENM after immersion in the respective solvent for 72 h.

First, the crosslinking effect of different crosslinkers was investigated and compared. Four different diamines: ethylenediamine (EDA), butylenediamine (BDA), hexamethylenediamine (HMDA), and *p*-xylylenediamine (*p*-XDA) and ammonia hydroxide solution were used as the crosslinkers. All the diamines were used in the form of 30 wt% aquous solution and ammonia hydroxide solution were used with a concentration of 27 wt%. For all the diamines, crosslinking reactions were performed at 50 ℃ for 24 h, and for ammonia, the reaction was performed at 50 ℃ for 3 h. After crosslinking, the swelling test was performed in 3 different solvents: DMF, DMAc and DMSO, and the results are in figure 5.3. The reason why different crosslinking time was used for diamines and ammonia is that diamines can not give effective crosslinking to PANGMA-ENMs within 3 h. All the ENMs crosslinked with diamines for 3h were dissolved in all the solvents quickly, the same with 6h, 9h and 12h. The swelling test shows that all of the crosslinked PANGMA-ENMs were nearly insoluble in DMF, DMAc and DMSO. As compared, all of the neat ENMs were dissolved immediately after dipped into these solvents. From figure 5.3 it is clear that all the samples will lose some weight after 3 days immersion in solvents. The weight loss is from 15 wt% (crosslinked with *p*-XDA) to less than 3 wt% (crosslinked with ammonia). As the crosslinker, *p*-XDA has the worst crosslinking ability while ammonia is the best one. This is probably because *p*-XDA has a large and rigid benzene ring in its structure, which will seriously hinder the movement of the *p*-XDA molecules and as a result decrease their contact possibility with PANGMA molecules. This results in a lower crosslinking degree and a higher weight loss in swelling test.

On the contrary, ammonia is much more active due to its high chemical activity and small molecular size. During the crosslinking, ammonia can easily move and enter into the PANGMA nanofibers, and then easily attack epoxy groups. Finally this causes much higher completeness of the reaction and a higher crosslinking degree, which bring a much lower weight loss and much better solvent resistance.[41-43]

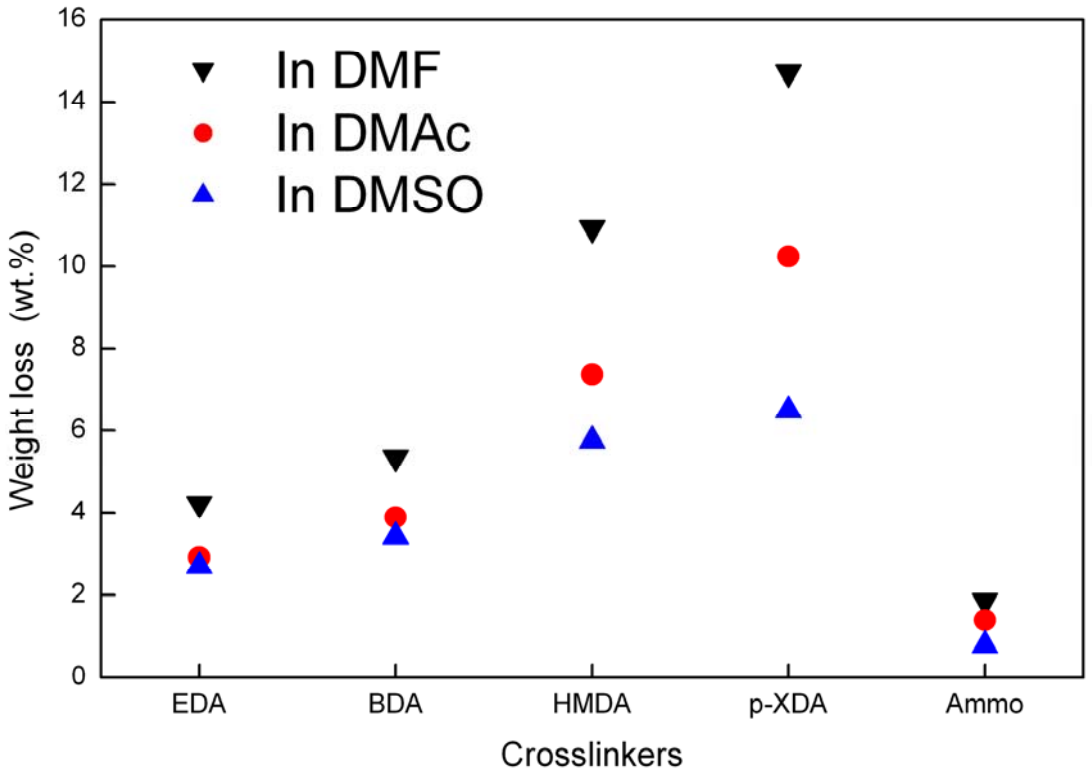

Figure 5.3 Weight loss of PANGMA-ENMs crosslinked with different crosslinkers after immersion in organic solvents for 72 h

From the above results and discussion it is clear that ammonia has the best crosslinking ability among these crosslinkers. Therefore ammonia was chosen as the crosslinker for the preparation of solvent resistant PANGMA-ENMs in later researches. All the results and discussions in the following passages will be only focused on the crosslinking with ammonia. The weight loss of PANGMA-ENM dependent on the crosslinking time is given in figure 5.4. The weight loss at

comparable crosslinking times decreases in the order of DMF, DMAc and DMSO. Correspondingly, the same trend was observed for the swelling rates which are 17 %, 8.9 % and 7.5 %, respectively. Generally, the weight loss decreases with increasing crosslinking time for all tested solvents. After 1 h crosslinking time the weight loss is more than 4 wt% in the case of DMF and only about 2 wt% for the samples immersed in DMSO. This decrease is moderate from below 2.5 wt% for 2 h crosslinking to below 1.5 wt% for 6 h crosslinking. After crosslinking for 3 h, the weight loss is less than 2 wt% in all solvents and it is already enough for the solvent resistance applications. So PANGMA nanofibers crosslinked for 3 h were chosen for further experiments.

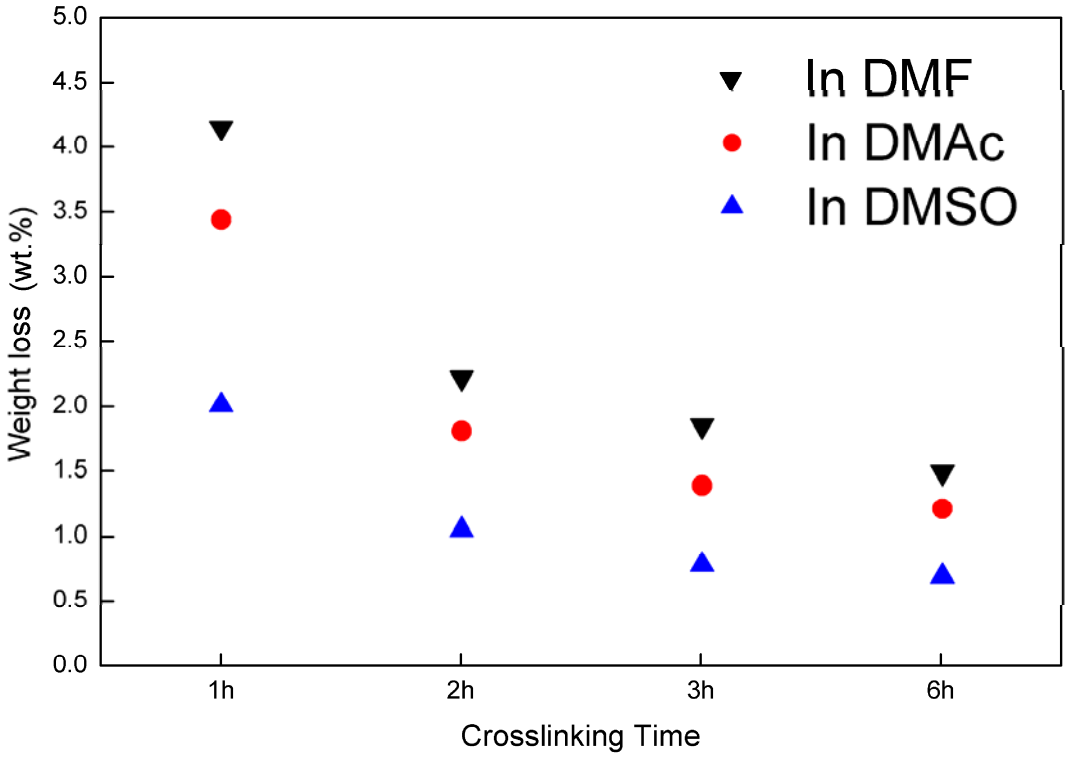

Figure 5.4 Weight loss of PANGMA-ENMs dependent on the crosslinking time after immersion in organic solvents for 72 h

FTIR measurements were performed to structurally verify the crosslinking of PANGMA nanofibers. Figure 5.5 shows the FTIR spectra (in transmittion mode) of neat (curve (a)) and crosslinked (curve (b)) nanofibers. On curve (a) there is a clear peak near 908 cm^{-1} (characteristic peak of epoxy group), which shows the existence of epoxy groups in neat PANGMA nanofibers. Meanwhile no obvious peak near 908 cm^{-1} can be found in the spectrum (b), which further proves that epoxy groups in PANGMA have been crosslinked by ammonia.[44,45]

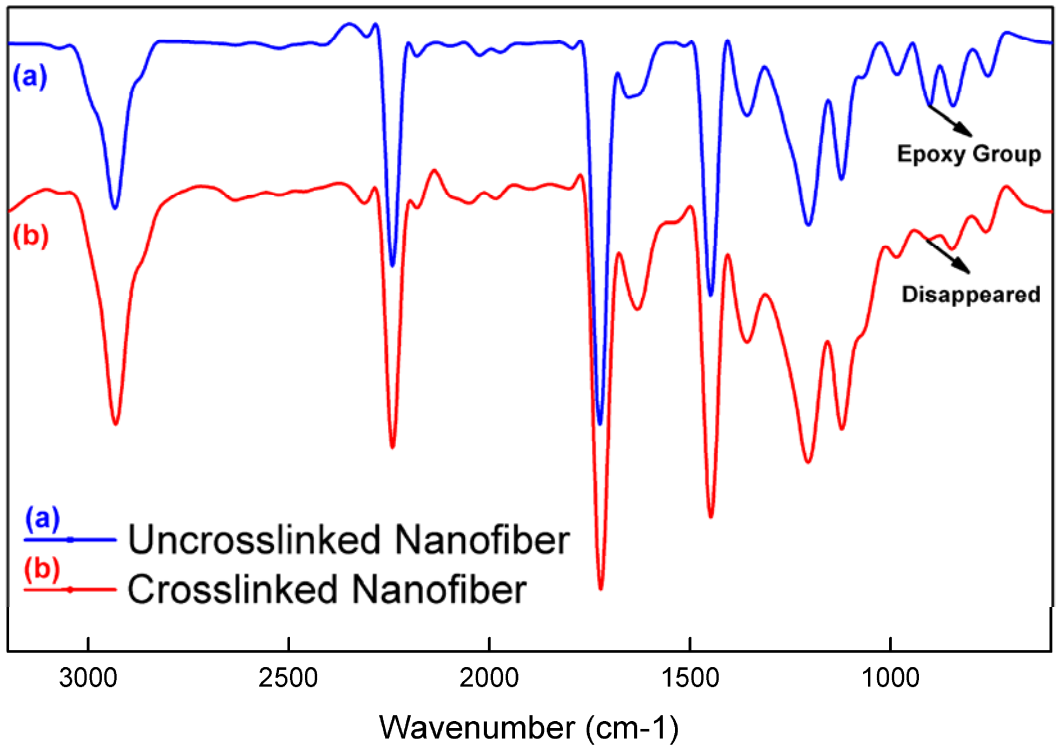

Figure 5.5 FTIR spectrum of PANGMA nanofibers: (a) before, and (b) after crosslinking, crosslinked samples prepared with ammonolysis at 50℃ for 3h

Figure 5.6 shows the SEM photos of the crosslinked PANGMA nanofibers after immersion in organic solvents for 72 h at room temperature. For comparison the neat PANGMA nanofibers are included in figure 5.6(a). It can be seen that the crosslinked nanofibers are rather unaffected in the case of THF, toluene and DMSO (Figures 5.6(b)

to 5.6(d)). Since PANGMA originally has only limited (in DMSO) or even no solubility (in THF and toluene) in these solvents, this is not surprising. In DMAc and DMF a higher swelling of the PANGMA nanofibers was observed as it was discussed before. Correspondingly, the shape of the fibers is changed (Figures 5.6(e), 5.6(f)) in comparison to the neat fibers (Figure 5.6(a)). Obviously, the nanofibers become more ribbon-like, especially in the case of DMF-treated fibers (Figure 5.6(f)). Generally, the structure of the nanomats is kept, although it seems that nanomats which have been immersed in DMF have a more densified inter-fiber structure. However, the results show that the crosslinked PANGMA-ENM have superior solvent resistance in a series of organic solvents and therefore are very suitable for the applications in such harsh environments.

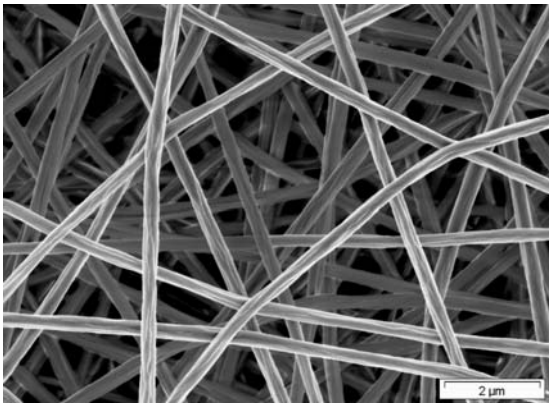

(a)

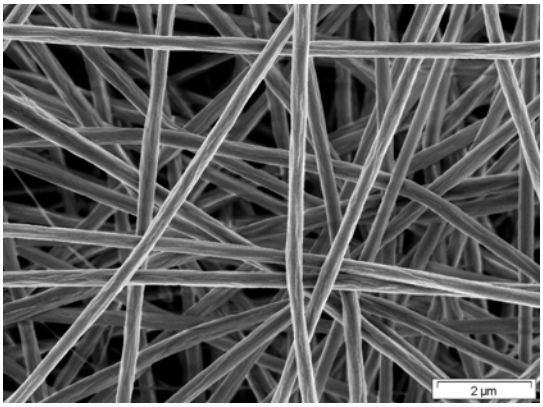

(b)

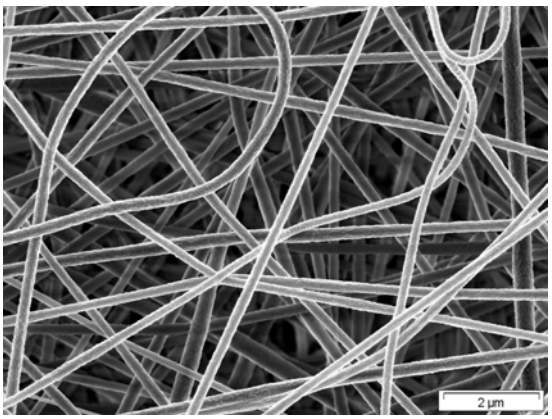

(c)

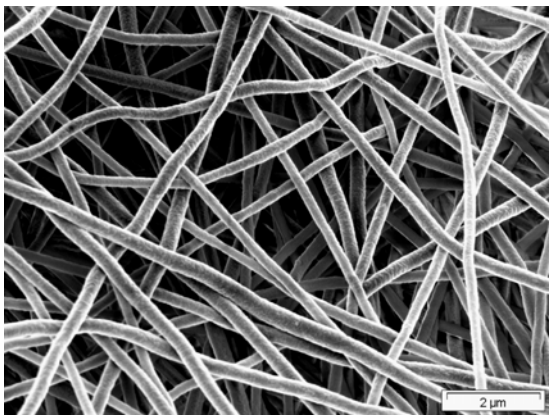

(d)

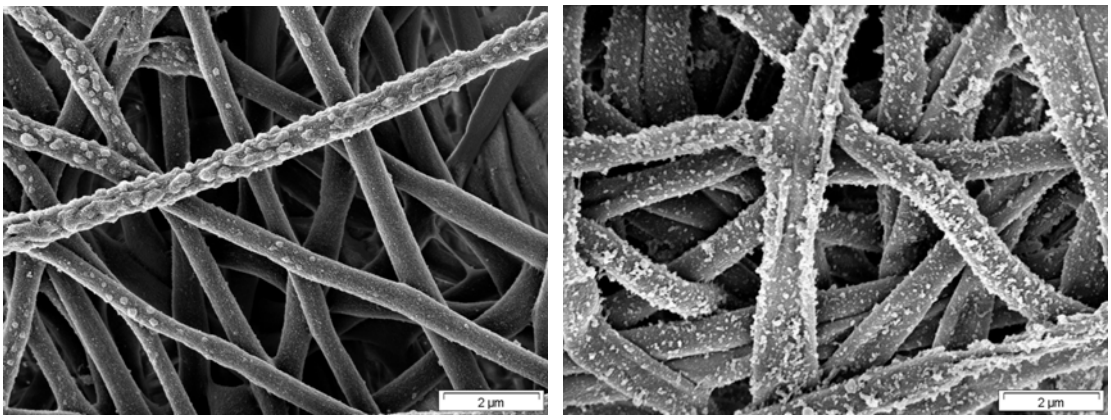

(e) **(f)**

Figure 5.6 SEM micrographs of PANGMA nanofibers: (a) neat, (b)-(f) after immersion in different solvents at room temperature for 72 h, (b) in THF; (c) in toluene; (d) in DMSO; (e) in DMAc; (f) in DMF

It is noteworthy that PANGMA nanofibers with only 10 mol% GMA content already have enough epoxy groups to obtain this excellent solvent resistance. It is feasible to synthesize PANGMA with a higher GMA content (higher than 15 mol%) and partially crosslink them after electrospinning in order to keep enough epoxy groups for the additional binding capacity for covalent immobilization of ligands of homogeneous catalysts or enzymes on the PANGMA nanofibers.

5.3.3 Thermal stability of PANGMA-ENMs

Crosslinking also improved the thermal stability of the PANGMA nanofibers and ENMs. Figure 5.7 shows the DSC thermograms for neat and crosslinked PANGMA-ENMs. After three hours of crosslinking the glass transition temperature (T_g) of the ENMs increases from 98.7 ℃ to 109 ℃, and then further increases with increase in crosslinking time to almost 130 ℃ after 48 h crosslinking. This is due to the decreasing flexibility of polymer chains as a result of the formation of a crosslinked

network. As a consequence, the glass transition temperature increases. These results indicate that PANGMA nanofibers and ENMs still have big potential for further improvement of thermal stability.

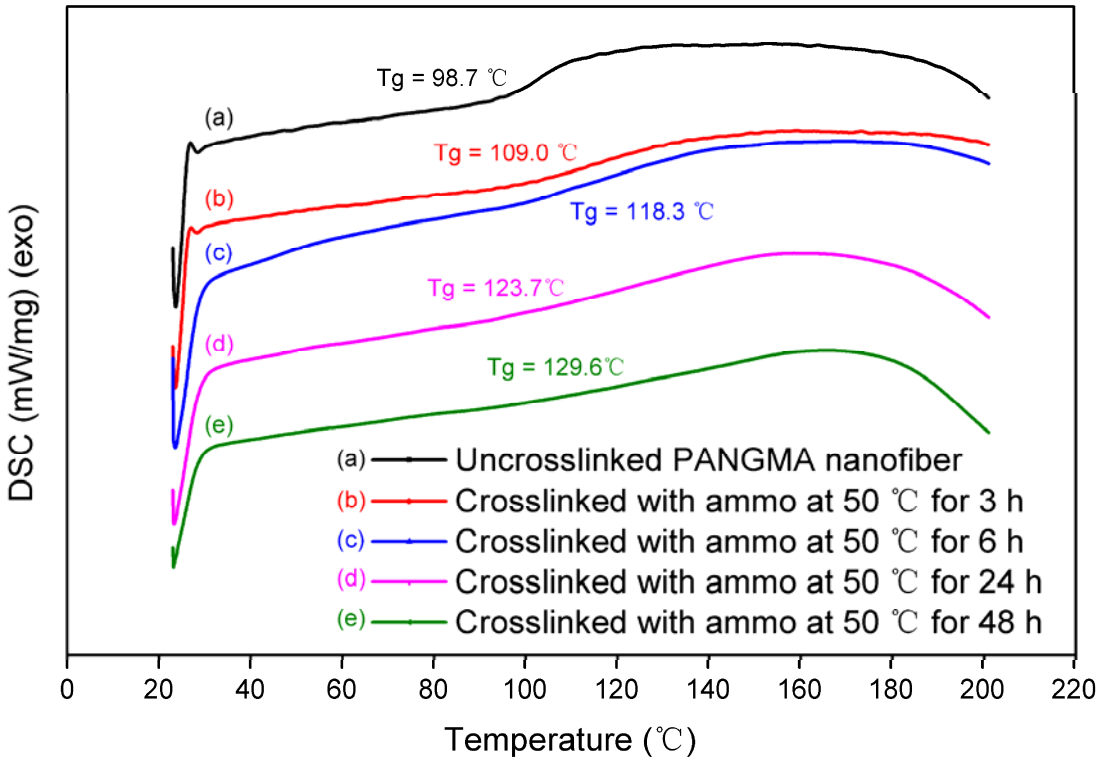

Figure 5.7 DSC curves of neat and crosslinked PANGMA-ENMs: (a) neat; (b) crosslinking time= 3 h; (c) crosslinking time= 6h; (d) crosslinking time=24 h; (e) crosslinking time= 48 h

Meanwhile, the thermal decomposition temperature (T_d) (here T_d is specially defined as the temperature at which the weight of PANGMA-EMNs changes by 5%)[46,47] of the PANGMA-ENMs increases from 272.8 ℃ of neat ENM to 335.1 ℃ of crosslinked for 48 h (Figure 5.8). The decomposition temperature increases with the increase of crosslinking time. This phenomenon is also one of the consequences of crosslinking. With longer crosslinking time, more completed crosslinking could be fufilled, which improves the thermo-stability of the crosslinked PANGMA-ENMs.

The thermal analysis results indicate that ammonia crosslinked PANGMA-ENMs can be served in a much harsher working condition than the neat ENMs.

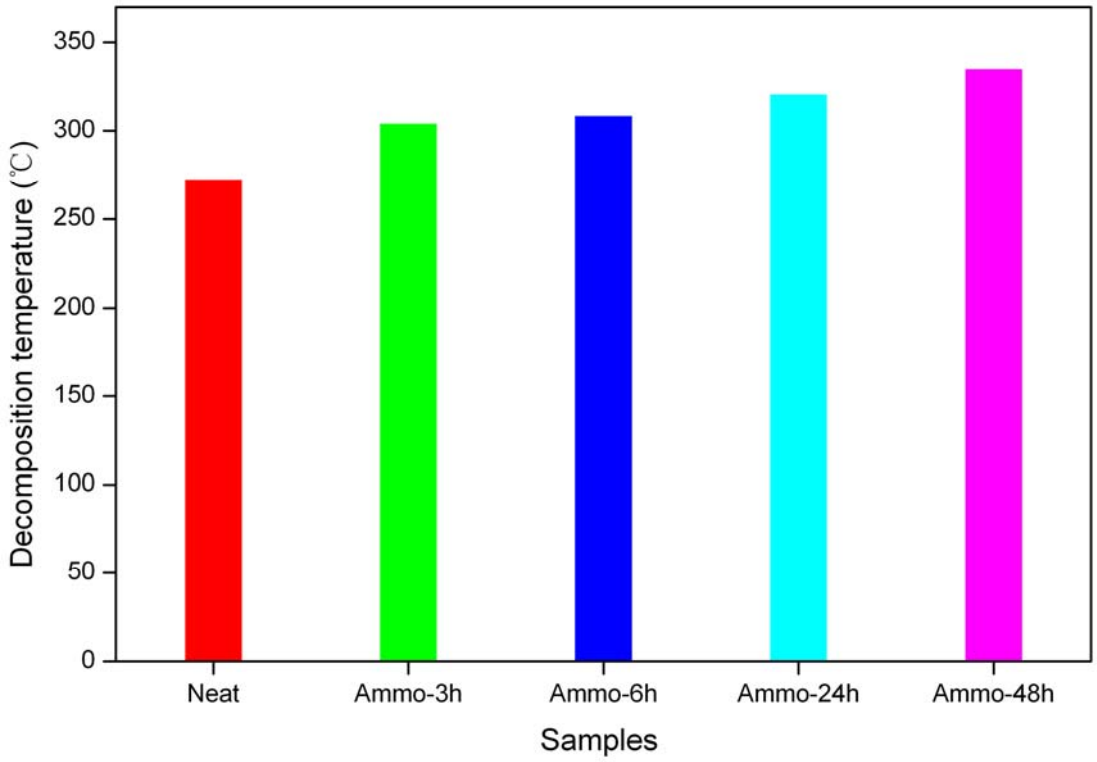

Figure 5.8 Decomposition temperature (T_d) of ammonia crosslinked PANGMA-ENMs with different crosslinking time (3, 6, 24 and 48 h)

5.3.4 Pore size distribution of PANGMA-ENMs

In figure 5.9 the pore size distribution of neat, crosslinked and solvent-treated PANGMA-ENMs are shown. For all studied ENMs, pore sizes ranging from 0.6 to 2.8 µm are determined. The maximum frequency of pore size for neat and crosslinked PANGMA-ENMs is found at about 1.4 µm. This maximum shifts to about 1 µm for crosslinked ENMs which have been stored in DMF for 72 hours at room temperature. The results correspond to those obtained from the SEM studies. After the treatment with DMF the nanofibers change their shape to ribbons thereby decreasing the inter-fiber distances and consequently, resulting in lower inter-fiber pore sizes.

Furthermore, it may be speculated whether a crosslinking temperature of 50 ℃ might induce a slight shrinkage of ENMs due to relaxations of frozen-in local stresses in the nanofibers. For the reduction after immersion in DMF, the swelling of the crosslinked ENMs will alter both the shape of nanofibers and the structure of the ENMs. The growth of the nanofibers caused by swelling will occupy part of the pore space, resulting in the reduction of pore size, and the shrinking of ENMs during the drying process after swelling will reduce the pore size too.

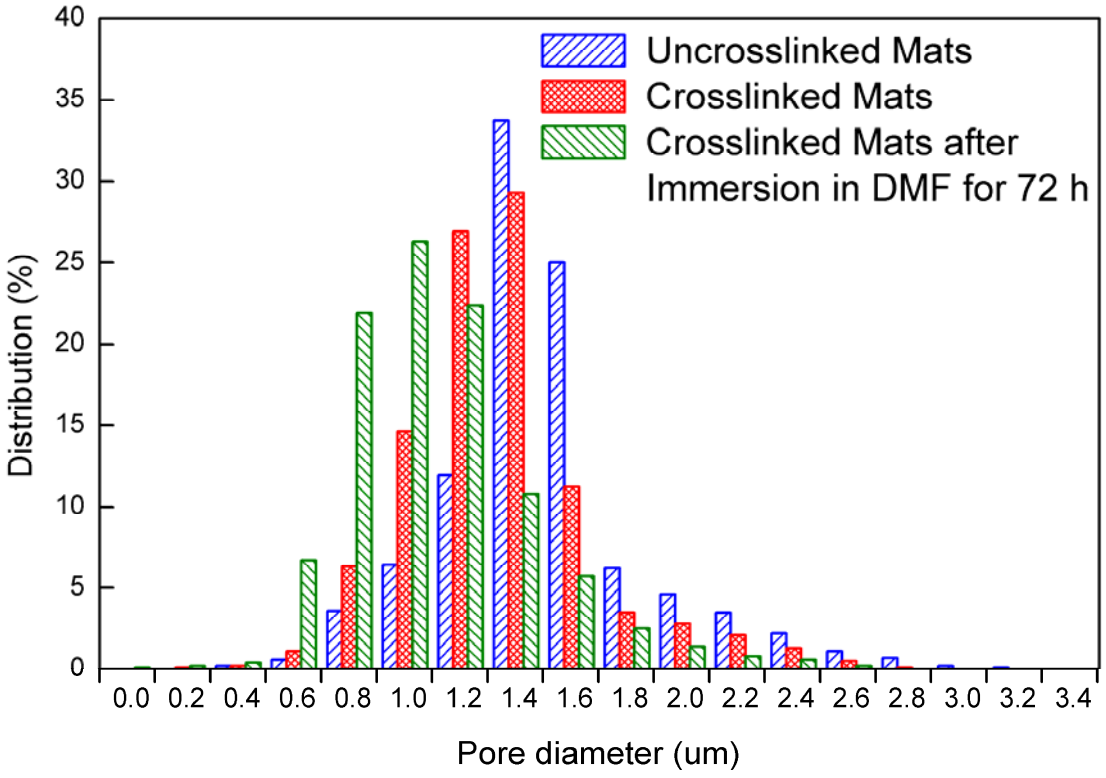

Figure 5.9 Pore size distribution of the neat and crosslinked PANGMA-ENM

5.4 Conclusions

In this chapter, we have demonstrated the preparation of a novel solvent resistant nanofibrous mat based on the electrospinning of PANGMA and the subsequent crosslinking of the nanofibers. PANGMA nanofibers were obtained by electrospinning PANGMA/DMF solutions with: solution concentration of 22 wt%,

applied voltage of 25 kV, feed rate of 1.5 mL/h, spinning distance of 25 cm and spinning time of 4 h. The fabricated ENMs have a uniform distribution of fiber size and are practically free of beads with the average diameter from 300 ~ 600 nm.

The as-spun PANGMA nanofibers can be successfully crosslinked by crosslinkers such as: different kinds of diamines and ammonia hydroxyl solution. Swelling test indicates that ammonia has much better crosslinking ability than all the diamines. The crosslinking temperature and time also have big influence on the crosslinking degree and the solvent resistance of PANGMA-ENMs. Within 3 hours of crosslinking time the weight loss of the crosslinked ENMs decreases dramatically with the increase of crosslinking time, while after 3 h crosslinking the weight loss almost keeps constant with the extension of the crosslinking time. FTIR spectrum shows that no peak near 908 cm^{-1} (epoxide peak) can be found after crosslinking, which further varifies the successful crosslinking of epoxy groups in PANGMA by ammonia. From the SEM pictures it also could be seen that there are no obvious deformation and break of nanofibers.

The crosslinked PANGMA-ENMs have better thermal stability than the neat ENMs. The glass transition temperature (T_g) of the ENMs increases from 98.7 ℃ of neat sample to 129.6 ℃ after 48 h crosslinking with ammonia. Meanwhile, the thermal decomposition temperature (T_d) of the ENMs also increases from 272.8 ℃ of neat sample to 335.1 ℃ of being crosslinked for 48 h.

The pore size of the PANGMA-ENM will reduce after being immersed into the solvents. The maximum frequency of pore size of the crosslinked ENMs shifts from

about 1.4 μm to about 1 μm after being stored in DMF for 72 hours at room temperature.

The optimal crosslinking condition is that crosslinking reaction carried out at 50 ℃ for 3 h by using 27 wt% ammonia hydroxide solution as the crosslinker. Crosslinked PANGMA-ENMs obtained under these conditions have weight loss below 2 wt% and very good thermal stability. Crosslinked PANGMA-ENMs have superior solvent resistance against most of the solvents which are commonly used in chemical and catalytic reactions, and therefore have potential as the solvent resistant membrane and the support for the immobilization of homogeneous catalysts and enzymes.

5.5 References

[1] L.S. White, J. Membr. Sci., 2006, 286, 26.
[2] X. Cao, X. Y. Wu, T. Wu, K. Jin, B. K. Hur, Biotechnol. Bioprocess. Eng., 2001, 6, 200.
[3] J. C. T. Lin, A. G. Livingston, Chem. Eng. Sci., 2007, 62, 2728.
[4] S. S. Luthra, X. J. Yang, L. M. Freitas dos Santos, L. S. White, A. G. Livingston, J. Membr. Sci., 2002, 201, 65.
[5] M. Mulder, Basic Principles of Membrane Technology, Kluwer Academic Publishers, Dordrecht, The Netherlands, 1997.
[6] J. A. Whu, B. C. Baltzis, K. K. Sirkar, J. Membr. Sci., 1999, 163, 319.
[7] C. A. McNamara, M. J. Dixon, M. Bradley, Chem. Rev., 2002, 102, 3275.
[8] M. Benaglia, A. Puglisi, F. Cozzi, Chem. Rev., 2003, 103, 3401.
[9] D. E. Bergbreiter, Chem. Rev., 2002, 102, 3345.
[10] Y. You, S. W. Lee, S. J. Lee, W. H. Park, Mater. Lett., 2006, 60, 1331.
[11] B. Ding, H. Y. Kim, S. C. Lee, C. L. Shao, D. R. Lee, S. J. Park, G. B. Kwag, G. K. J. Choi, J. Polym. Sci. Part B: Polym. Phys., 2002, 40, 1261.

[12] P. Gupta, S. R. Trenor, T. E. Long, G. L. Wilkes, Macromolecules, 2004, 37, 9211.

[13] R. M. Hodge, G. H. Edward, G. P. Simon, Polymer, 1996, 37, 1371.

[14] Y. Li, W. H. Thomas, G. E. Anthony, L. B. Gary, G. S. David, E. W. Gary, Chem. Mater., 2003, 15, 1860.

[15] P. Vandezande, L. E. M. Gevers, I. F. J. Vankelecom, Chem. Soc. Rev., 2008, 37, 365.

[16] B. D. Freeman, I. Pinnau, American Chemical Society, Washington, DC, 1999.

[17] K. Vanherck, P. Vandezande, S. O. Aldea, I. F. J. Vankelecom, Journal of Membrane Science, 2008, 320, 468.

[18] Z. W. Ma, M. Kotaki, S. Ramakrishna, J. Membr. Sci., 2006, 272, 179.

[19] Y. Z. Zhang, J. Venugopal, Z. M. Huang, C. T. Lim, S. Ramakrishna, Polymer, 2006, 47, 2911.

[20] S. H. Kim, S. Nair, E. Moore, Macromolecules, 2005, 38, 3719.

[21] F. Yi, Z. X. Guo, P. Hu, Z. X. Fang, J. Yu, Q. Li, Macromol. Rapid. Commun., 2004, 25, 1038.

[22] J. Zeng, H. Q. Hou, J. H. Wendorff, A. Greiner, Macromol. Rapid. Commun., 2005, 26, 1557.

[23] L. Li, Y. L. Hsieh, Polymer, 2005, 46, 5133.

[24] S. S. Choi, J. P. Hong, Y. S. Seo, S. M. Chung, C. Nah, J. Appl. Polym. Sci., 2006, 101, 2333.

[25] C. T. Wright, D. R. Paul, J. Membr. Sci., 1997, 129, 47.

[26] C. N. Dudley, B. Schöberl, G. K. Sturgill, H. W. Beckham, M. E. Rezac, J. Membr. Sci., 2001, 191, 1.

[27] L. Buttafoco, N. G. Kolkman, P. E. Buijtenhuijs, A. A. Poot, P. J. Dijkstra, I. Vermes, J. Feijen, Biomaterials, 2006, 27, 724.

[28] A. M. Mika, R. F. Childs, J. M. Dickson, B. E. McCarry, D. R. Gagnon, J. Membr. Sci., 1997, 135, 81.

[29] R. C. Ruaan, T. H. Wu, S. H. Chen, J. Y. Lai, J. Membr. Sci., 1998, 138, 213.

[30] H. G. Hicke, I. Lehmann, G. Malsch, M. Ulbricht, M. Becker, J. Membr. Sci., 2002, 198, 187.

[31] T. H. Dai, H. Yu, K, Zhang, M. F. Zhu, Y. M. Chen, H. J. Adler, J. Appl. Polym. Sci., 2008, 107, 2142.

[32] T. H. Dai, N. Miletić, K. Loos, M. Elbahri, V. Abetz, Macromolecular Chemistry and Physics, 2011, 212, 319.
[33] K. Ebert, D. Fritsch, J. Koll, C. Tjahjawiguna, J. Mem. Sci., 2004, 233, 71.
[34] Z. K. Zhong, Q. P. Guo, Polymer, 1998, 39, 3451.
[35] W. Gong, K. Zeng, L. Wang, S. X. Zheng, Polymer, 2008, 49, 3318.
[36] A. M. Atta, N. O. Shaker, N. E. Nasser, Journal of Applied Polymer Science, 2008, 107, 347.
[37] W. C. Shih, C. M. Ma, Journal of Applied Polymer Science, 1998, 69, 51.
[38] M. Grasselli, M. L. Carbajal, F. Yoshii, T. Sugo, Journal of Applied Polymer Science, 2003, 87, 1646.
[39] S. Brt, R. A. Goffe, S. B. Kessler, J. L. O'Connor, S. E. Zale, Biotechnology, 1988, 6, 779.
[40] S. Tsuneda, K. Saito, S. Furusaki, T. J. Sugo, J. Chromatogr., 1995, 689, 211.
[41] S. A. Camperi, A. A. Navarro del Canizo, E. E. Smolko, O. Cascone, M. Grasselli, Biotechnol. Prog., 1999, 15, 500.
[42] S. Zheng, H. Wang, Q. Dai, X. Luo, D. Ma, Macromol. Chem. Phys., 1995, 196, 269.
[43] T. J. Kemp, A. Wilford, O. W. Howarth, T. C. P. Lee, Polymer, 1992, 33, 1860.
[44] J. González-Benito, Journal of Colloid and Interface Science, 2003, 267, 326.
[45] A. Lopez-Quintela, P. Prendes, M. Pazos-Pellin, M. Paz, S. Paz-Abuin, Macromolecules, 1998, 31, 4770.
[46] M. J. Zohuriaan, F. Shokrolahi, Polymer Testing, 2004, 23, 575.
[47] K. J. Baranyai, G. B, Deacon, D. R. MacFarlane, J. M. Pringle, J. L. Scott, Australian Journal of Chemistry, 2004, 57, 2004, 145.

Chapter 6. PANGMA electrospun nanofibrous mat for the immobilization of *Candida Antarctica* Lipase B

6.1 Brief Introduction

As biocatalysts, enzymes exhibit a number of excellent features like high activity, high specificity and high selectivity, and also can catalyze many organic reactions under mild and environmentally friendly conditions.[1,2] Among a variety of enzymes, lipases are very popular ones and they are most useful in asymmetric synthesis.[3] Lipases can be applied into chemo-, regio- and stereoselective processes, such as kinetic resolution of racemic alcohols, acids, esters or amines and the desymmetrization of prochiral or meso compounds.[4,5] Other non-conventional processes such as Aldol reactions or Michael additions also can be catalyzed by some lipases.[5,6] *Candida antarctica* lipase B (Cal-B) has proven to be one of the most recognized and versatile member among the group of lipases.[7–9] Cal-B is among the best catalysts in the resolution of amines and the preparation of many amino compounds.[5] This enzyme has lots of outstanding advantages, including: good stability in acidic pH range, quality of end product, less side products and good performance at high temperatures. It can be used in a wide range of applications in chemical industry, such as: kinetic resolutions, aminolysis, esterification, and transesterification.[10–13]

However, most of the natural enzymes (of course also including Cal-B) will lose most of their powerful catalytic activity in organic solvents and also will easily denature under industrial conditions (high temperature, mechanical shear, etc.). Moreover, the direct recovery of enzymes from reaction solutions and the separation of enzymes

from substrates and products are generally difficult. These weak points and disadvantages of normal enzymes severely restrict their applications in many catalytical areas.[14-16]

Therefore, there have been many attempts aiming to stabilize enzyme activity and increase operational stability. Among them, enzyme immobilization is the most effective and popular strategy for most applications. Immobilization can, in general, improve the catalytic activity and selectivity of enzymes, in addition it can enhance the temperature and solvent stability, and the most important function is: immobilized enzymes can easily be recovered from the reaction medium and preferably be reused, which is particularly important because of the high enzyme costs.[17-19] Looking for an appropriate solid support and immobilizing enzyme on it properly is the topic which is being widely researched in all over the world. Numerous literatures have reported the development of the new support materials and the modification of existing supports.[20-22] In recent years nanostructured materials are widely used as the support for the immobilization of enzymes due to their large surface area which can effectively improve the enzyme loading per unit mass of support. Both nanoparticles and electrospun nanofibrous mats (ENMs) were attempted for this purpose.[23-26] In the cases of nanoparticles, for instance, Li et al.[27] covalently immobilized glucose oxidase (GOD) monolayer on the surface of gold nanoparticles (AuNPs) to fabricate bioconjugate complexes. The enzyme activity assays of the obtained bioconjugates display an enhanced thermostability and similar pH-dependence behavior in contrast with that of free enzyme. Šulek et al.[28] covalently immobilized cholesterol oxidase (ChOx) to magnetic nanoparticles of maghemite (γ-Fe_2O_3) and further functionalized by silica (SiO_2) and amino-silane molecules. The activity of the bound enzyme was

retained up to 60%. Miletić et al.[29] immobilized Cal-B on polystyrene (PS) nanoparticles and studied the hydrolytic activity of the immobilized Cal-B. Their results indicated that Cal-B immobilized on PS nanoparticles in buffer solution with pH 6.8 performed higher hydrolytic activity than pure enzyme powder and Novozyme 435. Nevertheless, nanoparticles have two common deficiencies: firstly, they have almost reached their upper limits concerning balancing the contradictory issues including surface area, diffusion resistance, and effective enzyme loading. Secondly and critically, their dispersion in reaction phase and subsequent recovery and recycling are often very difficult and complicated.[16,30-32]

On the contrary, compared with nanoparticles, electrospun nanofibrous mats (ENMs) have intrinsically high specific surface, inter-fiber porosity, easy handling and good mechanical strength, and most importantly, ENMs can be easily recovered from the catalytical reaction medium, which is of most benefit to the recycling and reusing of the enzymes. Therefore they are very suitable for the application on continuous operations.[33-36] The immobilization of enzymes on both natural and synthetic polymeric ENMs has been widely reported.[37–44] For instance, Ignatova et al.[37] electrospun novel bicomponent poly(styrene-*alt*-maleic anhydride) / poly(styrene-*co*-maleic anhydride) (P(St-*alt*-MA)/P(St-*co*-MA)) ENMs containing targeted amount of reactive maleic anhydride groups, and then immobilized laccase from Trametes versicolor was covalently attached onto. Results showed that the average amount of immobilized enzyme was 40 ± 0.7 mg/g mat. The catalytic activity of the immobilized enzyme was very high and more encouragingly it remained stable for about 30 successive reuses. Ye et al.[40] electrospun poly(acrylonitrile-*co*-maleic acid) (PANCMA) containing reactive carboxyl groups and covalently immobilized Lipase

from Candida rugosa onto the membrane surface. The enzyme loading and the activity retention of the immobilized lipase on the ENM were 21.2 ± 0.7 mg/g and 37.6%, respectively. This lipase-immobilized ENM can be used as biocatalysts for polyester synthesis. Huang et al.[43] fabricated ENMs from mixed chitosan/poly(vinyl alcohol) (PVA) solution by an electrospinning process. Lipase from Candida rugosa was immobilized on this ENM using glutaraldehyde (GA) as coupling reagent. Results showed that the observed lipase loading on this ENM was up to 63.6 mg/g and the activity retention of the immobilized lipase was 49.8% under the optimum condition. The reusability, pH stability, storage stability and thermal stabilities of lipase were obviously improved after immobilization.

PANGMA has the advantage of the further reacting ability from the free and active epoxy group on the GMA part on its chain. The epoxy group offers the opportunity for the employment of PANGMA on a variety of activation/coupling chemistries for the covalent binding of enzymes. An effective covalent binding of enzymes on the support not only can enhance the solvent and thermal abilities of the immobilized enzymes, but also can make the efficient reuse and recycling of the enzymes come to reality.[45,46] Godjevargova et al.[47] cast PANGMA ultrafiltration membrane by phase-inversion method and used this membrane as a carrier for the immobilization of glucose oxidase. They proved that the immobilized glucose oxidase has similar or even better activity comparing to the free enzyme, and much better operational stability, reusability and storage stability. After that, they successively immobilized glucose oxidase onto ultrafiltration membranes made from different acrylonitrile copolymers and used them for the catalytic application.[48-50]

In this chapter, we describe the fabrication and property for a novel Cal-B immobilized PANGMA-ENM, which can be obtained by two steps, first electrospinning PANGMA/DMF solution and second a chemical immobilization of Cal-B via activation and covalent binding. The enzyme loading, enzyme leaching, catalytical activity, pH value of immobilization, immobilization temperature, immobilization time, reusability, thermal and storage stability of the immobilized enzyme are investigated, described and discussed in detail. This novel Cal-B immobilized PANGMA-ENM has potential applications in the field of enzymatic catalysis.

6.2 Experimental

6.2.1 Materials

Poly(acrylonitrile-*co*-glycidyl methacrylate) (PANGMA) was synthesized by Helmholtz-Zentrum Geesthacht with a molecular weight (M_n) of ca. 100,000 g/mol and GMA contents of 13 mol%.[45] *Candida antarctica* lipase B (Cal-B) in the form of a dried powder was purchased from BioCatalytics Co. (Grambach, Austria). Novozyme 435 was provided by Novozymes® (Bagsværd, Denmark). Hexamethylenediamine (HMDA), glutaraldehyde solution (25 wt.%) (GA), phosphate buffered saline (PBS) and *p*-nitrophenyl acetate (*p*NPA) were purchased from Sigma-Aldrich Co. Ammonium hydroxide solution (27 wt.%) (Ammo) was purchased from Fluka Co. N'N-dimethylformamide (DMF), methanol and 1,4-dioxane were purchased from Merck KGaA. All the chemicals were directly used without purification.

6.2.2 Preparation of PANGMA-ENMs via electrospinning

PANGMA was dissolved in DMF at room temperature under moderate stirring for 48 h to form a homogeneous solution. The solution concentration was fixed to 20 wt%. The solution was placed in a 5 mL glass syringe with a metal needle with the inner diameter of 0.8 mm. A high voltage generator was connected to the middle of needle. A rectangular counter electrode covered with aluminium foil was used as the collector. Typically, electrospinning was performed at the applied voltage of 25 kV. The working distance (the distance between the needle tip and the collector) was 25 cm. The feed rate of the solution was controlled by a syringe pump (HARVARD PHD 4400, Harvard Apparatus Co.) to maintain at 1.2 mL/h and the electrospinning time was usually 5 h to obtain sufficient thickness of the ENM. After electrospinning, the ENM was detached and washed with methanol and distilled water to remove DMF and other impurities, and then was dried under vacuum at 30 ℃ for 24 h.[51]

6.2.3 Enzyme immobilization[34,51]

The immobilization of Cal-B on PANGMA-ENM was carried out by covalently binding Cal-B molecules to the epoxy groups on PANGMA via three different routes (Figure 6.1).

Route 1: Indirect enzyme immobilization with HMDA and GA

PANGMA-ENMs were first immersed in 10 wt.% HMDA aqua solution at room temperature for 1 h. Then the ENMs were washed with distilled water for several times. The washed ENMs were immersed in 10 wt.% GA aqua solution at 4 ℃ for another 1 h. After that, the activated PANGMA-ENMs were extensively and carefully

washed with distilled water and PBS buffer (PH 6.8) until total removal of unreacted HMDA and GA.

Enzyme immobilization was performed in lidded bottles loaded with Cal-B solution prepared with the concentration of 5 mg/mL in buffer solution with different pH values. The activated PANGMA-ENMs were immersed into the Cal-B solution and the mixture was shaken at 4 ℃, room temperature (RT, 20 ℃) and 30 ℃ for up to 32 h. After reaction, the ENMs were taken out and washed several times with PBS buffer (pH 6.8) under shaking condition until the complete removal of unbound enzymes. All the supernatants and washing solutions were collected carefully for the determination of enzyme loading capacity. The amount of residual protein after immobilization was determined by Bradford's method.[52] Bovine serum albumin (BSA) was used as the standard to construct the calibration curve. The amount of immobilized protein onto the nanomats was estimated by deducting the amount of residual protein from the initial amount of protein used in the immobilization procedure (5 mg/mL). The enzyme loading capacity was defined as the amount of bound protein (mg) per gram of the enzyme immobilized PANGMA-ENM. Each reported value was the average of at least three experimental values.

Route 2: Indirect enzyme immobilization with Ammo and GA

Route 2 was carried out by the same technique as by route 1 but changing HMDA to ammonia aqua solution (27 wt.%) (Ammo). The ammonolysis was performed at 50 ℃ for 1 h.

Route 3: Direct enzyme immobilization

The direct immobilization was carried out by the same technique with route 1 except for the activation treatment with HMDA and GA.

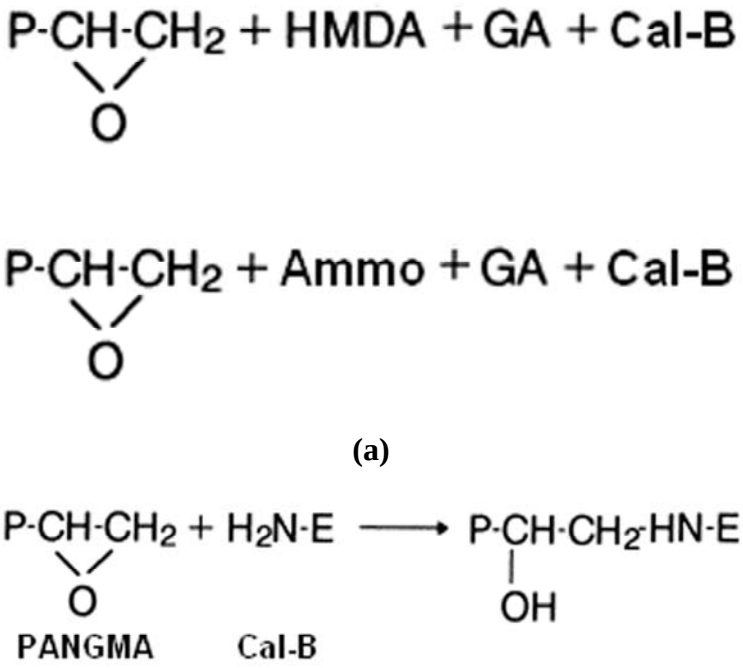

(a)

(b)

Figure 6.1 Different routes of immobilizing Cal-B onto PANGMA-ENMs: (a) indirect immobilizations; (b) direct immobilization[47]

6.2.4 Enzyme leaching test

The leaching of the immobilized Cal-B was investigated and characterized by the leaching test. A self-made water recycling setup (Figure 6.2) was built and used for the leaching test and the measurement of water flux. It consisted of several parts: a module (D) in which the membrane sample was placed, a pump (B) to drive the recycling water, a vessel (A) for loading the water, and a valve (E) was installed to control the flux direction. During the measurement, 500 mL deionized water was first loaded in the vessel and then passed through the sample and recycled by the pump for up to 168 hours.

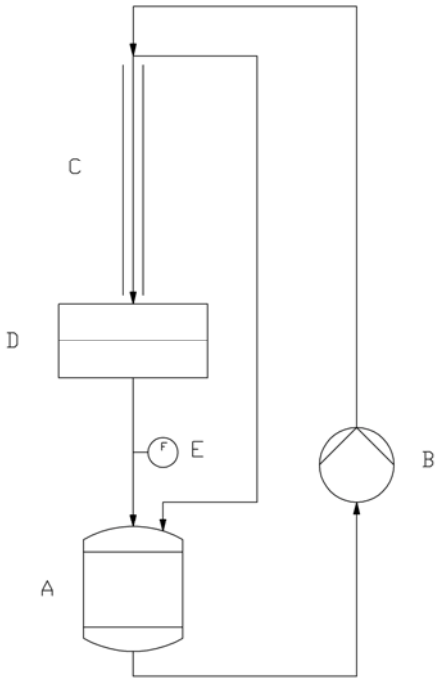

Figure 6.2 Water recycling setup for enzyme leaching test and water flux measurement

The Cal-B leaching was characterized by measuring the amount of dissociated Cal-B in the water flow by Bradford's method. Cal-B leaching was defined and calculated by:

$$L = (W_0 - W_t) / W_0 \times 100\% = W_{lt} / W_0 \times 100\% \quad (6\text{-}1)$$

where L is the enzyme leaching (wt%), W_0 (mg) is the initial amount of the bound Cal-B on PANGMA-ENM, W_t (mg) is the remaining amount of the bound Cal-B on ENM at the moment of t (t represents the time of leaching test progressing), W_{lt} is the amount of dissociated Cal-B in water at the moment of t (mg).

The water permeability of the Cal-B immobilized PANGMA-ENM was characterized by measuring the volume of the permeated water as a function of consumed time. Water flux was calculated by the following equation:

$$J = Q / (A \cdot \Delta t) \quad (6\text{-}2)$$

where J is the water flux (L m^{-2} s^{-1}), Q is the volume of the permeated water (L), A is the effective permeation area of the PANGMA-ENM in permeability measurement (m^2), Δt is the permeation time (s).

6.2.5 Hydrolytic activity assay of free and immobilized Cal-B

A 1,4-dioxane solution (5 ml) containing *p*NPA (40 mM) and methanol (80 mM) was added to 20 ml vials containing 0.500 mg of enzyme. The assay reactions were carried out for 50 min at 35 ℃ (250 rpm) and were terminated by removal of the enzyme by filtration. The concentration of the reaction product *p*-nitrophenol (*p*NP) was determined by UV-vis spectrophotometry (HITACHI U-3000, HITACHI) at λ_{max} (304 nm) of *p*NP. Enzyme hydrolytic activities for immobilized Cal-B are defined herein as the nanomoles of *p*NPA hydrolyzed in 1,4-dioxane per unit of weight of enzyme per time (nmol of *p*NP/min mg).[29,34,51]

6.2.6 Reusability, thermal stability and storage stability[34,51]

The reusability of the Cal-B immobilized PANGMA-ENMs was examined by a recycling hydrolytic activity assay. After each recycling reaction run, the immobilized ENMs were washed several times with PBS buffer (pH 6.8) to remove any residual substrates on the ENMs. The recycled ENMs were subjected to the new hydrolytic activity assay for the next cycle and so on. Activity retention was given as percentage of activity taken as 100% for the initial hydrolytic activity before recycling.

Thermal stabilities of Cal-B immobilized PANGMA-ENMs and free Cal-B were determined by incubating them in PBS buffer (pH 6.8) at 60 ℃ for 10 h. Periodically,

the samples were withdrawn and their residual hydrolytic activities were determined. Activity retention was given as percentage of activity taken as 100% for the initial hydrolytic activity before incubation.

Storage stabilities of Cal-B immobilized PANGMA-ENMs and free Cal-B were determined by storing them in PBS buffer (pH 6.8) at 4 ℃ for 30 days. The residual hydrolytic activities of the samples were measured at intervals of 1 to 5 days within the 30 days. Activity retention was given as percentage of activity taken as 100% for the initial hydrolytic activity before storage.

6.2.7 Measurements and characterizations

The morphology of the neat and Cal-B immobilized PANGMA nanofibers and ENMs was observed with a scanning electron microscope (LEO Gemini 1550 VP, Zeiss) at 10 kV accelerating voltage after sputter-coating with Au/Pd. The average diameters of the nanofibers were calculated from 10 different randomly chosen single values.

The structure of both neat and Cal-B immobilized PANGMA nanofibers and ENMs was characterized by Attenuated Total Reflection Fourier transform infrared spectroscopy (ATR-FTIR) with a FTIR spectrophotometer (Bruker Equinox 55, Bruker Optics) in the mid-infrared range from 4000 to 500 cm^{-1}.

6.3 Results and discussions

6.3.1 Fabrication of PANGMA-ENMs by electrospinning

In this work, PANGMA with GMA content of 10 mol% was electrospun into nanofibers. The morphology of the PANGMA nanofibers before and after Cal-B

immobilization was observed by using the scanning electron microscope. As shown in figure 6.3(a), an almost homogeneous network of the electrospun nanofibers with diameters in the range of 150 to 300 nanometers was obtained when the electrospinning solution concentration was 20 wt.% and the applied voltage was 25 kV. The nanofibers show a smooth surface and a uniform body with a narrow distribution of fiber diameter.

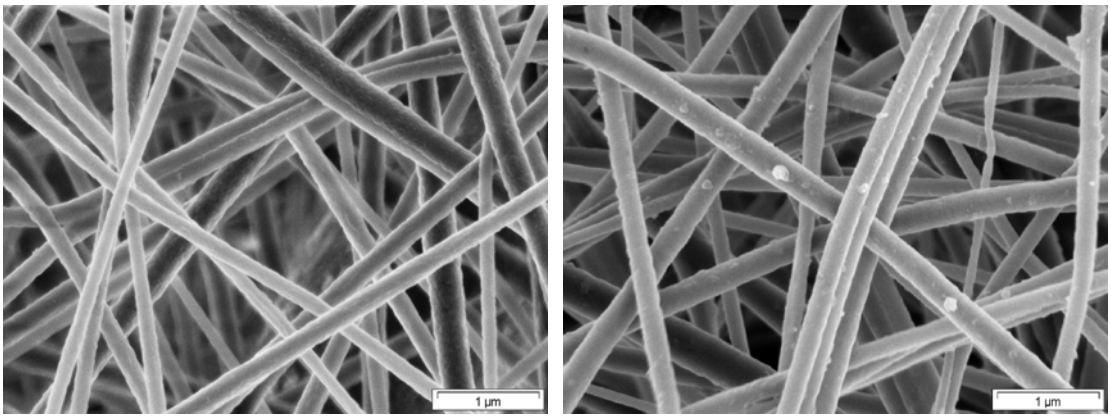

Figure 6.3 SEM micrographs of the PANGMA nanofibers: (a) neat nanofibers; (b) Cal-B immobilized nanofibers

From the SEM photo of Cal-B immobilized nanofibers (figure 6.3(b)) it can be found that the morphology of the nanofibers remains uniform and the structure of the ENMs remains complete after Cal-B immobilization reaction and washing with PBS buffer. As mentioned in introduction, PANGMA has a good chemical stability and mechanical strength. It is quite stable during the Cal-B immobilization reaction and the following hydrolytic activity assay.

6.3.2 Covalent immobilization of Cal-B onto PANGMA-ENMs

It is well known that the amount of immobilized enzyme and its activity depends on the physical and chemical structure of the carriers. PANGMA-ENMs contain epoxy

groups which are very suitable for direct and indirect immobilization of Cal-B. For indirect immobilization, PANGMA-ENMs were first modified with HMDA/Ammo (spacers) in order to introduce amine groups into their structure. The presence of amine groups is needed for the further GA activation. For direct immobilization, PANGMA-ENMs were directly coupled with Cal-B without any modification (Figure 6.4). The properties (enzyme loading and leaching, hydrolytic activity, reusability, thermal stability, storage stability, etc.) of the Cal-B immobilized PANGMA-ENMs prepared by different routes are compared and discussed.

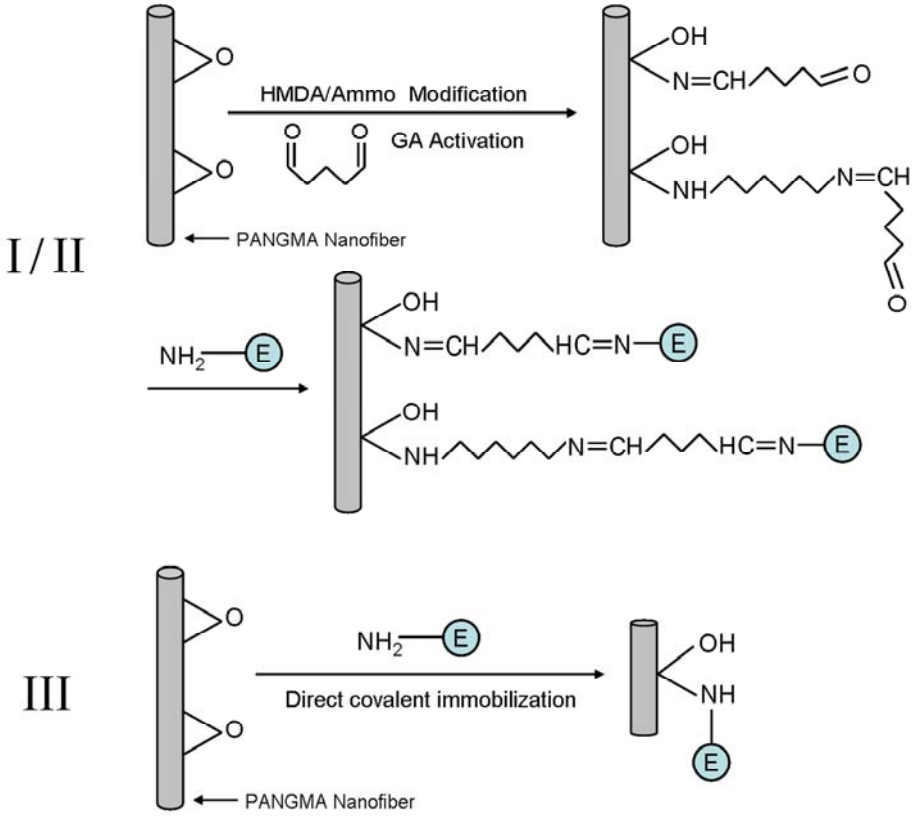

Figure 6.4 Schematic diagram for the pre-modification of the PANGMA-ENM support and the immobilization of Cal-B

FTIR results show the successful immobilization of Cal-B on PANGMA nanofiber. Figure 6.5 shows the FTIR spectrum of neat (curve (a)) and Cal-B immobilized (curve (b)) PANGMA nanofibers. It could be observed that first on curve (a) there is a clear

peak near 908 cm^{-1} (characteristic peak of epoxy group), which shows the existence of epoxy groups in neat PANGMA nanofibers. Meanwhile in curve (b), the epoxy peak is sharply diminished, which proves that epoxy groups in PANGMA have been reacted with Cal-B. In addition, a single peak near 1650 cm^{-1} represents the existence of secondary aldimine (RCH＝NR′), which is the result of the imine formation reaction between the amine groups in modified PANGMA nanofibers and Cal-B and the aldehyde groups in glutaraldehyde. A double peak near 3300 cm^{-1} and a single peak near 1550 cm^{-1} both show the evidence of secondary amine, which is generated during the opening of the epoxy group by the immobilization of Cal-B. A peptide peak at 2180 cm^{-1} and two peaks near 2000 cm^{-1} give the direct information of the Cal-B structure. Finally, a peak near 3600 cm^{-1} is the characteristic peak of the hydroxyl group converted from the epoxy group and the primary amine during the immobilization reaction (Figure 6.4).

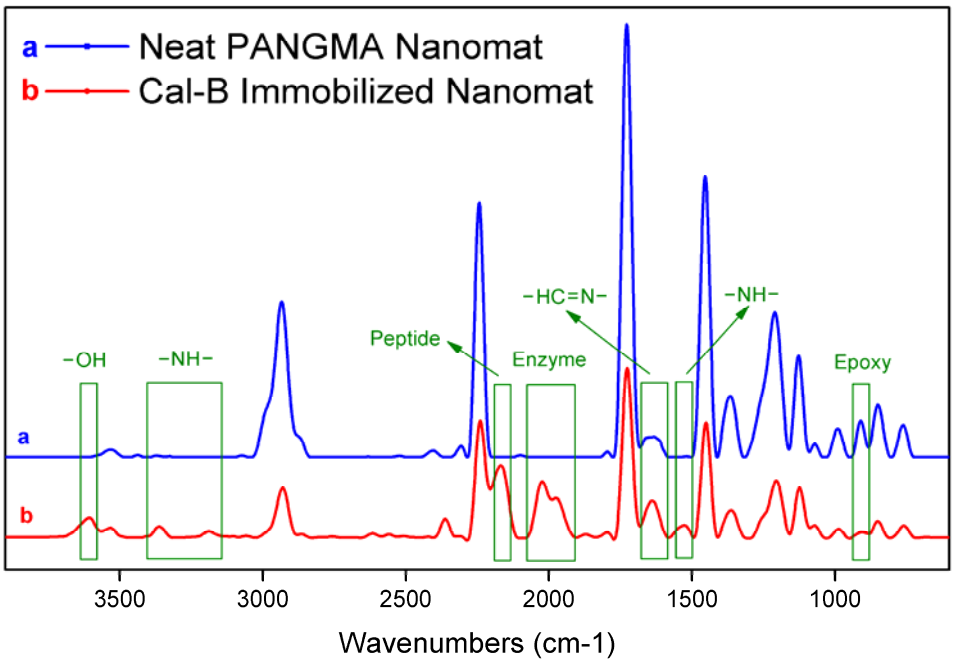

Figure 6.5 FTIR spectrum of neat (curve (a)) and Cal-B immobilized (curve (b)) PANGMA nanofibers, immobilized nanofibers prepared by HMDA and GA activation and immobilization in 5mg/mL Cal-B/PBS solution at 4 ℃

Moreover, it also can be seen clearly from the SEM photo of the Cal-B immobilized PANGMA-ENM (figure 6.3(b)) that there are some small agglomerations of Cal-B on the surface of the nanofibers after Cal-B was immobilized. This result also verifies the successful binding of the Cal-B onto the PANGMA-ENMs.

6.3.3 Cal-B loading

Figure 6.6 shows the Cal-B loading of samples prepared via different immobilization routes at different immobilization temperatures. For each sample studied, immobilization saturation is achieved within 10 h. It is obvious from figure 6.6(a) that GA activation can enhance the Cal-B loading of the PANGMA-ENMs (detailed data seen in table 6.1). ENMs with GA activation have much higher amount of bound Cal-B than those prepared by direct immobilization. As modifiers, HMDA and ammonia do not show significant differences in the amount of bound Cal-B. Samples modified with HMDA only give a little bit higher Cal-B loading than those modified with Ammo. It is reported that GA-activated epoxy resins attach more enzymes than epoxy resins themselves. For instance, López-Gallego et al.[53] immobilized glutaryl-7-aminocephalosporanic acid acylase (GAAA) onto both GA-activated and standard epoxy Sepabeads and found that 100% immobilization yield could be obtained for GA-activated epoxy Sepabeads whereas only 75% immobilization yield was got for standard one. Their reported results are consistent with the results we have obtained.

The immobilization temperature seems to have limited influence on the Cal-B loading (figure 6.6(b)). This behavior is due to the high reactivity between Cal-B and the GA molecules introduced onto PANGMA nanofibers, and therefore the effect of the

temperature does not play an important role on the loading. Nevertheless, small difference between immobilization temperatures is noticeable.

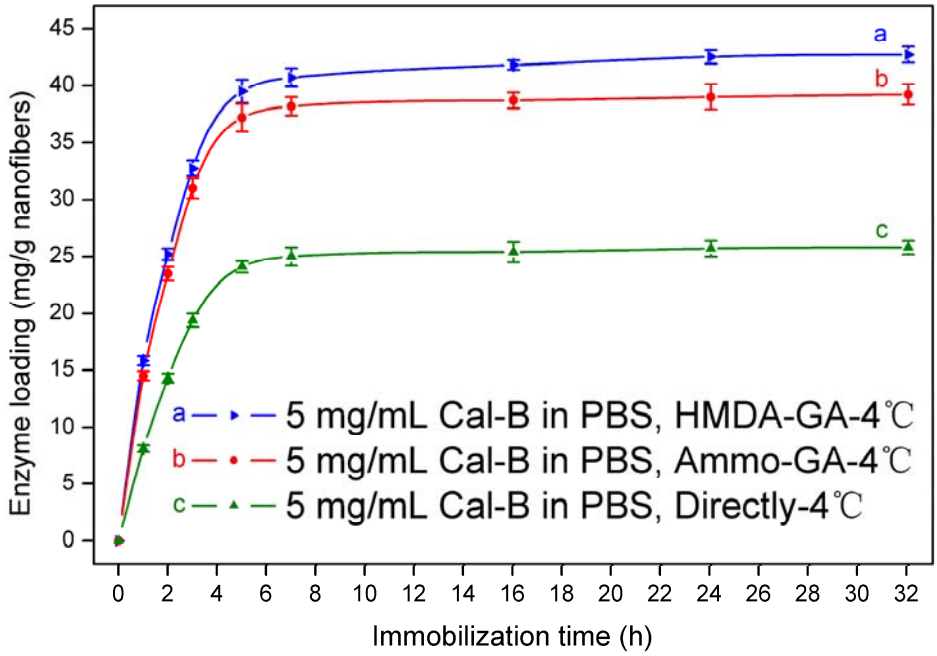

(a)

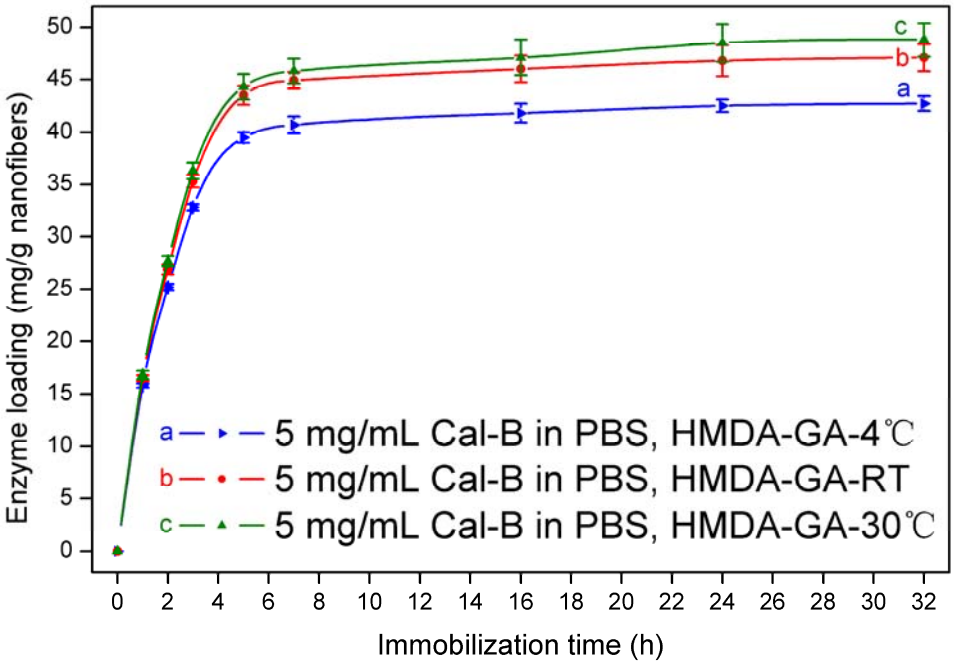

(b)

Figure 6.6 Comparison of enzyme loading of Cal-B immobilized PANGMA-ENMs: (a) via different immobilization routes; (b) at different immobilization temperature

6.3.4 Cal-B leaching

One of the most important advantages of the covalently immobilized enzymes is that covalently binding could effectively prevent the leaching of the enzymes compared with physical immobilization methods. The leaching of the immobilized Cal-B was investigated and measured by the leaching test. Figure 6.7 shows the Cal-B leaching of Cal-B immobilized onto PANGMA-ENMs with different immobilization routes. It is obvious that all these covalently immobilized Cal-B have very good stabilities in water. The highest leaching is below 4.5 wt% after very long time recycled in water (168 hours). Samples with GA activation have little bit higher leaching than the one without any activation. This is probably because GA activation improves the absorption ability of PANGMA-ENMs to Cal-B. It is clear that leaching is derived from the elution of those physically absorbed enzymes when the ENMs are impacted by the water flow during their performance. Samples with pre-modification and GA activation certainly absorb more Cal-B than the unactivated one during the immobilization, which results in the subsequently higher leaching of those physically absorbed Cal-B of GA activated samples.

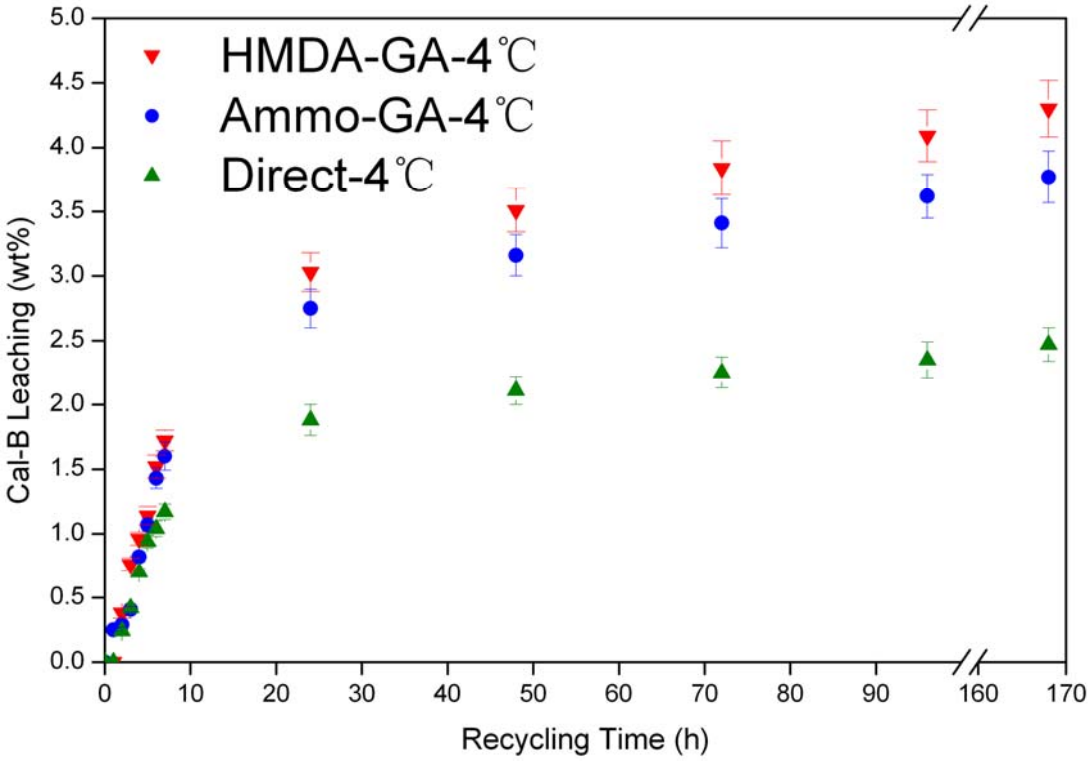

Figure 6.7 Comparison of enzyme leaching of Cal-B immobilized PANGMA-ENMs prepared with different immobilization routes

The water permeability of the Cal-B immobilized PANGMA-ENMs was characterized by water flux measurement. Figure 6.8 shows the water flux of samples with different immobilization methods on different recycling time. It can be found that the water flux of all the samples only slightly decreases after long time recycled in water, which indicates that no obvious fouling of the samples happens. The sample prepared with direct Cal-B immobilization has slightly higher water flux than the GA activated ones. The possible reason is that GA activated samples have much higher Cal-B loading, which will lead to more aggregations of Cal-B on the surface of PANGMA nanofibers. These Cal-B aggregations will somehow decrease the pore size of the ENM and perhaps also block up part of the pores, which results in the worse water permeability of these GA activated samples.

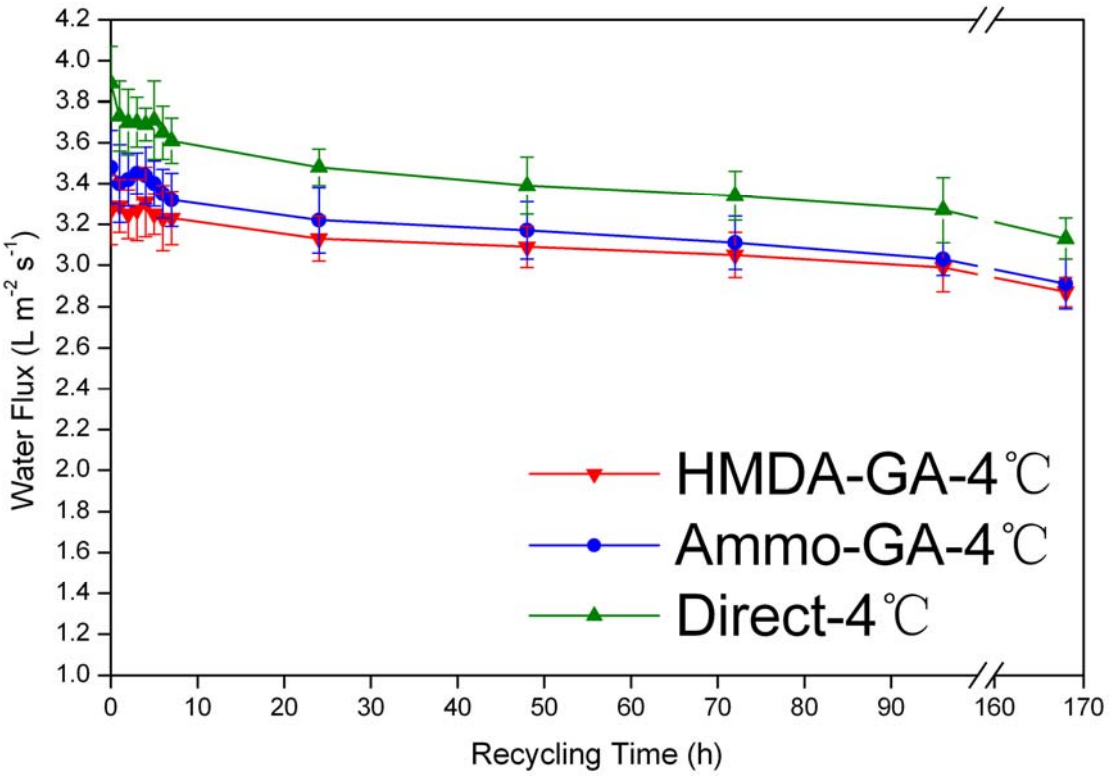

Figure 6.8 Water flux of different Cal-B immobilized PANGMA-ENMs recycled in water for up to 168 hours

Thus these Cal-B immobilized PANGMA-ENMs have very low Cal-B leaching and good water permeability after being served in water for quite a long time. They have much higher stability than those physically immobilized enzymes.

6.3.5 The hydrolytic activity of Cal-B immobilized PANGMA-ENMs

All these Cal-B immobilized PANGMA-ENMs were studied to assess how these parameters (pH value, temperature, recycling times, storage environment, etc.) affect their hydrolytic activity (hydrolysis of *p*-nitrophenol acetate).

Table 6.1 Cal-B immobilization on PANGMA-ENMs with different immobilization routes at different immobilization temperatures for 24 h: enzyme loading and hydrolytic activity

Catalyst	Modification	Activation	Immo. temp. (℃)	Enzyme loading (mg/g fiber)	Hydrolytic activity (nmol pNP/min mg Cal-B)
H-G-4	Hexamethylenediamine	Glutaraldehyde	4	42.1 ± 0.7	2285.6 ± 45.1
H-G-RT	Hexamethylenediamine	Glutaraldehyde	20	46.0 ± 1.3	2403.3 ± 72.5
H-G-30	Hexamethylenediamine	Glutaraldehyde	30	47.3 ± 1.6	2555.2 ± 60.6
A-G-4	Ammonia	Glutaraldehyde	4	38.6 ± 0.9	1995.3 ± 57.4
A-G-RT	Ammonia	Glutaraldehyde	20	42.5 ± 1.4	2037.4 ± 48.9
A-G-30	Ammonia	Glutaraldehyde	30	43.7 ± 1.1	2144.5 ± 69.3
D-4	/	/	4	25.7 ± 0.6	1691.9 ± 65.2
D-RT	/	/	20	28.8 ± 0.8	1775.2 ± 55.0
D-30	/	/	30	29.5 ± 0.8	1836.1 ± 81.6
Cal-B powder	/	/	/	/	1551.8 ± 32.9
Novozyme 435	/	/	/	200[61]	2457.9 ± 29.9

Table 6.1 shows the immobilization conditions and working parameters of all the ENMs studied in this chapter. For comparison purpose, hydrolytic activity results of free Cal-B powder and commercially available Cal-B preparation, Novozyme 435, are also included. As the Cal-B loading, also the hydrolytic activity is highly influenced by the immobilization route. Indirect immobilization (with pre-modification and GA activation) is found to give higher hydrolytic activity to the Cal-B immobilized PANGMA-ENMs than the direct immobilization. ENMs modified with HMDA show advantages on the hydrolytic activity than those modified with ammonia. Hydrolytic activity also increases a little bit with the increase of immobilization temperature. Results in table 6.1 indicate that Cal-B immobilized on all ENMs studied perform much higher hydrolytic activity than free enzyme powder. Furthermore, Cal-B

immobilized at 30 ℃ on PANGMA-ENM modified with HMDA has higher activity than Novozyme 435.[54]

6.3.6 Determination of proper pH value of the buffer solution for the optimal catalytic activity

It is well known that the pH value of the buffer solution for immobilization will affect the activity of the immobilized enzymes. Cal-B immobilization was carried out at different pH values and the optimal value was determined. The variation of the activity retention for the Cal-B immobilized PANGMA-ENMs with the pH value is given in figure 6.9. Here, the activity retention was defined as the percentage ratio of initial activity to the maximum initial activity achieved in this set. It can be seen that Cal-B immobilization in the pH range of 6.0–7.5 provided relatively high activity values. This is because the enzyme conformation, which is essential for the enzymatic activity, changes with different pH values. It is well known that the behavior of an enzyme molecule, such as conformation, is susceptible to its vicinal microenvironment. An alteration of the pH value results in a possible influence on the immediate vicinity of the enzyme environment. By this way, the pH value of the buffer solution finally affects the activity of the enzymes.[29,55-57] Therefore, there was an optimal pH value for enzyme activity in the enzyme immobilization process. In this case, the highest activity was observed at a pH 6.8, for all the samples prepared from the three different routes. This result is consistent with the previous work on the immobilization of Cal-B on polystyrene nanoparticles by physical adsorption.[29] Since the highest hydrolytic activity was found under the pH = 6.8, all other steps of this work were carried out at this pH value.

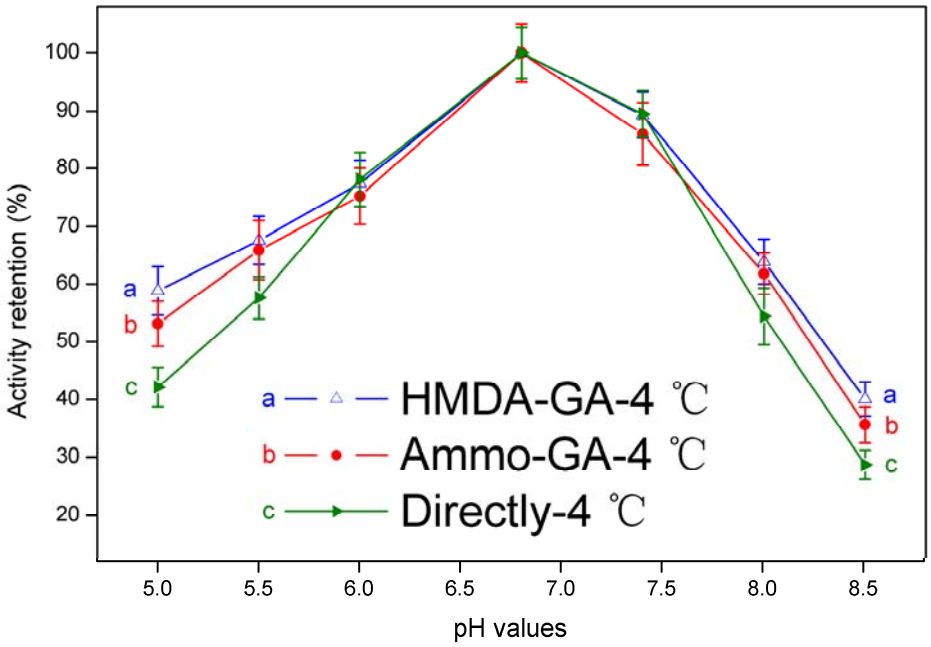

Figure 6.9 Hydrolytic activity of Cal-B immobilized PANGMA-ENMs versus pH value of the buffer solution used during immobilization

6.3.7 Reusability of Cal-B immobilized PANGMA-ENMs

The reusability of the immobilized enzymes is of importance for their practical application because of the sustained costliness of the enzymes. The effect of repeated use on the activity of Cal-B immobilized PANGMA-ENMs is presented in figure 6.10. The activity retention of the sample prepared with HMDA and GA at 4 ℃ was chosen as a representative since all the samples prepared under different conditions showed almost the same behavior and activity retention in reusability measurements. It can be found that the activity of the Cal-B immobilized ENM decays when being recycled. The ENM maintained about 72% of its initial activity after 5 cycles, about 60% after 10 cycles, and about 51% after 15 cycles, respectively. Such reusability is advantageous for the continuous use in industrial applications. The loss of activity could be explained by the inactivation of the enzyme due to the denaturation of protein and the less leakage of enzyme from the ENMs supports upon the repeated use.

The leaching of the residual surface-adsorbed enzymes could also decrease the activity during the first few cycles.[58]

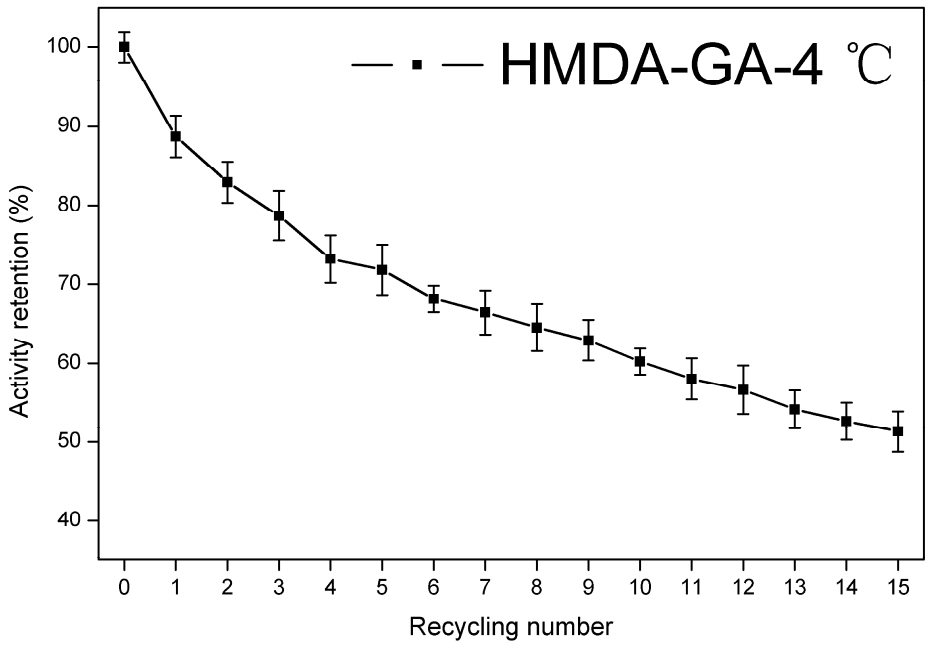

Figure 6.10 Reusability of the Cal-B immobilized PANGMA-ENMs (activated with HMDA and GA, immobilized in PBS buffer at 4 ℃)

6.3.8 Thermal stability of Cal-B immobilized PANGMA-ENMs

The drawback on the thermal stability of native enzymes is one of the most important limitations for their application in continuous reactors. It has been reported in several articles that the activation and the covalent binding between the enzyme and support can enhance the thermal stability.[55,59,60] Therefore, the thermal stability at 60 ℃ of Cal-B immobilized PANGMA-ENMs and free Cal-B were studied in this work. Fig. 6.11 shows the activity retentions of the Cal-B immobilized ENMs and the free Cal-B under the incubation at 60 ℃. It can be seen that the free Cal-B almost loses all of its initial activity after 2 h, while the Cal-B immobilized ENMs prepared from three different routes retain their initial activities of about 96% for HMDA-GA, 95% for Ammo-GA and 88% for direct immobilization after 2h heat incubation, respectively.

Even after 10 h incubation, all three Cal-B immobilized ENMs still maintain over 65% of their initial activities. These results indicate that the Cal-B immobilized ENMs are much more stable at high temperature than the free Cal-B. This also could be explained by the multipoint attachment of the Cal-B molecules with the epoxy groups on the ENMs. The formation of multiple covalent bonds between the enzyme and the ENMs supports restricts the conformation transition of the enzyme, resulting in the reduction of mobility and the protection of distortion of the enzymes at high temperature. This protects the enzymes from thermal deactivation.[55,56]

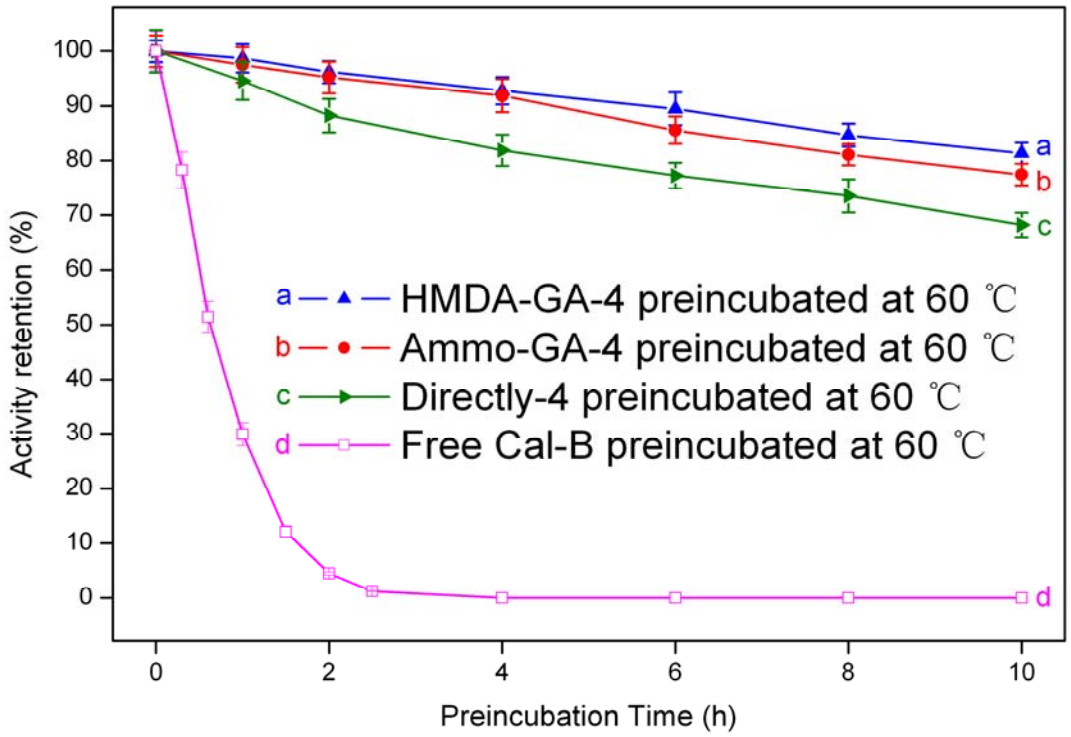

Figure 6.11 Thermal stabilities of Cal-B immobilized PANGMA-ENMs (curve a,b,c) and free Cal-B (curve d), preincubated in PBS buffer at 60 ℃

6.3.9 Storage stability of Cal-B immobilized PANGMA-ENMs

Storage stability of the immobilized enzymes is one of the significant parameters to evaluate the properties of enzyme, which can greatly benefit the transportation and storage of the immobilized enzymes. Figure 6.12 shows the activity retentions of the

Cal-B immobilized PANGMA-ENMs and the free Cal-B. Since there is no obvious difference of retentions among the Cal-B immobilized ENMs prepared under different conditions, the retention of the sample prepared with HMDA and GA at 4 ℃ is shown as a representative. It is obvious that as the time of storage increases, there is a remarkable difference in the activity retentions between the Cal-B immobilized ENM and the free one. The immobilized ENM still retained about 77% of its initial activity after being stored in PBS buffer (pH 6.8) at 4 ℃ for 30 days, while the free Cal-B lost most of its initial activity after the same period of time. This indicates that immobilization can prolong the storage period and consequently increase the service life of enzyme.[61] The good storage stability of Cal-B immobilized ENMs could be attributed to two reasons: first the covalent bonds between Cal-B and PANGMA nanomat support prevent the structural denaturation of the enzymes; and second the leaching of Cal-B is effectively held back by the firm covalent bonds.[55,61,62]

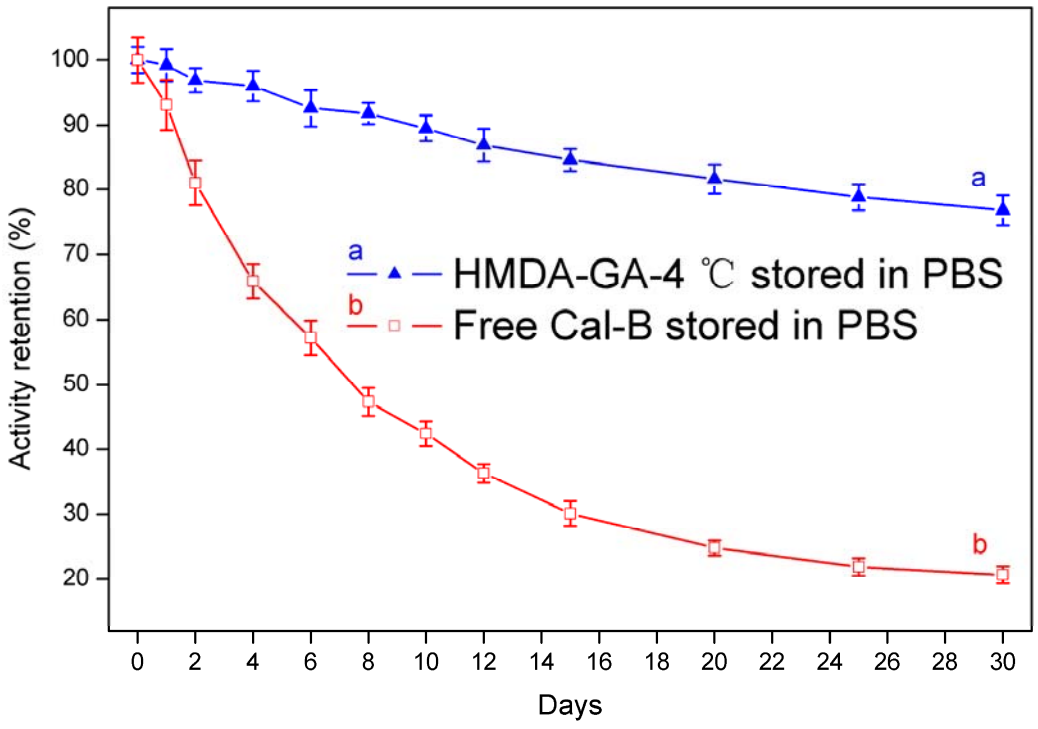

Figure 6.12 Storage stability of Cal-B immobilized PANGMA-ENM (curve a) and free Cal-B (curve b) in PBS buffer at 4 ℃ for 30 days

6.4 Conclusions

Poly(acrylonitrile-*co*-glycidyl methacrylate) (PANGMA) nanofibers and ENMs with the fiber diameter of 200 to 300 nanometers were fabricated by electrospinning a 20 wt.% PANGMA/DMF solution at the applied voltage of 25 kV. *Candida antarctica* lipase B (Cal-B) was covalently immobilized onto the PANGMA-ENMs via three different immobilization routes: (i) activated with hexamethylenediamine (HMDA) and glutaraldehyde (GA), (ii) activated with ammonia (Ammo) and GA, and (iii) direct immobilization.

SEM and FTIR results indicate that the Cal-B has been successfully immobilized onto PANGMA nanofibers. For immobilization, the best concentration of Cal-B/PBS solution is 5 mg/mL. ENMs with pre-modification and GA activation have higher Cal-B loading than those without activation. The observed Cal-B loading on these GA activated PANGMA-ENMs is up to approximately 50 mg/g. All the Cal-B immobilized ENMs have very low Cal-B leaching and good water permeability. Even after being served in water for 168 hours, the Cal-B leaching of all the ENMs are still lower than 4.5 wt% and no fouling of the ENMs is observed.

Pre-modification and GA activation also could enhance the catalytic ability of the immobilized ENMs. The hydrolytic activity of the Cal-B immobilized PANGMA-ENMs is up to approximately 2500 nmol/min/mg. All these Cal-B immobilized ENMs perform much higher hydrolytic activity than free Cal-B powder, the ENM activated with HMDA and GA, immobilized with Cal-B at 30 ℃ even has higher activity than Novozyme 435.

The optimal pH value of the buffer solution for the Cal-B immobilization is 6.8. Cal-B immobilized PANGMA-ENMs retain over 50% of their initial activity after 15 cycles of reuse. They also have good thermal and storage stabilities, retaining over 65% of their initial hydrolytic activities after 10 hours heat incubation at 60 ℃, and over 75% after 30 days storage, which are obviously higher than those of the free Cal-B.

In summary, the optimal fabrication conditions of Cal-B immobilized PANGMA-ENMs are: first pre-modified with HMDA and activated with GA, then immobilized in 5mg/mL Cal-B/PBS solution with pH of 6.8 at 30 ℃ for 24 h. Samples fabricated under these conditions have very good catalytic activity and retentions. This kind of enzyme immobilized ENM could have good potential applications in the field of enzymatic catalysis.

6.5 References

[1] R. A. Gross, A. Kumar, B. Kalra, Chem. Rev., 2001, 101, 2097.
[2] A. Schmid, J. S. Dordick, B. Hauer, A. Kiener, M. Wubbolts, B. Witholt, Nature, 2001, 409, 258.
[3] D. Wiktelius, Synlett, 2005, 2113.
[4] A. Ghanem, H. Y. Aboul-Enein, Tetrahedron: Asymmetry, 2004, 15, 3331.
[5] V. Gotor-Fernández, E. Busto, V. Gotor, Advanced Synthesis & Catalysis, 2006, 348, 797.
[6] U. T. Bornscheuer, R. J. Kazlauskas, Angew. Chem. Int. Ed., 2004, 43, 6032.
[7] V. Gotor-Fernandez, E. Busto, V. Gotor, Adv. Synth. Catal., 2006, 348, 797.
[8] O. Kirk, M. Würtz, Organic Process Research & Development, 2002, 6, 446.
[9] A. Kumar, R. A. Gross, J. Am. Chem. Soc., 2000, 122, 11767.
[10] L. Costa, V. Brissos, F. Lemos, F. Ramo, R. Cabral, Biosyst. Eng., 2008, 31, 323.

[11] A. I. S. Brígida, Á. D. T. Pinheiro, A. L. O. Ferreira, L. R. B. Gonçalves, Appl Biochem Biotechnol 2008, 146, 173.
[12] B. Chen, J. Hu, E. M. Miller, W. C. Xie, M. M. Cai, R. A. Gross, Biomacromolecules, 2008, 9, 463.
[13] E. M. Anderson, K. M. Larsson, O. Kirk, Biocatal. Biotransform., 1998, 16, 181.
[14] C. Mateo, J. M. Palomo, G. Fernandez-Lorente, J. M. Guisan, R. Fernandez-Lafuente, Enzyme and Microbial Technology, 2007, 40, 1451.
[15] D. E. Bergbreiter, Catalysis Today, 1998, 42, 389.
[16] H. F. Jia, G. Y. Zhu, B. Vugrinovich, W. Kataphinan, D. H. Reneker, P. Wang, Biotechnol. Prog., 2002, 18, 1027.
[17] K. H. Lee, C. S. Ki, D. H. Baek, G. D. Kang, D. W. Ihm, Y. H. Park, Fiber. Polym., 2005, 6, 181.
[18] P. Ye, Z. K. Xu, A. F. Che, J. Wu, P. Seta, Biomaterials, 2005, 26, 6394.
[19] T. G. Kim, T. G. Park, Biotechnol. Prog., 2006, 22, 1108.
[20] V. Grazu, L. Betancor, T. Montes, F. Lopez-Gallego, J. M. Guisan, R. Fernandez-Lafuente, Enzyme Microb. Technol., 2006, 38, 960.
[21] C. Mateo, O. Abian, M. Bernedo, E. Cuenca, M. Fuentes, G. Fernandez-Lorente, Enzyme Microb. Technol., 2005, 37, 456.
[22] J. Fan, J. Lei, L. M. Wang, C. Z. Yu, B. Tu, D. Y. Zhao, Chem. Commun., 2003, 5, 2140.
[23] J. F. Diaz, K. J. Balkus, J. Mol. Catal. B: Enzyme, 1996, 2, 115.
[24] S. Liu, J. Li, L. Jiang, Colloid. Surface A, 2005, 257, 57.
[25] M. Namdeo, S. K. Bajpai, Journal of Molecular Catalysis B: Enzymatic, 2009, 59, 134.
[26] Y. H. Wang, Y. L. Hsieh, J. Polym. Sci.: Part A: Polym. Chem., 2004, 42, 4289.
[27] D. X. Li, Q. He, Y. Cui, L. Duan, J. B. Li, Biochemical and Biophysical Research Communications, 2007, 355, 488.
[28] F. Šulek, Z. Knez, M. Habulin, Applied Surface Science, 2010, 256, 4596.
[29] N. Miletić, V. Abetz, K. Ebert, K. Loos, Macromolecular Rapid Communications, 2010, 31, 71.
[30] H. F. Jia, G. Y. Zhu, P. Wang, Biotechnology and Bioengineering, 2003, 84, 406.
[31] A. Moradzadegan, S. Ranaei-Siadat, A. Ebrahim-Habibi, M. Barshan-Tashniz, R. Jalili, S. Torabi, K. Khajeh, Eng. Life Sci., 2010, 10, 1.
[32] J. Xie, Y. L. Hsieh, J. Mater. Sci., 2003, 38, 2125.

[33] M. Stasiak, C. Röben, N. Rosenberger, F. Schleth, A. Studer, A. Greiner, J. H. Wendorff, Polymer, 2007, 48, 5208.
[34] N. Miletić, R. Rohandi, Z. Vuković, A. Nastasović, K. Loos, Reactive & Functional Polymers, 2009, 69, 68.
[35] M. M. Tomadakis, T. J. Robertson, Journal of Composite Materials, 2005, 39, 163.
[36] N. Miletić, R. Rohandi, Z. Vuković, A. Nastasović, K. Loos, Journal of Molecular Catalysis B: Enzymatic, 2009, 56, 196.
[37] M. Ignatova, O. Stoilova, N. Manolova, D. G. Mita, N. Diano, C. Nicolucci, I. Rashkov, European Polymer Journal, 2009, 45, 2494.
[38] X. J. Huang, Z. K. Xu, L. S. Wan, C. Innocent, P. Seta, Macromol. Rapid Commun., 2006, 27, 1341.
[39] L. S. Wan, B. B. Ke, J. Wu, Z. K. Xu, J. Phys. Chem. C., 2007, 111, 14091.
[40] P. Ye, Z. K. Xu, J. Wu, C. Innocent, P. Seta, Biomaterials, 2006, 27, 4169.
[41] Z. G. Wang, B. B. Ke, Z. K. Xu, Biotechnology and Bioengineering, 2007, 97, 708.
[42] L. L. Wu, X. Y. Yuan, J. Sheng, Journal of Membrane Science, 2005, 250, 167.
[43] X. J. Huang, D. Ge, Z. K. Xu, European Polymer Journal, 2007, 43, 3710.
[44] J. P. Chen, K. H. Ho, Y. P. Chiang, K. W. Wu, Journal of Membrane Science, 2009, 340, 9.
[45] H. G. Hicke, I. Lehmanna, G. Malsch, M. Ulbricht, M. Becker, Journal of Membrane Science, 2002, 198, 187.
[46] K. V. Peinemann, K. Ebert, H. G. Hicke, N. Scharnagl, Environmental Progress, 2001, 20, 17.
[47] T. Godjevargova, V. Konsulov, A. Dimov, Journal of Membrane Science, 1999, 152, 235.
[48] T. Godjevargova, R. Dayal, S. Turmanov, Macromol. Biosci., 2004, 4, 950.
[49] R. Dayal, T. Godjevargov, Macromol. Biosci., 2005, 5, 222.
[50] T. Godjevargov, R. Nenkov, N. Dimov, Macromol. Biosci., 2005, 5, 760.
[51] T. H. Dai, N. Miletić, K. Loos, M. Elbahri, V. Abetz, Macromolecular Chemistry and Physics, 2011, 212, 319.
[52] M. M. Bradford, Analytocal Biochemistry 1976, 72, 248.
[53] F. López-Gallego, L. Betancor, A. Hidalgo, C. Mateo, J. M. Guisán, R. Fernández-Lafuente, Journal of Biotechnology, 2004, 111, 219.

[54] Y. Mei, A. Kumar, R.A. Gross, Macromolecules, 2003, 36, 5530.

[55] M. V. Kahraman, G. Bayramoglu, N. Kayaman-Apohan, A. Güngör, Food Chemistry, 2007, 104, 1385.

[56] J. P. Chen, D. H. Chu, Y. M. Sun, J. Chem. Tech. Biotechnol., 1997, 69, 421.

[57] E. B. Pereira, G. M. Zanin, H. F. Castro, Brazilian Journal of Chemical Engineering, 2003, 20, 343.

[58] B. L. Tee, G. Kaletunc, Biotechnol. Prog., 2009, 25, 436.

[59] C. Otero, A. Ballesteros, J. M. Guisan, Appl. Biochem. Biotechnol., 1988, 19, 163.

[60] J. Pedroche, M. M. Yust, C. Mateo, R. Fernandez-Lafuente, J. Giron-Calle, M. Alaiz, J. Vioque, J. M. Guisan, F. Millan, Enzym. Microb. Technol., 2007, 40, 1160.

[61] S. G. Wu, B. L. Liu, S. J. Li, International Journal of Biological Macromolecules, 2005, 37, 263.

[62] G. Mateo, O. Abian, G. Fernández-Lorente, B. C. C. Pessela, V. Grazu, J. M. Guisan, R. Fernandez-Lafuente, Methods in Biotechnology: Immobilization of Enzymes and Cells, 2nd Edition, Humana Press Inc., Totowa NJ., 47.

Chapter 7. BSA modified PANGMA electrospun nanofibrous mat applied for the filtration of protein in water

7.1 Brief Introduction

The filtration of heavy metal particles, over waterborn contaminants, hazardous biological agents, and toxic pollutants is a key issue in industrial catalysis, agriculture, pharmaceuticals, and biotechnology processes.[1-4] Among a variety of filtration membranes, the electrospun nanofibrous mat (ENM), which possesses highly effective porosity, low basis weight, good flexibility, interconnectivity, microscale interstitial space, huge specific surface area and potential to incorporate functionality on nanoscale, is an attractive candidate compared with other membranes for applications in filtration area.[5-9]

However, normal electrospun nanofibrous mats (ENMs) have two general and critical problems which limit their practical applications in ultra- or nanofiltration: large pore size and weak mechanical property. Generally speaking, it is necessary and important that the sizes of the channels and pores in the filter material match the sizes of the particles to be filtered in order to obtain high filtration efficiency. But the diameters of electrospun fibers are generally in the range of micrometers or sub-micrometers, thus ENMs correspondingly have a large pore size in the range of several micrometers resulting in the difficulty of filtrating submicro- or nano-scaled particles from water or solution.[6] However, many of the toxic metal particles, proteins and toxins in pollutants are nanometer-scaled and therefore they are very difficult to be filtrated by normal ENMs. Moreover, the relatively wide distribution of both fiber size and pore size of ENMs will also reduce the filtration efficiency.[10-12] On the other hand,

sometimes the mechanical strength of ENMs is not sufficient to withstand macroscopic impacts from the fluids during the filtration. Without a sufficient mechanical strength, the nanofibers in the ENMs are very difficult to preserve integrity under a high pressure from the fluid liquid and tend to deformation and delamination, which results in a poor permeability to the filtration objects. The damping of permeability will behave much more obviously especially when the membrane is under a higher feed pressure. A bad permeability of the membrane results in a lower flux and thus abates the filtration efficiency dramatically.[13-15] In some cases of the applications involving protein solution, the adsorbed protein on the surface of ENMs may cause serious fouling of membrane due to the inherent hydrophobicity of most neat ENMs. So the improvement of the surface hydrophilicity of the ENMs should also be considered.[16,17]

How to solve those abovementioned problems? The idea of affinity membrane is an excellent approach. Affinity membrane is a broad sort of membranes which are able to selectively capture specific target molecules by binding a specific capturer onto the membrane surface. In environmental industry, affinity membranes can be applied for the removal of toxic heavy metal particles in industrial waste water. In biotechnology, affinity membranes can be used in protein purification and toxin removal from bioproducts.[18-20] The desirable properties for a qualified affinity membrane are well-known, including high porosity, large internal and external surface areas, high chemical, biological and mechanical stabilities, a certain degree of hydrophilicity, low non-specific adsorption of bioactive species and chemical groups for functionalization.[21,22]

ENMs have high porosity and large surface area thereby they are very appropriate for the application as an affinity membrane, but a proper surface functional modification is necessary for improving their biological and mechanical stabilities and hydrophilicity. After introducing a suitable capturer onto the ENM, the tiny metal nanoparticles, proteins and toxins can be effectively captured by its bound capturer. By this way, the bad filtration ability of the ENMs due to their big pore size could be greatly compensated.[23,24] A proper binding of appropriate capturers on the surface of ENMs could also improve other properties such as mechanical strength and hydrophilicity of the ENMs.[25,26]

To the limit of our knowledge, no publications could be found concerning the topic of applying ENMs as the affinity membrane for the filtration and separation of metal nanoparticles. In all of the prior work which referred to using ENMs for particles filtration, ENMs were made use of just in terms of their pore size but not their affinity properties.[27,28] So most of the ENMs were applied as a filter for the filtration of microparticles. In the case of nanoparticles filtration, ENMs filters were usually in the configuration of multi-layers in order to gain enough thickness for getting enough tortuosity for obstructing more tiny particles. Therefore these ENMs filters normally required a higher pressure drop due to their high fiber volume fraction and low hydraulic permeability as a result of high tortuosity.[29-31]

On the other hand, only very few relevant works can be found in regard to the fabrication and application of affinity ENMs for the protein capture. Bamford et al.[32] electrospun polyurethane nanofiber, then functionalized it by means of isocyanate couplings and finally activated it by attachment of an appropriate active moiety based

on free-radial reactions or direct coupling. This functionalized and activated nanofiber membrane finally gained the ability of capture and was used for the binding of protein A and human immunoglobulin G (IgG). Some primary results were obtained but no further publications and reports from them could be found. After that, Ma et al.[33] electrospun polysulphone (PSU) nanofiber mesh and then surface modified the nanofiber by introducing PMAA onto the fiber surface via grafting copolymerization of MAA. The PMAA grafted PSU nanofiber mesh showed the ability to capture bovine serum albumin (BSA) with a capture capacity of 17 mg/g mesh. Following their previous work, they tried to modify the PSU mesh with another reactive general purpose ligand called cibacron blue F3GA (CB) dye. CB was covalently immobilized on the fiber surface through a series of complicated chemical reactions. Firstly methacrylic acid (MAA) was graft polymerized on the PSU fiber surface after introducing carboxyl groups by Ce(IV) and reacting them with diamino-dipropylamine (DADPA) using carbodiimide as the coupling agent. Finally, CB was covalently attached on the PSU fiber surface through reaction with the amino groups. By this new modification, they were able to improve the capture capacity for BSA to 22 mg/g mesh.[34,35] They also fabricated cellulose acetate (CA) nonwoven mesh by electrospinning and again covalently attached CB on the modified CA nanofiber surfaces. The CA nanofiber mesh was first alkaline treated to obtain regenerated cellulose (RC) nanofiber mesh for the covalent binding of CB. CB was covalently coupled to the RC nanofiber surface via the nucleophilic reaction between the chloride of its triazine ring and the hydroxyl groups of the cellulose molecules under alkaline conditions. The CB derived RC nanofiber membrane showed the ability to capture BSA and bilirubin specifically with capacities of 13 and 4 mg/g, respectively.[36]

From the abovementioned short review of the prior work, it could be found that firstly these works only touched upon the capture of proteins but did not further involve details. Secondly and most importantly, these works still did not improve the common deficiencies of normal filtration membranes very well, such as lower filtration efficiency and weak mechanical properties. Especially the weak mechanical properties were not addressed in these literatures. Thirdly, these methods and routes for the modification of the membranes were really complex, normally involving plasma treatments, chemical pre-functionalizations and a lot of complicated coupling reactions.

How to improve the affinity and mechanical properties of the normal ENMs? How to avoid the complex modification reactions and simplify the reaction routes? The idea is to introduce proteins directly onto ENMs as a very effective capturer for target particles or molecules during filtration. The well-known protein-protein interaction which has been reported in many publications offers many possibilities for the ENMs to capture target proteins by the ENM-bound proteins.[37,38] There have some strong protein-protein interactions between different kind of proteins, such as ionic interaction, hydrogen bonding, van der Waals interaction, and hydrophilic interaction. These interactions are helpful for the affinity filtration of proteins in water.[39]

Bovine serum albumin (BSA) is a very conventional and cheap serum albumin protein, which has been widely used in numerous biochemical applications.[40-42] Poly(acrylonitrile-*co*-glycidyl methacrylate) (PANGMA) is a polymeric material which is the a very good candidate for electrospinning ENM as the carrier of protein capturers. It has not only the advantage of the chemical stability from the sturdy

backbone of polyacrylonitrile but also the more critical functionality of further reacting ability from the free and active epoxy group on GMA. The epoxy group offers the opportunity in a variety of activation/coupling chemistries for the covalent binding of capturers or ligands. In this case, the extremely simple and widespreadly used epoxy-amino reaction between the amine groups on BSA and epoxy groups on PANGMA-ENM.[43,44]

In this chapter, we present the fabrication of a novel nanofibrous affinity membrane by electrospinning PANGMA and the subsequent modification with BSA, and the application of this PANGMA electrospun nanofibrous mat (PANGMA-ENM) in the filtration of proteins in water. This new fabrication method for the affinity ENMs is extremely effective, simple, and easy to operate compared with the previous reported methods. Furthermore, the BSA modification of the PANGMA-ENM not only binds BSA onto it but also improves the mechanical properties and hydrophilicity of the PANGMA-ENM, which is very important and beneficial for its application for the water filtration. The fabrication of neat PANGMA-ENM and the subsequent BSA modification are described in detail. The physical properties of the neat and BSA modified ENMs including: porosity, pore size, thermal property, methanical property, wettability are investigated, discussed and compared particularly. Water flux measurement was performed to study the water permeability of the neat and BSA modified ENMs. Finally, the filtration efficiency of the BSA modified ENMs is studied by filtration test and the results are discussed in detail. The filtration results indicate that BSA modified PANGMA-ENM has great rejection ability to proteins in water. It is very suitable for the application as the affinity nano-membrane in the filtration area.[45]

7.2 Experimental

7.2.1 Materials

Poly(acrylonitrile-*co*-glycidyl methacrylate) (PANGMA) was synthesized by Helmholtz-Zentrum Geesthacht with a molecular weight (Mn) of ca. 100,000 g/mol and GMA contents of 10 mol%.[46] Bovine Serum Albumin (BSA) (dried powder) and phosphate buffered saline (PBS) were purchased from Sigma-Aldrich Co. *Candida antarctica* lipase B (Cal-B) in the form of a dried powder was purchased from BioCatalytics Co. (Grambach, Austria). N,N-dimethylformamide (DMF) and methanol were purchased from Merck KGaA. All the chemicals were directly used without purification.

7.2.2 Preparation of PANGMA-ENMs via electrospinning

The electrospinning processes and conditions in this chapter are same as those mentioned in §6.2.2 but only changing the applied voltage to 20 kV and the feed rate to 1.0 mL/h.

7.2.3 BSA modification

The BSA modification of PANGMA-ENMs was performed in lidded bottles loaded with BSA/PBS buffer solution with the concentration of 5 mg/mL and the pH values of 6.8. PANGMA-ENMs were immersed into the BSA/PBS buffer and the mixture was moderately shaken at 55 ℃ for 24 h. After reaction, the ENMs were taken out and washed several times by PBS buffer (pH 6.8) under shaking condition until the complete removal of unbound BSA. All the supernatants and washing solutions were collected carefully for the determination of BSA binding capacity (crosslinking degree). The amount of residual protein after immobilization was determined by

Bradford's method.[47] BSA was used as the standard to construct the calibration curve. The amount of bound BSA onto the PANGMA-ENMs was estimated by deducting the amount of residual BSA from the initial amount of BSA used in the immobilization procedure (5 mg/mL). The BSA binding capacity was defined as the amount of bound BSA (mg) per gram of the PANGMA-ENMs. Each reported value was the average of at least three experimental values. Finally, the BSA crosslinked PANGMA-ENMs were carefully washed with deionized water again and dried under vacuum at 30 ℃ for 24 h.

7.2.4 BSA leaching test

The leaching of the bound BSA was investigated and characterized by the leaching test, which has been detailed in §6.2.4

7.2.5 Water permeability analysis

Water flux measurement was applied to characterize the properties of the PANGMA-ENMs during their service in filtration, such as the permeability and the structural stability (integration). Both neat and BSA modified PANGMA-ENMs in the circular shape with the diameter of 20 mm were stamped and used for the flux measurement. A poly(*p*-phenylene sulfide) (PBS) nonwoven layer was used as the substrate for the ENM to place on (Figure 7.1). A custom-built pressure filtration set-up was designed for the permeability measurement (Figure 7.2). The dried sample was placed in the membrane cell (module) and the water in the vessel was pushed through the membrane cell once at a time by the compressed air with 1 bar pressure. The flux of water permeate was calculated by equation (7-1):

$$J = Q / A\Delta t \qquad (7\text{-}1)$$

where J is the water permeate flux (L m^{-2} s^{-1}), Q is the permeated volume of water (Q = 300 mL), A is the effective area of the ENMs (m^2), and Δt is the sampling time (s), which is recorded by measuring the time for 300 mL distilled water permeating through the membrane. All the flux measurement experiments were repeated three times to obtain average results.

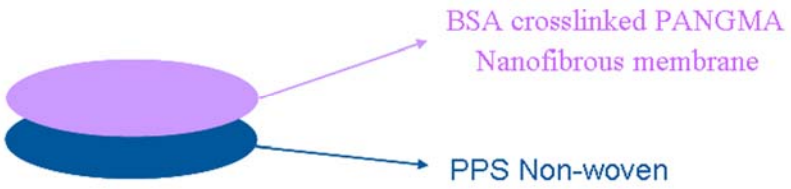

Figure 7.1 Configuration of samples used in the water flux measurements and filtration tests

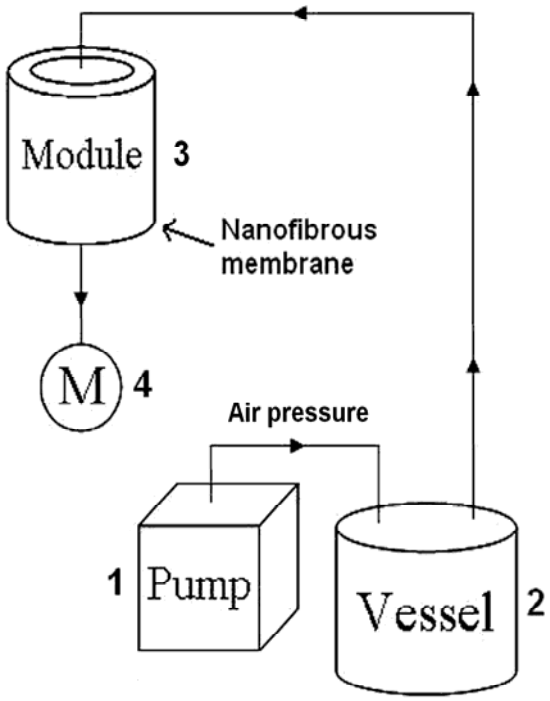

Figure 7.2 Schematic digram of the setup for the water flux measurements

7.2.6 Filtration test

The filtration performance of the PAMGMA-ENMs was tested by filtering BSA and Cal-B from water using neat and crosslinked PANGMA-ENMs and the subsequent

concentration measurements. BSA and Cal-B were chosen as the representative of proteins.

Filtration was carried out by a handmade setup (Figure 7.3). PANGMA-ENM samples with the same preparation process discribed in the water permeability analysis were use for the filtration test. A piece of prepared sample was placed on a self-made stainless steel membrane cell. The effective filtration area was calculated to be 2 cm^2. 20 mL of proteins (BSA and Cal-B) water solution with original concentration of 2 mg/L was used to test the filtration performance of the neat and BSA modified PANGMA-ENMs. Water could permeate through the ENMs even in the absence of any extra pressure. To achieve a higher flux, a gravitational water pressure of about 20 mPa was applied to drive the filtration. After the first filtration, the collected permeate were sampled first and then directly used as the feed for the second filtration. This was called one cycle and five cycles were done for each sample.

The concentrations of proteins in the original feed and filtrate were determined by Bradford's method which has been detailed in the statement above.[47] BSA was used as the standard to construct the calibration curve. The concentration of feed and permeate were calculated and compared. The filtration efficiency (FE) was determined using the formula below:

$$SF = (1 - C_{permeate}/C_{feed}) \times 100\% \quad (7\text{-}2)$$

where $C_{permeate}$ and C_{feed} are the concentration of proteins in the permeate and in the feed, respectively.

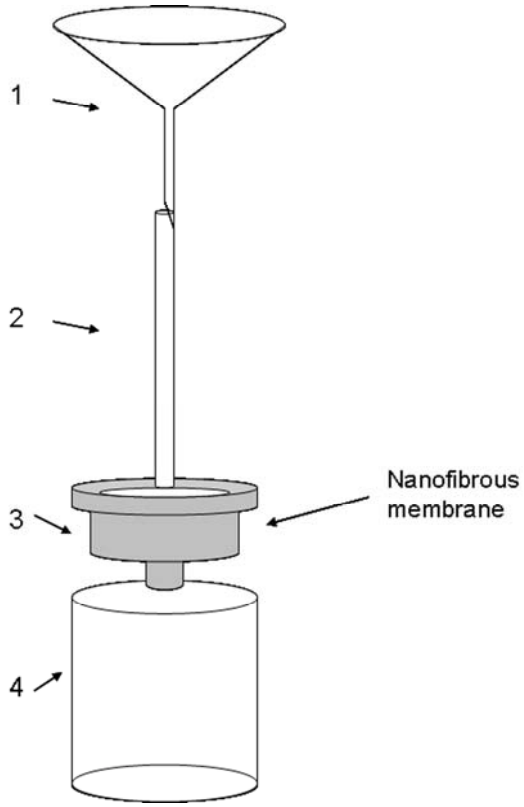

Figure 7.3 Schematic diagram of the setup for the filtration tests

7.2.7 Measurements and characterizations

The morphologies and structures of the neat and BSA modified PANGMA-ENMs were investigated by the same characterization methods and equipments mentioned in §6.2.7.

The inter-fiber pore sizes and thermal properties of the neat and BSA modified PANGMA-ENMs were investigated by the same characterization methods and equipments mentioned in §5.2.4.

The mechanical properties of the neat and BSA modified PANGMA-ENMs were studied by tensile strength tests, which were performed according to the ASTM D882-00 using a Zwick-Roell equipment with a 0.02 N load cell. The tensile strength,

stiffness and elongation of the samples were recorded automatically by the machine and the average data of them were calculated from at least ten independent specimens.

The water wettability of the neat and BSA modified PANGMA-ENMs were characterized by water contact angle measurement, which was performed according to the sessile drop method on a contact angle meter (Krüss DSA100E) with high performance image processing system from Data Physics Instruments. The liquids used were H_2O (HPLC grade) and were added by a motor driven syringe at room temperature. Ten measurements were carried out for each PANGMA-ENM. The presented results were calculated using the final average values.

The porosity of the neat and BSA modified PANGMA-ENMs was calculated by the equation (7-3):

$$\text{Porosity} = (1 - d/D) \times 100\% \qquad (7\text{-}3)$$

where d stands for the apparent density (g/cm^3) of the PANGMA-ENMs and D is the density of the pure block PANGMA (g/cm^3), respectively. The apparent density (d) of the PANGMA-ENMs was obtained by dividing its dry mass by its volume which is calculated from the area and thickness of the PANGMA-ENMs.

7.3 Results and discussions

7.3.1 Electrospinning of PANGMA-ENMs

The morphology of the neat and BSA modified PANGMA-ENMs was observed by SEM. As shown in figure 7.4(a), the neat electrospun nanofibers with diameters of 200 ~ 400 nanometers were obtained when the electrospinning solution concentration

was 20 wt% and the applied voltage was 20 kV. The nanofibers showed a smooth surface and a uniform body with a narrow distribution of fiber diameter.

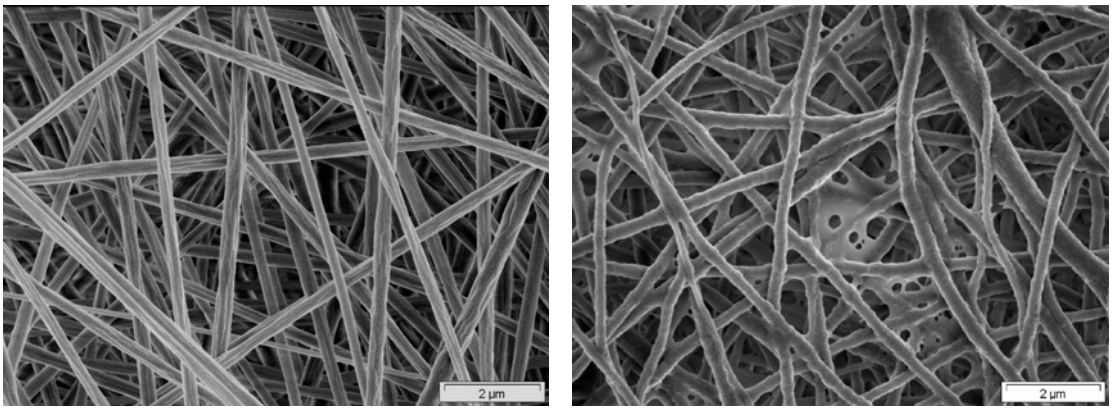

(a) **(b)**

Figure 7.4 SEM micrographs of the PANGMA nanofibers: (a) neat nanofibers; (b) BSA modified nanofibers

7.3.2 Modification of PANGMA-ENMs by BSA

PANGMA-ENM contains epoxy groups which are very suitable for the direct binding of BSA, on the other hand, BSA also crosslinks PANGMA-ENM during the binding process. So we surfacely modified PANGMA-ENM with BSA by making use of the crosslinking reaction between PANGMA and BSA. Briefly, during this crosslinking reaction, the epoxy groups on the PANGMA nanofibers are attacked by the primary amine groups in BSA and then secondary amine groups and hydroxyl groups are formed as a result of the ring-opening reaction of epoxide (Figure 7.5). BSA contains lots of primary amine groups and these amine groups tend to react with epoxy groups on different PANGMA nanofibers due to the nearer distance and lower steric hindrance of two epoxy groups on two different nanofibers, leading to the formation of the crosslinked structure. Small amount of crosslinking also happens between the epoxy groups on the same PANGMA nanofiber (Figure 7.5).

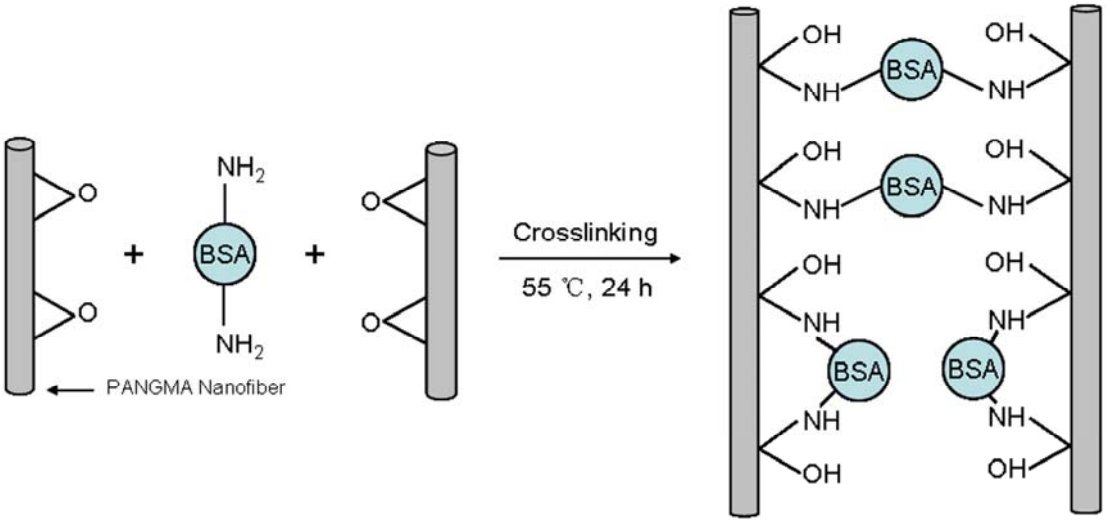

Figure 7.5 Schematic diagram of the modification of PANGMA-ENM with BSA

FTIR results show the successful modification of PANGMA-ENMs with BSA. Figure 2 shows the FTIR spectrum of neat (curve (a)) and BSA modified (curve (b)) PANGMA-ENMs. It could be observed that first on curve (a) there is a clear peak near 908 cm^{-1} (characteristic peak of epoxy group), which shows the existence of epoxy groups in neat PANGMA nanofibers. Meanwhile in curve (b), the epoxy peak is sharply diminished, which proves that epoxy groups in PANGMA have been crosslinked with BSA. In addition, two very obvious peaks near 1650 cm^{-1} and 1530 cm^{-1} are the vibration peak of amide I and amide II, which represent the amide groups (also nominated as the peptide link in biochemistry) in BSA molecules. A peak near 3300 cm^{-1} showed the evidence of secondary amine, which is generated during the opening of the epoxy group by the primary amine groups in BSA (Figure 7.6).[48,49]

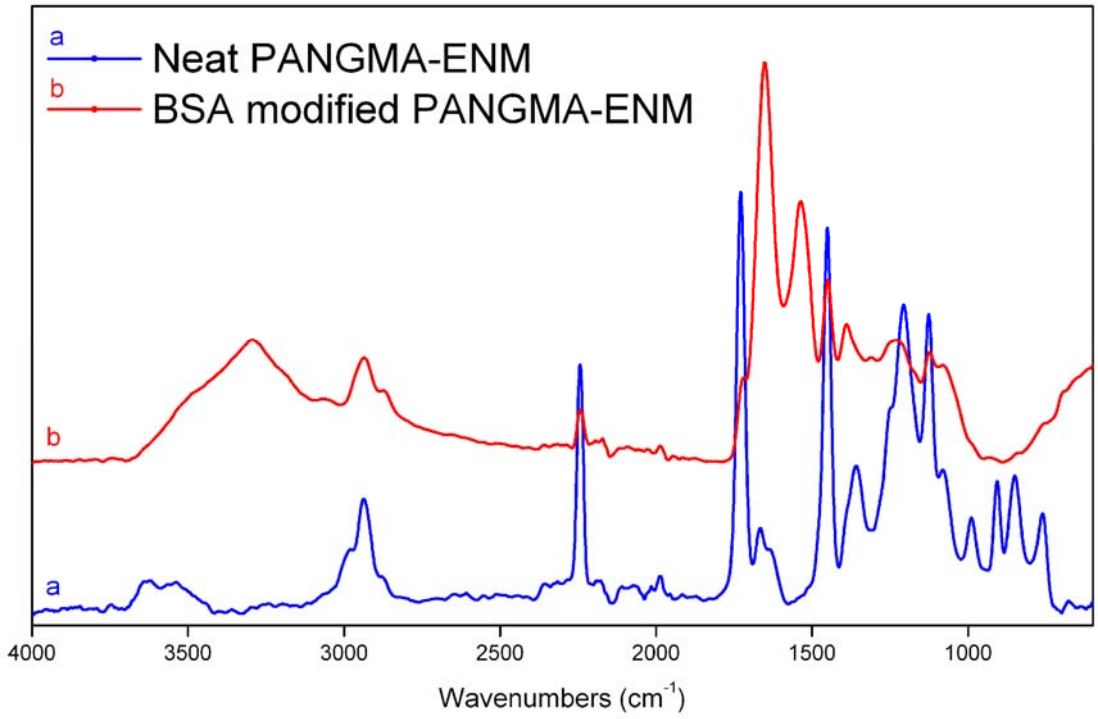

Figure 7.6 FTIR spectrum of PANGMA-ENMs: (a) neat; (b) BSA modified, BSA modified ENMs crosslinked in BSA/PBS buffer at 55 ℃ for 24 h

From the SEM photo of figure 7.4(b) it can be also found that the morphology of the nanofibers still remained uniform and the structure of ENM kept very well after BSA modification, only small degree of swelling and adhesion between fibers were observed. As mentioned in the introduction, PANGMA has good chemical stability and mechanical strength therefore is very stable during the crosslinking reaction. There were also some agglomerations of BSA on the surface of the nanofibers and in some pores of the ENM after modification, which verifies the successful binding of the BSA on the PANGMA nanofibers.

Figure 7.7 shows the BSA binding of PANGMA-ENMs bound at different temperatures. For each sample studied, binding saturation was achieved within 10 h.

The binding temperature has huge influence on the BSA binding. It could be found in figure 7.7 that BSA binding amount of the samples bound at 4 and 25 ℃ are very low, below 6 mg per gram ENM, while the PANGMA-ENMs bound at 55 ℃ gains a much higher binding amount of 27.2 mg per gram ENM. The reason is obvious since most of the chemical reactions need a higher ambient temperature to fulfill faster and more completely due to the higher activity of the reactant molecules in a higher temperature. But the binding temperature should also be controlled under a certain value to avoid the damage of BSA from heat since the onset temperature of the conformation change of BSA is 58.1 ℃ and the temperature of its denaturation is 62 ℃.[50,51] According to these reasons, the binding reaction was performed at 55 ℃ for 24h to obtain the best BSA binding.

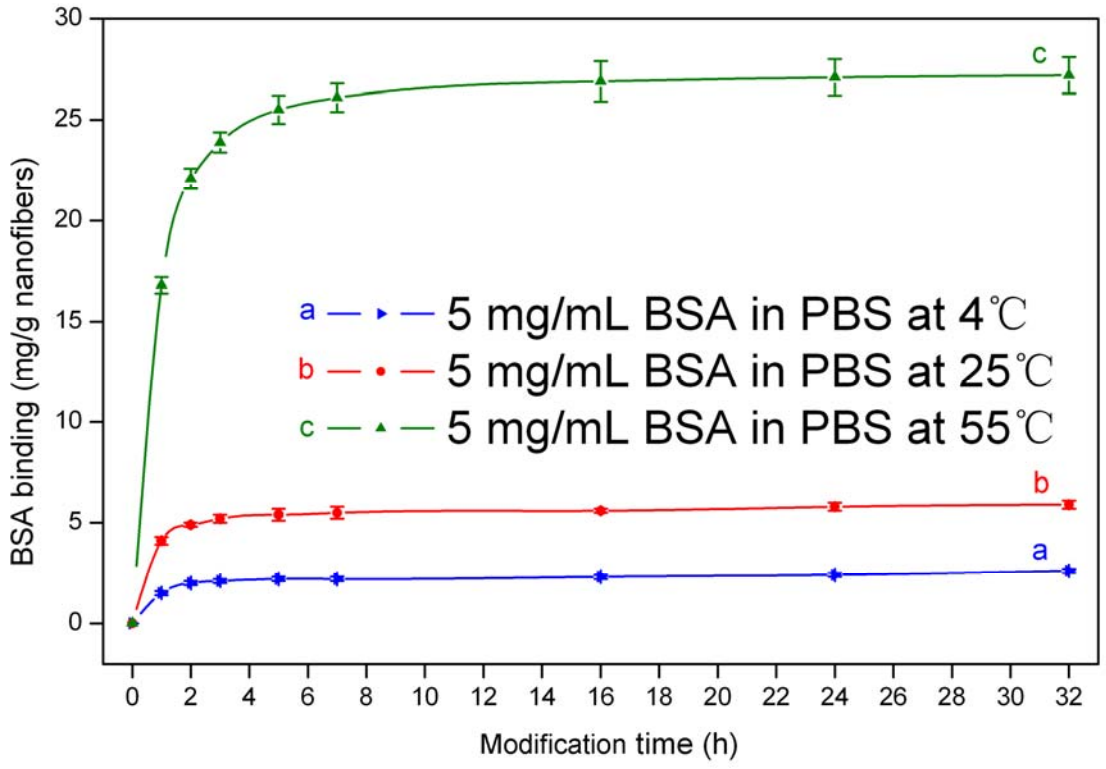

Figure 7.7 BSA binding amount at different binding temperature:

(a) 4 ℃, (b) 25 ℃, and (c) 55 ℃

After BSA modification, BSA should be covalently bound onto the PANGMA-ENMs and therefore they should not leach into the water during their service in the filtration process. This is very important for a qualified affinity membrane. Thus the leaching of the bound BSA was investigated and measured by the leaching test and the results are shown in figure 7.8. It is obvious that the ENM-bound BSA have very good stabilities in water. After 168 hours recycled in water, the leaching of the bound BSA are still less than 1.2 wt%. It has been mentioned in chapter 6 that leaching is derived from the elution of those physically absorbed enzymes when the ENMs are impacted by the water flow during their performance. After the BSA modification, all the samples were carefully and thoroughly washed by phosphate buffered solution. Almost all the physically absorbed BSA had been washed out, which results in a very low BSA leaching.

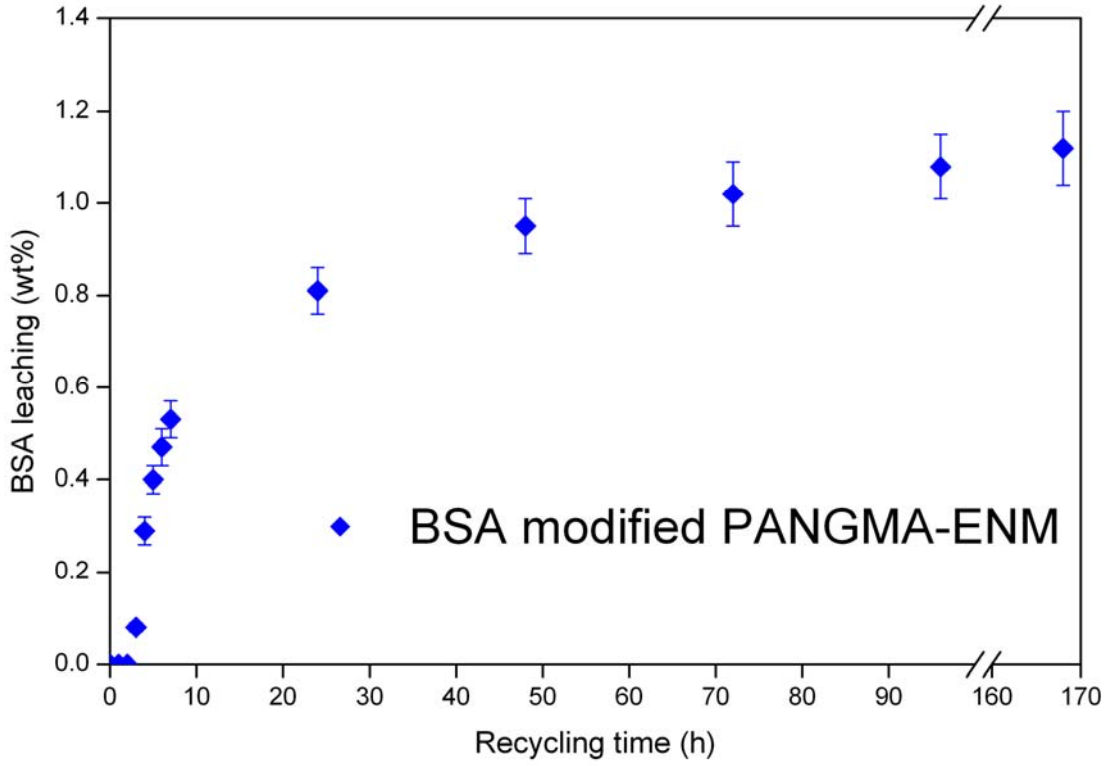

Figure 7.8 BSA leaching of BSA modified PANGMA-ENM in water for 168 h

7.3.3 Physical properties of neat and BSA modified PANGMA-ENMs

The binding of BSA onto PANGMA-ENMs not only modified the membrane into the affinity membrane but also enhanced lots of physical properties of PANGMA-ENMs. The porosity, pore size, thermal properties, water wettability, and mechanical properties of both neat and BSA modified PANGMA-ENMs will be compared and discussed in detail in the following. All the relevant data are displayed in table 7.1.

Table 7.1 Some physical properties of neat and BSA modified PANGMA-ENMs

	Porosity (%)	**Pore size (μm)**	**T_g (℃)**	**T_d (5%) (℃)**	**Contact angle (°)**
Neat PANGMA-EMNs	84.4	2.4	98.4	272.8	133.5
BSA modified PANGMA-EMNs	83.0	1.7	107.8	296.7	0

PANGMA-ENM does not lose its high porosity after BSA modification. The average porosity of BSA modified PANGMA-ENMs still reaches 83 %, which is very close to that of the neat one. Compared with some commercial membranes, PANGMA-EMNs have outstandingly high porous structure which is very good and critical for the filtration applications.[52,53]

After BSA modification, it was found that the average pore size of PANGMA-ENMs shifted from 2.4 to 1.7 μm (Table 7.1). The main reason causing the obvious decrease of pore size is that the bound BSA will alter both the shape of nanofibers and the structure of the ENMs. The possible growth of the nanofibers as a result of the bound BSA on their surface will occupy part of the pore space, resulting in the reduction of pore size. It may be also speculated whether a crosslinking temperature of 55 ℃

might induce a slight shrinkage of ENMs due to relaxations of frozen-in local stresses in the nanofibers. Moreover, the shrinking of PANGMA-ENMs during the drying process after crosslinking reaction will reduce the pore size too.

BSA modification also improved the thermal stability of the PANGMA-ENMs. It could be seen in table 7.1 that the glass transition temperature (T_g) and the thermal decomposition temperature (T_d) (In this Ph.D work, T_d is specially defined as the temperature at which the weight of PANGMA-EMNs changes by 5%)[54,55] of the PANGMA-ENMs increased from 98.7 ℃ and 272.8 ℃ to 107.8 ℃ and 296.7 ℃, respectively. This is due to the decreasing flexibility of polymer chains as a result of the formation of a crosslinked network. The thermal analysis results indicate that BSA modified PANGMA-ENMs can serve in a harsher working condition than the neat one.

The water wettability of the PANGMA-ENMs was characterized by water contact angle measurement and the results are shown in table 7.1 and figure 7.9. The water contact angle of the neat PANGMA-ENMs was measured to be (133.5° ± 7.2°) due to their inherent surface roughness and trapped air pockets same as most of the as-spun ENMs. Neat PANGMA-ENMs showed obvious hydrophobicity (Figure 7.9(a)). After modified with BSA for 24 h, the water contact angle of the BSA modified PANGMA-ENMs decreased dramatically to zero just after contacting with water for a few seconds as indicated in figure 7.9(b). The BSA modified ENMs showed the instantaneous wetting by water, suggesting that the rough surface of PANGMA-ENMs had been covered with the bound hydrophilic BSA, leading to the ultra-hydrophilic properties of the BSA modified PANGMA-ENMs.

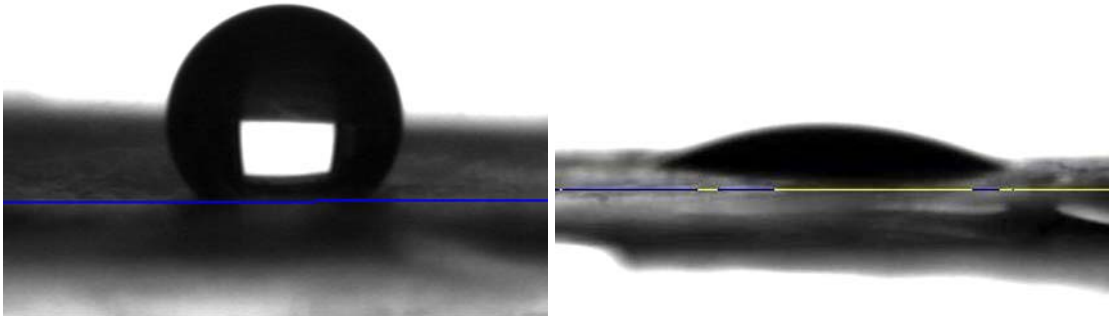

(a) **(b)**

Figure 7.9 Water contact angle of the PANGMA-ENMs: (a) neat; (b) BSA modified

Figure 7.10(a) shows the stress–strain curves for neat and BSA modified PANGMA-ENMs. The tensile behavior for all the modified ENMs presents like typical bulk rubber sheets or films, especially at relatively lower elongation regions. It was reported in literatures that the tensile behavior is strongly affected by the number and type of netting points in the nanofibrous mat.[56,57] The improved tensile performance in this case can be explained by the increased number of permanently netting points between netting nanofibers, as well as by the increased stiffness of the nanofibers themselves by the crosslinking of PANGMA molecules inside the nanofibers.[57] Several representative tensile properties including: tensile strength (ultimate stress), elongation (breaking strain) and stiffness (Young's modulus) are summarized in figure 7.10(b). Each datum in the plots provided the mean value of ten measurements. After BSA modification, the tensile strength of the modified ENM was about 4 times of the neat one. A similar increasing trend was also found for the stiffness of the PANGMA-ENMs. The Young's modulus of BSA modified ENM was 70 MPa, a substantial increment from 50 MPa for the neat one. But a decreased elongation was

observed after modification, which was very normal in many cases as a consequence of the increase of the tensile strength and stiffness. Thus, it can be concluded that BSA modification can improve the mechanical properties significantly. The high tensile strength of BSA modified PANGMA-ENMs extend their applications in the fields of filtration and seperation.

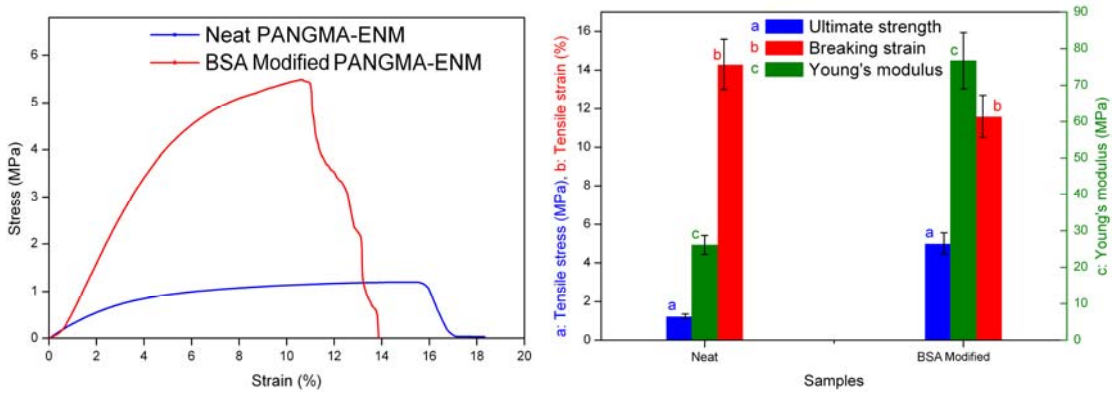

(a) **(b)**

Figure 7.10 Mechanical properties of neat and BSA modified PANGMA-ENMs: (a) s-s curves; (b) mechanical properties

7.3.4 Water permeability of PANGMA-ENMs

Pure water flux measurements were performed to study the water permeability and structural stability of the neat and BSA modified PANGMA-ENMs. The water fluxes of ENMs measured under different water pressure are shown in figure 7.11. It could be seen that the neat and BSA modified PANGMA-ENMs showed different behaviors in different working environments. When they were served under lower applied water pressure, neat and BSA modified PANGMA-ENMs show the similar water permeability. The neat ENM even give a slightly better water flux than the BSA modified one. But when they were served under higher applied pressure, they behaved totally reversely. BSA modified ENM showed a higher flux (91 ± 6 L m^{-2} s^{-1}) than the

neat one (79 ± 5 L m^{-2} s^{-1}). This is probably due to the following reasons: in the condition of low water pressure, the pore size of the ENMs plays a critical role on the water permeability of ENMs. As abovementioned, neat PANGMA-ENMs have bigger average pore size (2.4 μm) than BSA modified ENMs (1.7 μm). It is well known that water will pass through big pores more easily, so the water flux of neat ENMs was expected to be higher than that of BSA modified ENMs. But it should also be considered that BSA modified ENMs turn to be superhydrophilic while neat ENMs are superhydrophobic. The superhydrophilicity of the BSA modified ENMs will certainly compensate the loss of their water permeability due to their smaller pore size. So finally an almost similar water flux of these two ENMs was displayed. On the other hand, when they were under higher water pressure, the stronger mechanical properties of BSA modified ENMs play a critical role in the pure water flux. Under a higher water pressure, integration of the nanofibers will happen on the neat ENMs due to the relatively weak mechanical strength of the neat PANGMA nanofibers. Those nanofibers which are on the surface of the ENM will integrate each other and then result in the disappearance of pores and the deformation of the whole ENM. Finally the water flux decreased. But the modified PANGMA nanofibers have stronger mechanical strength which makes the modified ENMs keep their structure well even under higher pressure. Therefore the BSA modified ENMs still kept very good water permeability in that kind of environment. However, the effect of mechanical properties on water flux only could be exposed under a higher applied water pressure on the ENMs. Under a lower applied pressure, the impact from the water flow to the ENMs is so weak that those ENMs which have weaker mechanical resistance against water also can survive. The integrity of those ENMs will not change so much. In that kind of environmental condition, the decided factor for the water permeability is the

pore size but not the mechanical properties of the ENMs. Moreover, the hydrophilicity of the BSA modified ENMs also definitely plays a role in the pure water flux. The effect of the hydrophilicity on pure water flux exhibits more apparently in the initial stage. In contrast to neat PANGMA-EMNs, the BSA modified ones maintain their high water permeability under a high water pressure. This verifies that BSA modification can prevent the deformation and delamination of the PANGMA-ENMs during their service in the condition with stronger water impact. Without question, the BSA modified PANGMA-ENMs will be valuable for many affinity filtration and microfiltration applications.[58]

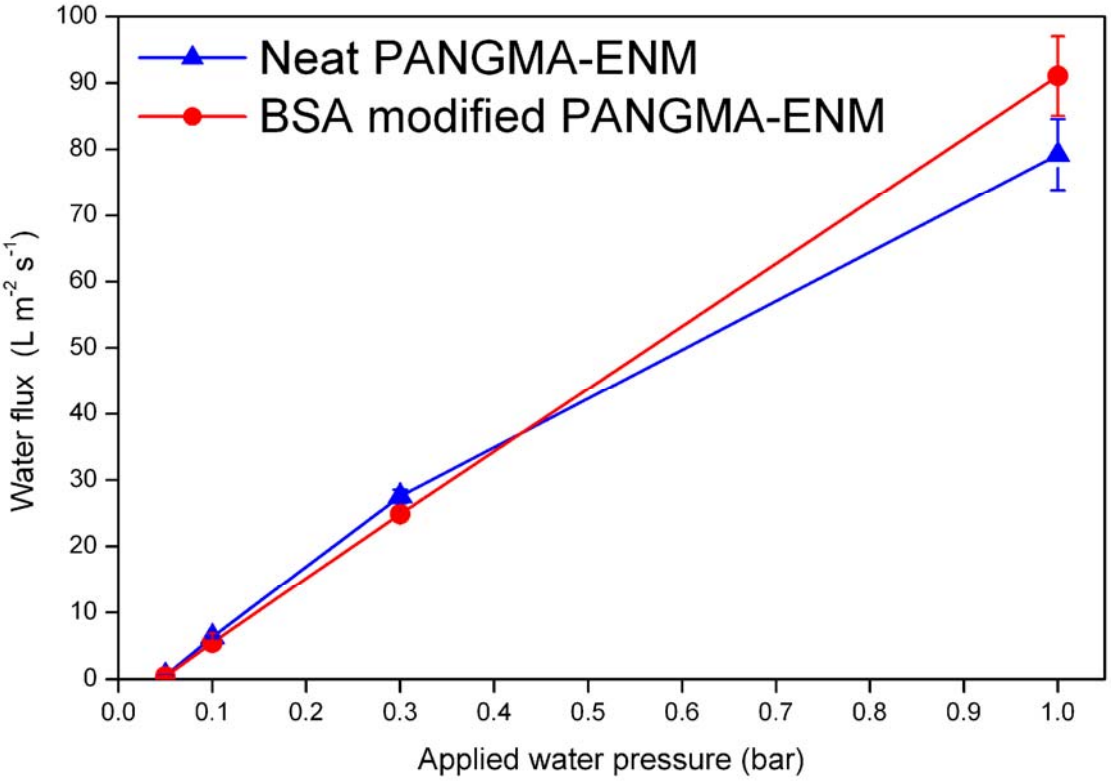

Figure 7.11 Water flux of neat and BSA modified PANGMA-ENMs under different applied pressures

7.3.5 Filtration of proteins in water

As mentioned in the introduction section, so far only few literatures about the application of ENMs as the affinity membranes for the filtration of proteins in water could be found. In this part, we report the first results for the affinity filtration of proteins in water using BSA modified PANGAM-ENMs. Bovine serum albumin (BSA) and *Candida antarctica* lipase B (Cal-B) were employed as the model filtration objects to study the filtration efficiency of PANGMA-ENMs because they are among the most well-known proteins used for the study of the affinity properties of affinity membranes.[59-61] The filtration efficiency of BSA and Cal-B by neat and BSA modified PANGMA-ENMs at different filtration cycles were plotted in figure 7.12. About 70 % of the BSA in initial feed solution was filtrated by the novel BSA modified affinity membrane after the first cycle, while only about 5 % of the initial BSA was rejected by the neat PANGMA-ENM at the same condition. After five times filtration, over 88 % of BSA in the initial feed solution had been captured by the BSA modified PANGMA-ENM, but in the case of neat PANGMA-ENM, more than 90 % of the BSA still easily passed through it the together with water. These results prove that BSA modified PANGMA-ENM can capture BSA in water effectively.

Similar to the filtration behavior of PANGMA-ENMs for the filtration of BSA in water, BSA modified PANGMA-ENMs have much better filtration ability than neat ones in the case of filtrating Cal-B. The filtration efficiency for the BSA modified PANGMA-ENMs after first cycle reached 59 % while a negligible filtration efficiency of 5 % for the neat PANGMA-ENMs was obtained. This indicated that most of the Cal-B in water was captured by the BSA modified PANGMA-ENMs but almost all of the BSA passed through the neat ones with water. After five filtration

cycles finished, the final filtration efficiency of BSA modified ENMs could be above 80 % but that of the neat ones only had a slight increment and still was under 10 %. Again it verifies that the neat PANGMA-ENMs almost can not capture BSA at all and the excellent BSA capturing ability of the BSA modified ones is completely attributed to the specific interaction between the bound BSA and the protein in water. It is worth to notice that the flux of proteins water solution during the whole filtration period did not change so much, indicating no permanent fouling of the ENMs (data not shown).[29] It could be concluded that the bound BSA on the PANGMA-ENMs would make a good candidate specifically isolating proteins in water.

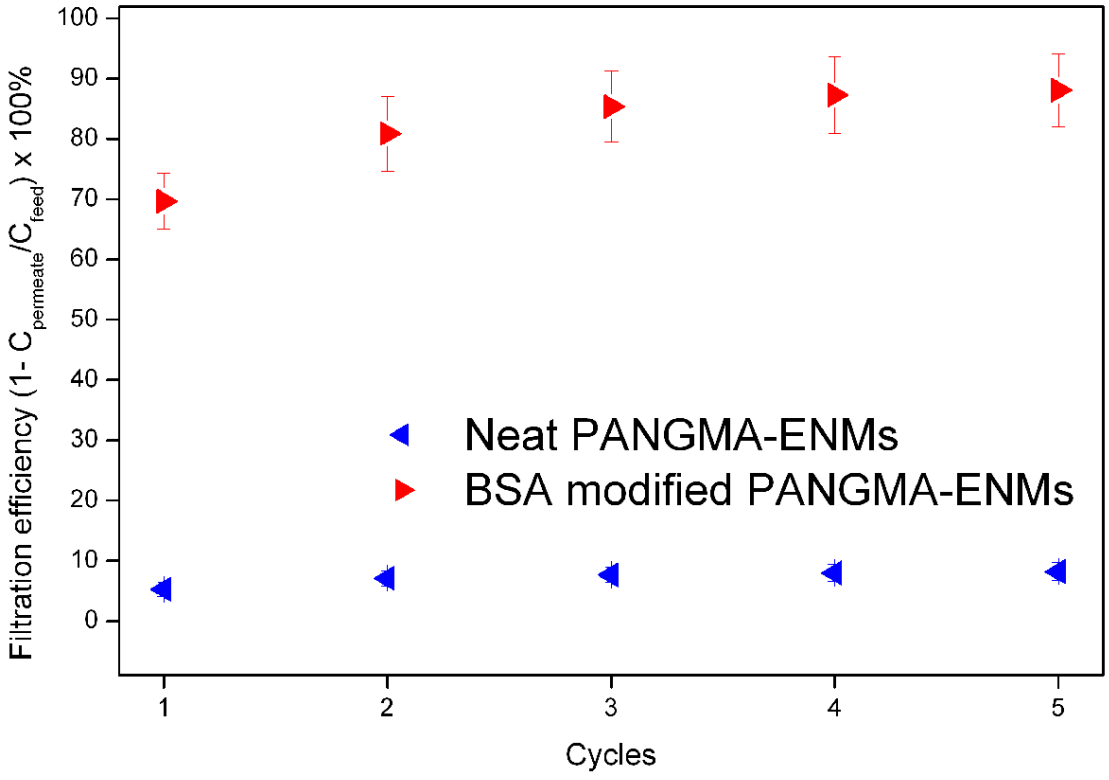

(a)

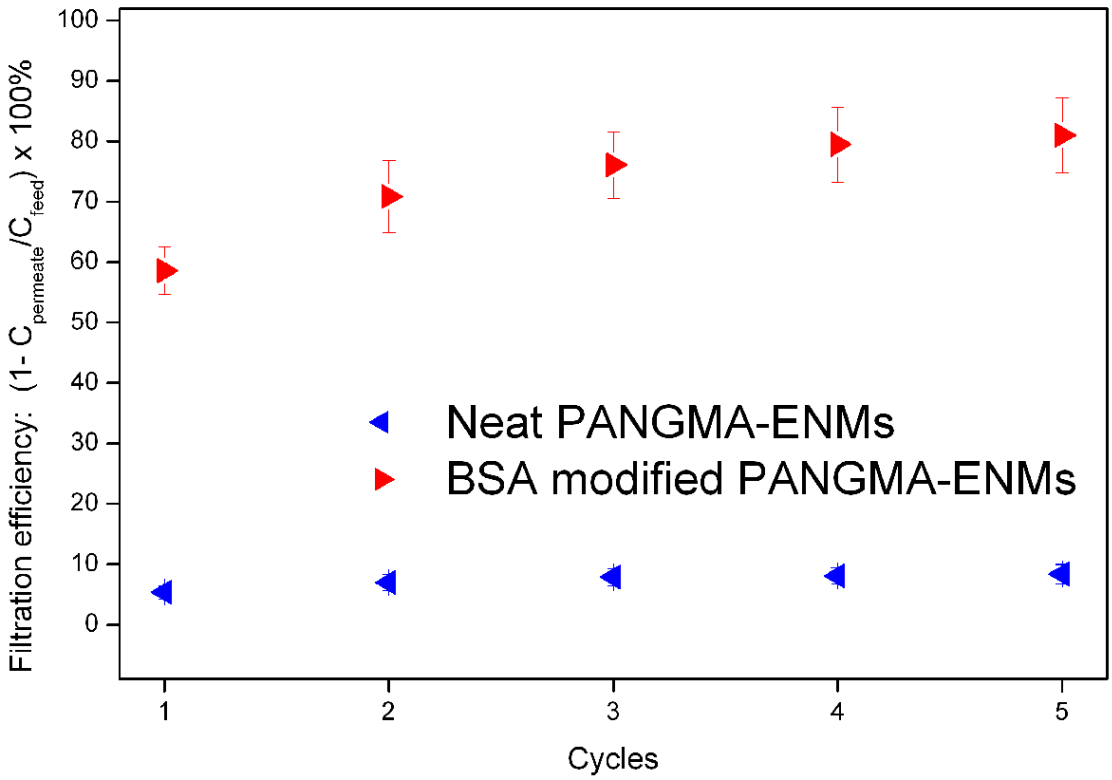

(b)

Figure 7.12 Filtration efficiency of the neat and BSA modified PANGMA-ENMs: (a) filtration of BSA in water, (b) filtration of Cal-B in water

It is also very obvious from the SEM photos that BSA modified PANGMA-ENMs have a good affinity to the proteins in water. Figure 7.13 shows the SEM photos of the BSA modified ENMs after the first cycle of the filtration of BSA in water. It could be seen clearly that there were lots of aggregations of BSA on the surface of BSA modified PANGMA nanofibers (Figure 7.13(b)) and these aggregations bestrewed over each layer of ENM (Figure 7.13(d)) and also inter-layers of the ENM (Figure 7.13(f)) after only one time of filtration. Meanwhile, almost no adherence of BSA on the neat nanofibers and ENM were observed by SEM (Figures 7.13 a, c, and e). The SEM photo provided a direct evidence of the successful capture of BSA by BSA

modified PANGMA-ENMs. The filtration of Cal-B shows the similar results therefore the SEM photos of that experiment were not displayed again.

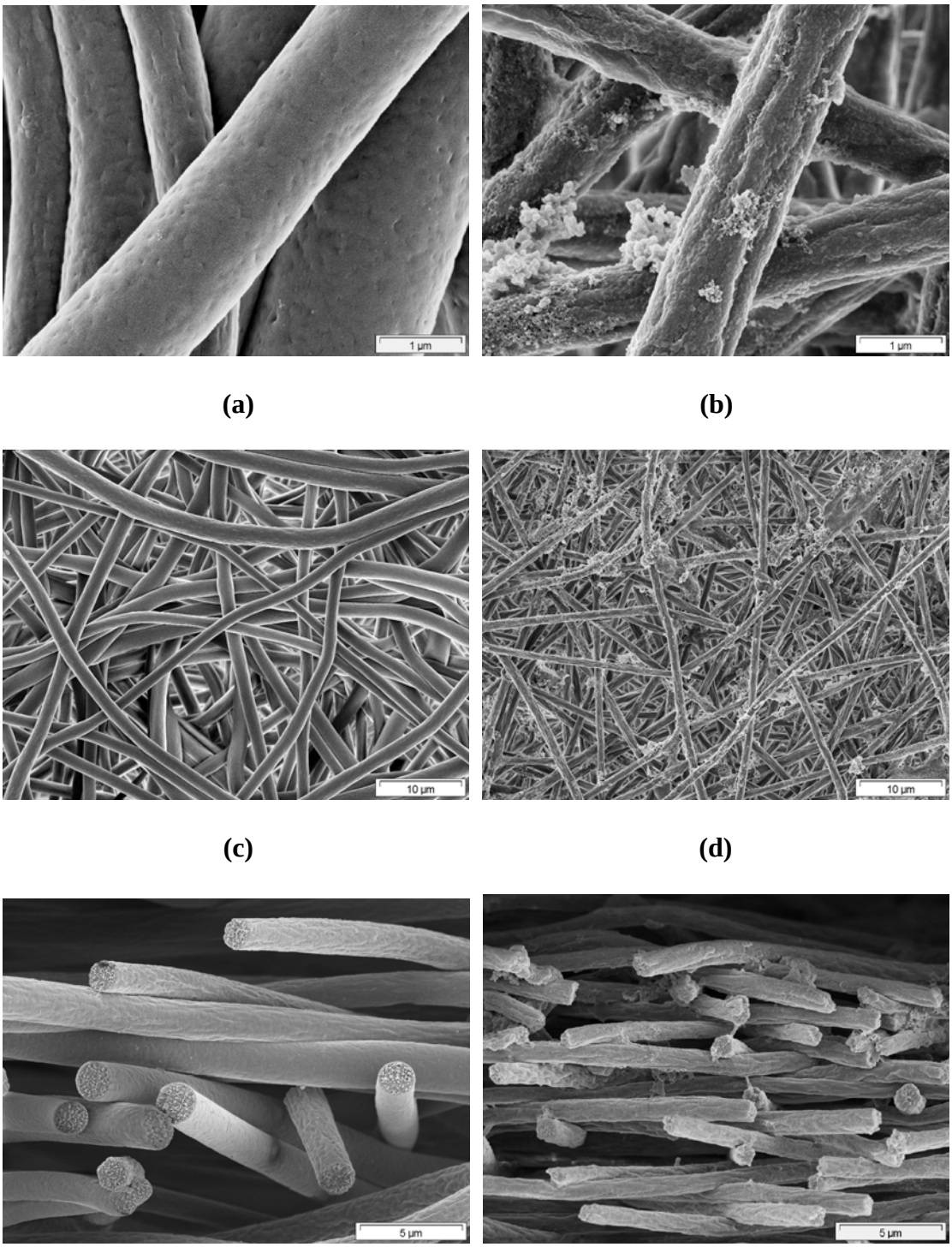

(a) **(b)**

(c) **(d)**

(e) **(f)**

Figure 7.13 SEM photos of PANGMA-ENMs after filtration of BSA: (a), (c) neat; (b),(d) BSA modified; (e) cross-section of neat; (f) cross-section of BSA modified

7.4 Conclusions

To sum up, a novel affinity electrospun nanofibrous membrane (ENM) was fabricated by electrospinning of poly(acrylonitrile-co-glycidyl methacrylate) (PANGMA) and the subsequent modification with bovine serum albumin (BSA). The modification reaction was performed in BSA/PBS solution with the concentration of 5mg/mL at 55 ℃ for 24h to obtain the best BSA binding. The binding amount could reach to 27.2 mg BSA per gram ENM. FTIR and SEM results also show the successful binding of BSA onto PANGMA-ENMs.

The BSA modified PANGMA-EMN had better thermal and mechanical properties than the neat PANGMA-ENM. After BSA modification, the glass transition temperature (T_g) and the thermal decomposition temperature (T_d) of the PANGMA-ENMs increased from 98.7 ℃ and 272.8 ℃ to 107.8 ℃ and 296.7 ℃, respectively. The tensile strength of the modified ENM was about 4 times of the neat one, from 1.24 MPa to 5.01 MPa. The Young's modulus of the ENMs also increased from 26.1 Mpa for neat ENM to 76.7 MPa for the BSA modified one.

The water wettability of PANGMA-ENM was also improved by the BSA modification. After modification, the modified ENM showed a contant angle of 0° and turned from super hydrophobic to super hydrophilic. The results of pure water flux measurement indicated that the BSA modified ENMs had better water permeability and structure integrity during their service under higher water pressure than the neat ones.

This novel BSA modified ENM was used as an affinity membrane to filtrate the proteins in water. BSA and Cal-B were used as the model filtration objects. Filtration test for the BSA showed that after the first filtration cycle, around 70 % of the BSA in initial feed solution could be filtrated by the BSA modified PANGMA-ENM. After five times filtration, finally over 88 % of BSA in the initial feed solution had been captured by this novel affinity ENM. Meanwhile, for the filtration of Cal-B, the filtration efficiency for the BSA modified PANGMA-ENMs after first cycle reached 59 %, and the final filtration efficiency of the affinity ENMs could be above 80 % after five filtration cycles. These results proved that BSA modified PANGMA-ENM can capture proteins in water effectively. This novel affinity ENM is highly suitable for the filtration and separation tiny particles and contaminations in water.

7.5 References

[1] T. H. Bae, T. M. Tak, Journal of Membrane Science, 2005, 249, 1.

[2] G. Nakhla, K. Wong, W. Wan, N. Maximous, Separation and Purification Technology, 2010, 73, 294.

[3] Z. X. Guo, Y. Liu, S. P. Li, Z. G. Yang, Rapid Communications in Mass Spectrometry, 2009, 23, 3983.

[4] T. G. I. Ling, B. Mattiasson, Biotechnology and Bioengineering, 1989, 34, 1321.

[5] S. S. Homaeigohar, K. Buhr, K. Ebert, Journal of Membrane Science, 2010, 365, 68.

[6] H. W. Liang , L. Wang , P. Y. Chen , H. T. Lin , L. F. Chen, D. He, S. H. Yu, Adv. Mater., 2010, 10, 1.

[7] M. Y. Ki, J .H. Christopher, Y. Matsubayashic, M. Kawabec, F. Iskandara, K. Okuyamaa, Chemical Engineering Science, 2007, 62, 4751.

[8] A.Greiner. J. H. Wendorff, Angew. Chem. Int. Ed., 2007, 46, 5670.

[9] T. Subbiah, G. S. Bhat, R. W. Tock, S. Parameswaran, S. S. Ramkumar, Journal of Applied Polymer Science, 2005, 96, 557.

[10] S. Kaur, R. Gopal, W. J. Ng, S. Ramakrishna , T. Matsuura, MRS Bull., 2008, 33, 21.

[11] A. Srivastava, O. N. Srivastava, S. Talapatra, R. Vajtai, P. M. Ajayan, Nat. Mater., 2004, 3, 610.

[12] K. H. Yoon, B. S. Hsiao, B. Chu, Polymer, 2009, 50, 2893.

[13] D. Aussawasathien, C. Teerawattananon, A. Vongachariya, J. Membr. Sci., 2008, 315, 11.

[14] T. Grafe, K. Graham, Nonwoven. Technol. Rev., INJ Spring, 2003, 51.

[15] R. Gopal, S. Kaur, C. Y. Feng, C. Chan, S. Ramakrishna, S. Tabe, T. Matsuura, J. Membr. Sci., 2007, 289, 210.

[16] F. Q. Sun, X. S. Li, J. K. Xu, P. T. Cao, Chinese Journal of Polymer Science, 2010, 28, 705.

[17] D. S. Wavhal, E. R. Fisher, J. Membr. Sci., 2002, 209, 255.

[18] E. Klein, Journal of Membrane Science, 2000, 179, 1.

[19] Z. K. Xu, X. J. Huang, L. S. Wan, Surface engineering of polymer membranes, Springer, 2009.

[20] A. A. Vetcher1y, R. Gearheart, V. N. Morozov, Polym. Adv. Technol., 2008, 19, 1276.

[21] C. H. Bamford, K. G. Al-Lamee, M. D. Purbrick, T. J. Wear, Journal of Chromatography A, 1992, 606, 19.

[22] H. T. Zhang, C. Y. Wu, Y. L. Zhang, C. J. B. White, Y. Xue, H. L. Nie, L. M. Zhu, J. Mater. Sci., 2010, 45, 2296.

[23] S. Agarwal, J. H. Wendorff, A. Greiner, Polymer, 2008, 49, 5603.

[24] J. S. Choi, H. S. Yoo, Journal of Bioactive and Compatible Polymers, 2007, 508.

[25] H. A. Rebyeh, F. Korber, K. S. Rehberg, J. Reusch, D. Josic, J. Chromatogr., 1991, 566, 341.

[26] T. C. Beeskow, W. Kusharyoto, F. B. Anspach, K. H. Kroner, W. D. Deckwer, J. Chromatogr. A, 1995, 715, 49.

[27] A. Podgorski, A. Balazy, A. Gradon, Chemical Engineering Science, 2006, 61, 6804.

[28] C. Shin, G. G. Chase, D. H. Reneker, Colloids and Surfaces A-Physicochemical and Engineering Aspects, 2005, 262, 211.

[29] R. Gopal, S. Kaur, Z. W. Ma, C. Chan, S. Ramakrishna, T. Matsuura, Journal of Membrane Science, 2006, 281, 581.

[30] X. Wang, X. Chen, K. Yoon, D. Fang, B. S. Hsiao, B. Chu, Environ. Sci. Technol., 2005, 39, 7684.

[31] P. Gibson, H. S. Gibson, D. Rivin, Colloids Surf. A: Physicochem. Eng. Aspects, 2001, 187–188, 469.

[32] C. H. Bamford, K. G. Al-Lamee, M. D. Purbrick, T. J. Wear, Journal of Chromatography, 1992, 606, 19.

[33] Z. W. Ma, M. Kotaki, S. Ramakrishna, Journal of Membrane Science, 2006, 272, 179.

[34] Z. W. Ma, K. Masaya, S. Ramakrishna, Journal of Membrane Science, 2006, 282, 237.

[35] Z. W. Ma, Z. W. Lan, T. Matsuura, S. Ramakrishna, Journal of Chromatography B, 2009, 877, 3686.

[36] Z. W. Ma, M. Kotaki, S. Ramakrishna, Journal of Membrane Science, 2005, 265, 115.

[37] S. Srivastava, A. Verma, B. L. Frankamp, V. M. Rotello, Advanced Materials, 2005, 17, 617.

[38] T. Cedervall, I. Lynch, S. Lindman, T. Berggård, E. Thulin, H. Nilsson, K. A. Dawson, S. Linse, PNAS, 2007, 104, 2050.

[39] X. L. Kong, L. C. L. Huang, C. M. Hsu, W. H. Chen, C. C. Han, H. C. Chang, Anal. Chem., 2005, 77, 259.

[40] A. S. Arthur, J. Kathryn, J. E. Fletcher, Journal of lipid research, 1969, 10, 56.

[41] K. Hirayama, S. Akashi, M. Furuya, K. I. Fukuhara, Biochemical and Biophysical Research Communications, 1990, 173, 639.

[42] B. R. Ware1, W. H. Flygare, Chemical Physics Letters, 1971, 12, 81.

[43] K. V. Peinemann, K. Ebert, H. G. Hicke, N. Scharnagl, Applications Environmental Progress, 2001, 20, 17.

[44] T. Godjevargova, V. Konsulov, A. Dimov, Journal of Membrane Science, 1999, 152, 235.

[45] M. Elbahri, S. S. Homaeigohar, T. H. Dai, R. Abdelaziz, A novel bio functionalized electrospun nanofibrous membrane; developed for nanofluid filtration and subsequent nanocomposite fabrication, Patent Pending.

[46] H. G. Hicke, I. Lehmann, G. Malsch, M. Ulbricht, M. Becker, Journal of Membrane Science, 2002, 198, 187.

[47] M. Bradford, Anal. Biochem., 1976, 72, 248.
[48] J. González-Benito, Journal of Colloid and Interface Science, 2003, 267, 326.
[49] M. Gonzalez, P. Kadlec, P. Stepanek, A. Strachota, L. Matejka, Polymer, 2004, 45, 5533.
[50] V. J. C. Lin, J. L. Koenig, Biopolymers, 1976, 15, 203.
[51] R. G. Reed, R. C. Feldhoff, O. L. Clute, Biochemistry, 1975, 14, 4578.
[52] A. D. Marshall, P. A. Munro, G. Trägårdh, Journal of Membrane Science, 1993, 91, 65.
[53] A. Mehta, A. L. Zydney, Journal of Membrane Science, 2005, 249, 245.
[54] M. J. Zohuriaan, F. Shokrolahi, Polymer Testing, 2004, 23, 575.
[55] K. J. Baranyai, G. B. Deacon, D. R. MacFarlane, J. M. Pringle, J. L. Scott, Australian Journal of Chemistry, 2004, 57, 145.
[56] A. R. Uribe, L. Arizmendi, M. E. R. Guzman, S. S. Guzman, R. C. Silva, Applied materials and interfaces, 2009, 1, 2502.
[57] S. S. Choi, J. P. Hong, Y. S. Seo, S. M. Chung, C. Nah, J. of Appl. Polym. Sci., 2006, 101, 2333.
[58] O. W. Reif, V. Nier, U. Bahr, R. Freitag, J. Chromatogr. A, 1994, 664, 13.
[59] M. Kim, K. Saito, S. Furusaki, T. Sato, T. Sugo, I. Ishigaki, Journal of Chromatography A, 1991, 585, 45.
[60] H. F. Zou, Q. Z. Luo, D. M. Zhou, Journal of Biochemical and Biophysical Methods, 2001, 49, 199.
[61] C. J. van Koppen, D. M. zu Heringdorf, K. T. Laser, C. Y. Zhang, K. H. Jakobs, M. Bünemann, L. Pott, The Journal of Biological Chemistry, 1996, 271, 2082.

Chapter 8. Summary

This Ph.D thesis introduces the fabrication of a novel electrospun nanofibrous mat (ENM) and its applications in three different fields. This novel ENM is fabricated by electrospinning of poly(acrylonitrile-*co*-glycidyl methacrylate) (PANGMA). PANGMA is a novel copolymer of polyacrylonitrile (PAN) and glycidyl methacrylate (GMA), which was developed at Helmholtz-Zentrum Geesthacht. It has both the advantage of the excellent mechanical stability of PAN backbone and the chemically active epoxy group on its GMA part. The epoxy group offers the opportunity for the employment of PANGMA in a variety of activation/coupling chemistries for lots of further applications, for instance: crosslinking reaction with amines, enzyme immobilization reaction and capturer binding reaction.

The fabrication method used in this Ph.D work for producing these novel nanofiber and nanofibrous mat is electrospinning. PANGMA nanofibers and ENMs were successfully fabricated by electrospinning PANGMA/DMF solution with precisely controlling the spinning conditions. Increasing solution concentration will increase the average diameter and unify the fiber morphology. Average fiber diameter also decreases slightly with the increase of the applied voltage. On the other hand, the feed rate and spinning distance have no obvious influence on the nanofiber diameter. Adding additives, such as citric acid and triethylbenzylammonium chloride (TEBAC) can further decrease the average diameter. The morphology of the PANGMA nanofibers also can be controlled by adjusting the spinning conditions properly. The parameters of the PANGMA-ENM, such as thickness and pore size of the ENM can be controlled and optimized by adjustment of the relevant spinning conditions. Higher

feed rate and longer electrospinning time can increase the thickness of the ENMs. Higher feed rate also can decrease the average pore diameter and narrow the pore size distribution of PANGMA-ENMs.

In this Ph.D thesis, three different applications of this novel PANGMA-ENM were introduced and discussed in particular. There are solvent-resistant nanomembranes, supports for the enzyme immobilization and affinity nanofilter for the protein filtration, respectively. The results of this Ph.D thesis prove that after some proper post-modification, these novel modified ENMs have very good perfomances in those three applications. They can greatly improve the restrictions and disadvantages of the existing ordinary ENMs on their applications in those areas.

In the first application, we demonstrated the fabrication of the novel solvent resistant ENM based on the electrospinning of PANGMA and the subsequent crosslinking of the ENM with ammonia. The fabricated ENMs have a uniform distribution of fiber size and are practically free of beads with the average diameter in the range of 300 ~ 600 nm. The neat PANGMA-ENMs can be successfully crosslinked by ammonia hydroxide solution. Swelling test and FTIR spectrum indicate verify the successful crosslinking of epoxy groups in PANGMA by ammonia. The crosslinked PANGMA-ENMs have better thermal stability than the neat ENMs. The pore size of the PANGMA-ENM will reduce after being immersed into the solvents. All the results indicate that this novel crosslinked PANGMA-ENM has superior solvent resistance against most of the solvents which are commonly used in chemical and catalytic reactions, and therefore have potential as the solvent resistant membrane and the support for the immobilization of homogeneous catalysts and enzymes.

In the second application, PANGMA nanofibers and ENMs with fiber diameters of 200 to 300 nm were fabricated by electrospinning a 20 wt% PANGMA/DMF solution at an applied voltage of 25 kV. *Candida antarctica* lipase B (Cal-B) was covalently immobilized onto the PANGMA-ENMs via three different immobilization routes. SEM and FTIR results indicate that Cal-B has been successfully immobilized onto PANGMA nanofibers. The observed Cal-B loading on these GA activated PANGMA-ENMs is up to approximately 50 mg/g and meanwhile no fouling of the ENMs is observed. The hydrolytic activity of the Cal-B immobilized PANGMA-ENMs is up to approximately 2500 nmol/min/mg. All these Cal-B immobilized ENMs perform much higher hydrolytic activity than free Cal-B powder, the ENM activated with HMDA and GA, immobilized with Cal-B at 30 ℃ even has higher activity than Novozyme 435. The novel Cal-B immobilized PANGMA-ENMs have much better thermal, storage, and reuse stabilities. They have good potential applications in the field of enzymatic catalysis.

In the last application, a novel affinity ENM was fabricated by electrospinning of PANGMA and the subsequent modification with BSA. The binding amount can reach 27.2 mg BSA per gram ENM. FTIR and SEM results also show the successful binding of BSA onto PANGMA-ENMs. This BSA modified PANGMA-EMN has better thermal and mechanical properties than the neat PANGMA-ENM. The water wettability of PANGMA-ENM is improved by the BSA modification. After modification, the modified ENM turns from super hydrophobic to super hydrophilic. The results of pure water flux measurement indicate that the BSA modified ENM has better water permeability and structure integrity during their service under higher water pressure than the neat one. Filtration test for the proteins shows that after the

first filtration cycle, around 70 % of the BSA and 60 % of the Cal-B in initial feed solution can be filtrated by the BSA modified PANGMA-ENM, which proves that BSA modified PANGMA-ENM can capture proteins in water effectively. This novel affinity ENM is highly suitable for the filtration and separation proteins, bio-harzards, tiny particles and contaminations in water.

Zusammenfassung

Diese Doktorarbeit stellt die Herstellung einer neuartigen elektrogesponnenen nanofibrösen Matte (ENM) und ihre Anwendungen in drei verschiedenen Bereichen vor. Diese neue ENM ist durch Elektrospinnen von Poly(acrylnitril-*co*-glycidylmethacrylat) (PANGMA) hergestellt worden. PANGMA ist ein neuartiges Copolymer aus Acrylnitril (AN) und Glycidylmethacrylat (GMA), welches beim Helmholtz-Zentrum Geesthacht entwickelt wurde. Es hat sowohl den Vorteil der ausgezeichneten mechanischen Stabilität des PAN-Rückgrats und den chemisch aktiven Epoxidgruppen der GMA Teile. Die Epoxidgruppe bietet die Möglichkeit für den Einsatz von PANGMA in einer Vielzahl von Aktivierungs- bzw.. Kopplungschemie für viele weitere Anwendungen, zum Beispiel: Vernetzungsreaktionen mit Aminen, Enzymimmobilisierung, und Bindungsreaktionen.

Das Herstellungsverfahren in dieser Doktorarbeit für die Herstellung dieser neuartigen Nanofaser und nanofibrösen Matte ist Elektrospinnen. PANGMA Nanofasern und ENMn wurden erfolgreich durch Elektrospinnen von der PANGMA/DMF Lösung mit präziser Steuerung der Spinnbedingungen hergestellt. Zunehmende Konzentration der Lösung erhöht den mittleren Durchmesser und führt zu einer Vereinheitlichung der Fasermorphologie. Durchschnittliche Faserdurchmesser verringern sich auch etwas

mit der Erhöhung der angelegten Spannung. Auf der anderen Seite haben die Vorschubgeschwindigkeit und Elektrodendistanz keinen offensichtlichen Einfluss auf die Nanofaserdurchmesser. Zugabe von Additiven, wie Zitronensäure und Triethylbenzylammoniumchlorid (TEBAC) führen zu einer weiteren Abnahme des mittleren Durchmessers. Die Morphologie der PANGMA Nanofasern kann auch durch Einstellen der Spinnbedingungen gesteuert werden. Die Parameter der PANGMA-ENM, wie Dicke und Porengröße der ENM, können durch Anpassung der einschlägigen Spinnbedingungen kontrolliert und optimiert werden. Höherer Vorschub und mehr Elektrospinnzeit können die Dicke des ENM erhöhen. Höherer Vorschub kann auch den durchschnittlichen Porendurchmesser verringern und die Porengrößenverteilung von PANGMA-ENMn verengen.

In dieser Doktorarbeit wurden drei verschiedene Anwendungen dieses neuartigen PANGMA-ENM im Besonderen eingeführt und diskutiert. Es gibt lösemittel-beständige Nanomembranen, Träger für die Immobilisierung von Enzymen und Affinität-Nanofilter für die Proteinfiltration. Die Ergebnisse dieser Doktorarbeit zeigen, dass nach einer geeigneten Post-Modifikation diese neuartigen modifizierten ENM sehr gute Eigenschaften in jenen drei Anwendungen haben. Sie können die Einschränkungen und die Nachteile der bestehenden gewöhnlichen ENMn auf ihre Anwendungen in jenen Bereichen erheblich verbessern.

In der ersten Anwendung zeigten wir die Herstellung des neuen lösemittelbeständigen ENM, das auf dem Elektrospinnen von PANGMA und die anschließende Vernetzung der ENM mit Ammoniak beruht. Die fabrizierten ENMs haben eine gleichmäßige Verteilung der Fasergröße und sind praktisch frei von Kügelchen mit dem mittleren

Durchmesser im Bereich von 300 ~ 600 nm. Diese homogenen PANGMA-ENMn können erfolgreich durch Ammoniakhydroxidlösung vernetzt werden. Quelltests und FTIR Spektrum bestätigen die erfolgreiche Vernetzung der Epoxidgruppen in PANGMA durch Ammoniak. Die vernetzten PANGMA-ENMn haben eine bessere thermische Stabilität als die nicht vernetzten ENMn. Die Porengröße des PANGMA-ENMn wird reduziert, nachdem sie in den Lösungsmitteln eingetaucht wurden. Alle Ergebnisse deuten darauf hin, dass dieses neuartigen vernetzten PANGMA-ENM eine überlegene Widerstandsfähigkeit gegen die meisten Lösungsmittel zeigen, welche häufig in der chemischen und katalytischen Reaktionen eingesetzt werden. Deshalb haben sie Potenzial als Lösungsmittel beständige Membran und als Unterstützung für die Immobilisierung von homogenen Katalysatoren und Enzymen.

In der zweiten Anwendung wurden PANGMA Nanofasern und ENMn mit Faserdurchmesser von 200 bis 300 nm durch Elektrospinnen von einer 20 Gew.% PANGMA/DMF Lösung bei einer angelegten Spannung von 25 kV hergestellt. *Candida antarctica* Lipase B (Cal-B) wurde an die PANGMA-ENMn über drei verschiedene Immobilisierungsrouten kovalent immobilisiert. SEM und FTIR Ergebnisse zeigen, dass Cal-B erfolgreich auf PANGMA Nanofasern immobilisiert wurde. Die beobachtete Cal-B Belastung auf diese mit Glutaraldehyd (GA) aktivierten PANGMA-ENMn ist bis ca. 50 mg/g und keine Verschmutzung der ENMn wird in der Zwischenzeit beobachtet. Die hydrolytische Aktivität der auf PANGMA-ENMn immobilisierten Cal-B ist bis zu ca. 2500 nmol/min/mg. Alle diese mit Cal-B funktionalisierten ENMn zeigen eine viel höhere hydrolytische Aktivität als frei Cal-B-Pulver. Das ENM, das mit HMDA und GA aktiviert und mit Cal-B bei 30 ℃ immobilisiert, hat sogar höhere Aktivität als Novozyme 435. Die neuartigen mit Cal-

B funktionalisierten PANGMA-ENMn zeigen eine viel bessere thermische, Stabilität und Wiederverwendbarkeit. Sie haben gute Einsatzmöglichkeiten im Bereich der enzymatischen Katalyse.

In der letzten Anwendung wurde eine neuartige Affinität-ENM durch das Elektrospinnen von PANGMA und der folgenden Modifikation mit BSA hergestellt. Die auf PANGMA-ENM angebundene Menge von BSA kann 27.2 mg BSA pro Gramm ENM erreichen. FTIR und SEM Ergebnisse zeigen auch die erfolgreiche Anbindung von BSA auf PANGMA-ENM. Das mit BSA modifizierte PANGMA-EMN hat bessere thermische und mechanische Eigenschaften als das nicht modifizierte PANGMA-ENM. Die Wasserbenetzbarkeit von PANGMA-ENM wird durch die Modifikation mit BSA verbessert. Durch die Modifikation wird das superhydrophoben ENM superhydrophil. Die Ergebnisse der reinen Wasserflussmessung zeigen, dass das BSA modifizierte ENM besser wasserdurchlässig ist und Strukturintegrität während seines Einsatzes unter höherem Wasserdruck als das unmodifizierte ENM hat. Filtriertests für die Proteine zeigen, dass nach dem ersten Filtrationzyklus, rund 70% des BSA und 60% der Cal-B in der Anfangszufuhrlösung durch das mit BSA modifizierte PANGMA-ENM filtriert werden kann. Das zeigt, dass die mit BSA modifizierte PANGMA-ENM die Proteine im Wasser effektiv abfangen kann. Diese neuartige Affinität-ENM eignet sich hervorragend für die Filtration und Separation von Proteinen, Bio-harzards, kleine Partikel und Verunreinigungen im Wasser.

Acknowledgements

First and foremost I would like to express my heartfelt gratitude towards my Doktorvater Professor Volker Abetz for his academic guidance, continuous support and encouragement throughout this project. He is an erudite and remarkable teacher and a great and pleasant person. I appreciate his generosity in financially supporting me to finish my Ph.D work and providing me the opportunity to attend international conferences that gave me good academic exposure. He has been very cooperative all along and gave me his precious time and advice whenever I needed it.

I would like to give my sincere thanks to my supervisor Professor Mady Elbahri for his kind and patient academic instructions. He is a man who always has hundreds and thousands novel and creactive inspirations. He always illuminated me when I had problems and difficulties during the experimental and composing works of my Ph.D.

I am deeply thankful to Mr. Joachim Koll, Mr. Shahin Homaeigohar and Mr. Ahnaf Usman Zillohu for their help and co-operations in my work. My heartfelt gratitude extends to Mrs. Clarissa Abetz, Mrs. Prause and Mr. Silvio Neumann for their kind and wonderful measurements work. I also would like to specially thank to Mrs. Ilona Zillich for her kind help.

I want to give a special acknowledgement to my parents for their unconditional love and support, even when I was in a bad temper due to the frustration of my thesis. Finally, I also want to thank my lovely girl friend for her self-giving and continuous support and care to me. I love you all and would not have been able to make everything through without your supports. You are the best!

List of publications

Papers

1. **Tianhe Dai**, Nemanja Miletić, Katja Loos, Mady Elbahri, Volker Abetz*, Electrospinning of poly(acrylonitrile-co-glycidyl methacrylate) nanofibrous mats for the immobilization of candida antarctica lipase B, Macromolecular Chemistry and Physics, Vol. 212, Issue 4, 319–327, 15-Feb-2011.

2. **Tianhe Dai**, Katrin Ebert*, Electrospinning of the solvents-resistant nanofibers based on poly(acrylonitrile-co-glycidyl methacrylate), Journal of Applied Polymer Science, accepted on 11-Jun-2010.

3. **Tianhe Dai**, Mady Elbahri*, Novel electrospun nanofibrous membrane for the filtration of proteins in water, Manuscript for submission.

4. **Tian-He Dai,** Hao Yu*, Kai Zhang, Mei-Fang Zhu, Yan-Mo Chen and Hans-Juergen Adler, Fabricating novel thermal crosslinked ultrafine fibers via electrospinning, Journal of Applied Polymer Science, Vol. 107, Issue 4, 2142–2149, 15-Feb-2008.

Patents

1. Mady Elbahri, Shahin Homaeigohar, **Tianhe Dai,** Ramzy Abdelaziz, A novel bio functionalized electrospun nanofibrous membrane; developed for nanofluid filtration and subsequent nanocomposite fabrication, Patent pending.

Conference Attended

1. Electrospinning 2010: Theory, practice and applications, Melbourne, Australia, Jan 26-29, 2010, Poster contributed.